Todd Kozlowski

Cosmic WISPers

Bari, 08.09.2023

COSMIC WISPERS
CA21106

cost
EUROPEAN COOPERATION IN SCIENCE & TECHNOLOGY

MADMAX

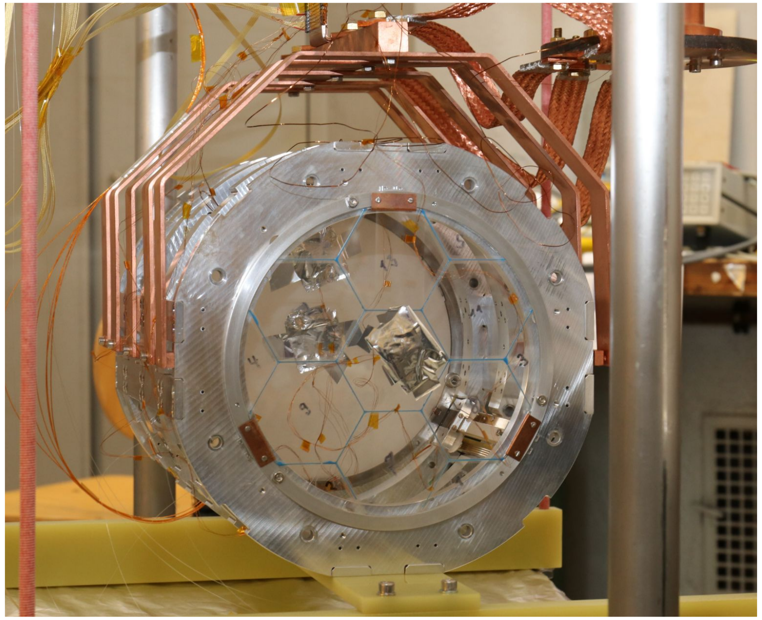

IAXO

ALPS II

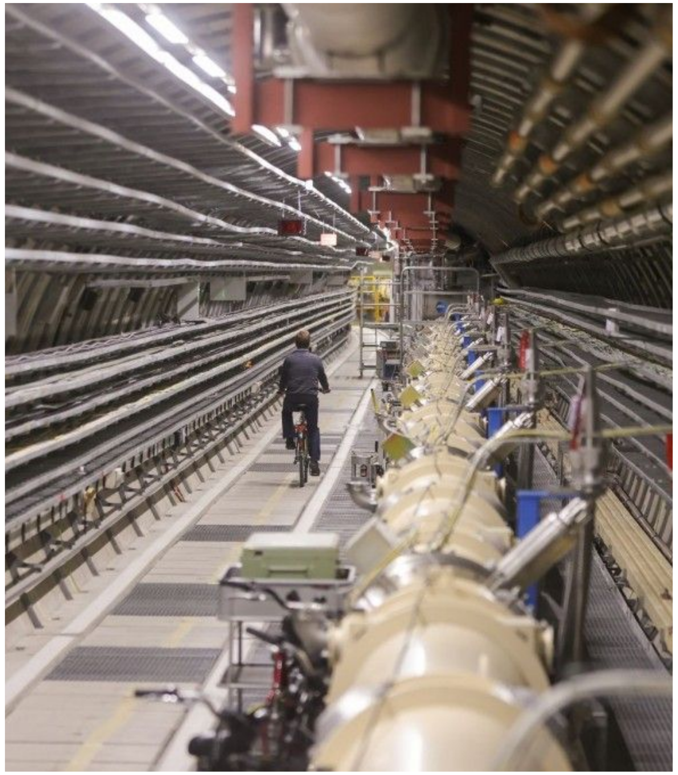

Axion Searches at DESY.

Outline

Introduction and Theoretical Motivation

- Axions and axion-like particles
- Basic axion search experiment concepts

Searching for Axion Dark Matter: MADMAX

- Improving sensitivity with a dielectric haloscope
- Research and development

A Solar Axion Telescope: (baby)IAXO

- Solar axion spectrum
- Next-generation technology

Light-Shining-Through-a-Wall: ALPS II

- A resonantly enhanced design
- First results from the initial science run!

Axions and Axion-like Particles

Axions:

- hypothetical particle beyond the standard model, pseudo-NGB from new U(1) symmetry
- favored solution to the strong charge-parity symmetry (CP) problem in QCD
- axion-photon interactions described by axion-extended Standard Model lagrangian:

$$\mathcal{L}_{a\gamma} = -\frac{1}{4} g_{a\gamma\gamma} a F_{\mu\nu} \tilde{F}^{\mu\nu} = g_{a\gamma\gamma} a \vec{E} \cdot \vec{B}$$

a → axion field

g → coupling strength

E → electric field (i.e. light)

B → background magnetic field

Axions and Axion-like Particles

Axion-like particles (ALPs):

- a family of so-called "Weakly-Interacting sub-eV Particles" (WISPs)
- properties similar to the classical axion
    - scalar or pseudo-scalar bosons
- motivated by ***astrophysical hints***
- excellent ***dark matter candidate***

$$\mathcal{L}_{a\gamma}^{ps} = -\frac{1}{4} g_{a\gamma\gamma} a F_{\mu\nu} \tilde{F}^{\mu\nu} = g_{a\gamma\gamma} a \vec{E} \cdot \vec{B}$$

pseudo-scalar:

$$\vec{E} \parallel \vec{B}$$

$$\mathcal{L}_{a\gamma}^{sc} = -\frac{1}{4} g_{a\gamma\gamma} a F_{\mu\nu} F^{\mu\nu} = g_{a\gamma\gamma} a \left(\vec{E}^2 - \vec{B}^2\right)$$

scalar:

$$\vec{E} \perp \vec{B}$$

Axions and Axion-like Particles

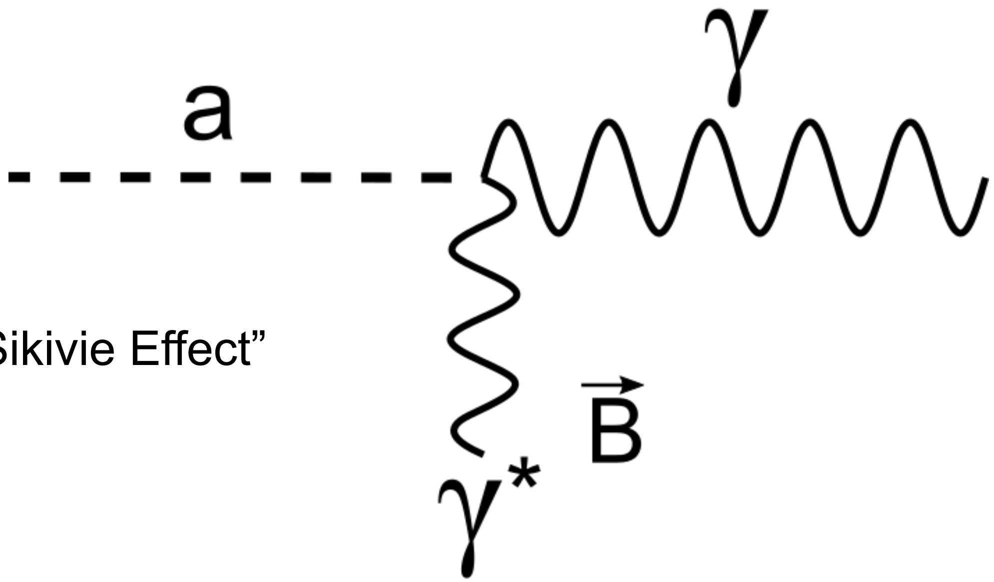

"Sikivie Effect"

P. Sikivie
Phys. Rev. Lett. **51**, 1415 (1983)

$$P_{a\to\gamma} \approx \frac{1}{4}(g_{a\gamma\gamma}BL)^2$$

Searching for Axion-like Particles

Haloscopes:
using a powerful magnet, dark matter axions from the galactic halo convert into EM waves in a tunable microwave cavity or resonant detector

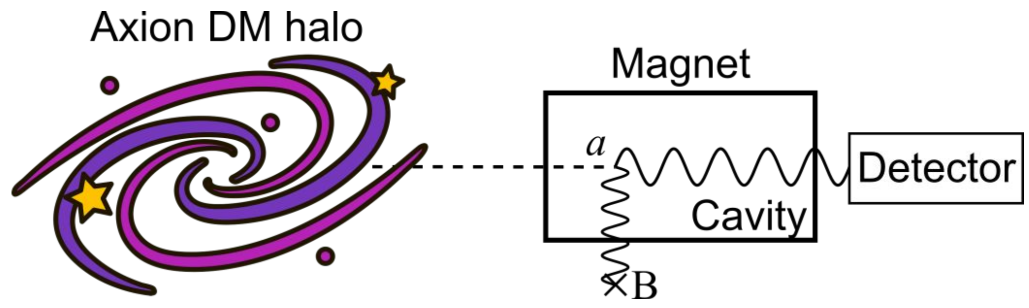

Helioscopes:
ALPs, generated in the core of the Sun, are re-converted in a experimental magnetic field and detected as X-rays

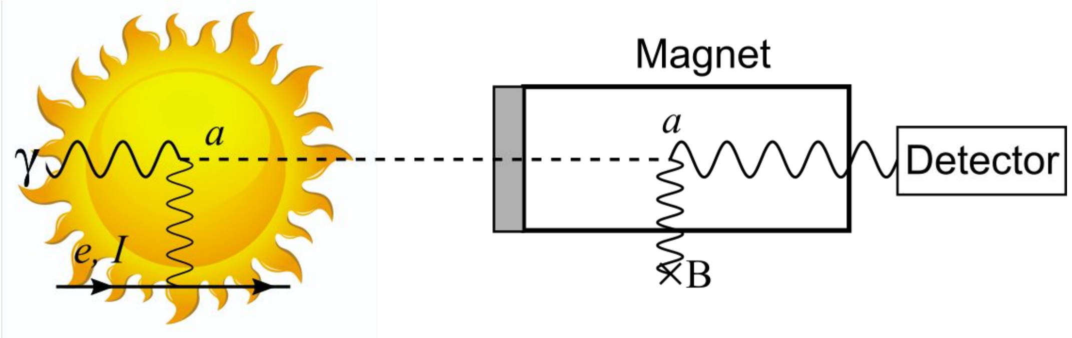

Light-shining-through-a-Wall (LSW):
laser light is converted into ALPs in a 'production' magnetic field. ALPs pass through an opaque barrier and re-convert in a 'regeneration' field for detection

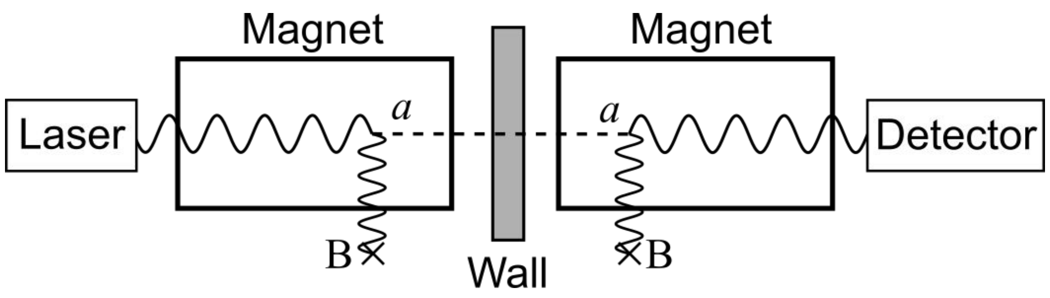

Searching for Axion-like Particles

Haloscopes:
using a powerful magnet, dark matter axions from the galactic halo convert into EM waves in a tunable microwave cavity or resonant detector

Helioscopes:
ALPs, generated in the core of the Sun, are re-converted in a experimental magnetic field and detected as X-rays

Light-shining-through-a-Wall (LSW):
laser light is converted into ALPs in a ‘production’ magnetic field. ALPs pass through an opaque barrier and re-convert in a ‘regeneration’ field for detection

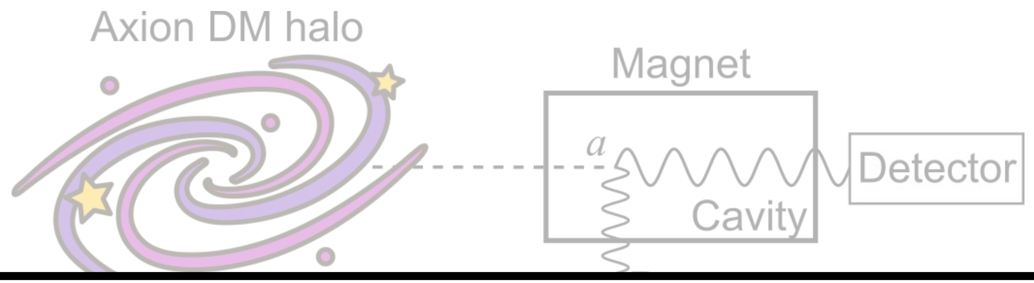

Experimental Tests of the "Invisible" Axion, P. Sikivie
Phys. Rev. Lett. 51, 1415 (1983)

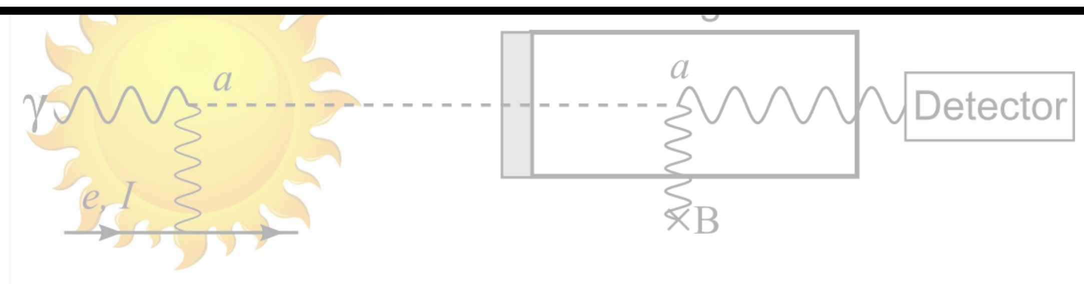

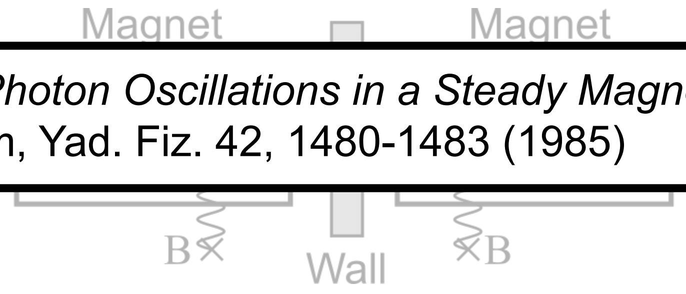

Arion ⇋ Photon Oscillations in a Steady Magnetic Field, A. Anselm, Yad. Fiz. 42, 1480-1483 (1985)

Searching for Axion-like Particles

Haloscopes:
using a powerful magnet, <u>dark matter</u> axions from the galactic halo convert into EM waves in a tunable microwave cavity or resonant detector

Helioscopes:
ALPs, generated in the core of the Sun, are <u>re-converted</u> in a experimental magnetic field and detected as X-rays

Light-shining-through-a-Wall (LSW):
laser light is converted into ALPs in a ‘<u>production</u>’ magnetic field. ALPs pass through an opaque barrier and re-convert in a ‘<u>regeneration</u>’ field for detection

Source	Experiments	Model dependence
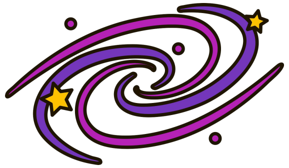 **Relic CDM axions**	MADMAX ADMX, many worldwide …	**High**
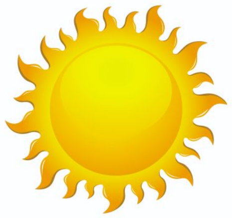 **Solar axions**	IAXO CAST, SUMICO	**Low**
 **Laboratory-prepared axions**	ALPS II ALPS I, OSQAR	**Very Low**


HERA North
HERA South


HERA North
HERA South
MADMAX


HERA North
HERA South
MADMAX


ALPS II
HERA North
MADMAX
IAXO
HERA South

Searching for Axion-like Particles

Axion mass-coupling parameter space

- **MADMAX**, **IAXO** and **ALPS II** provide complementary and model-distinct windows into the dark universe
- New models of monopole-philic QCD axions moves the predicted band into experimental accessible territories

Sokolov-Ringwald: [JHEP06(2021)123]

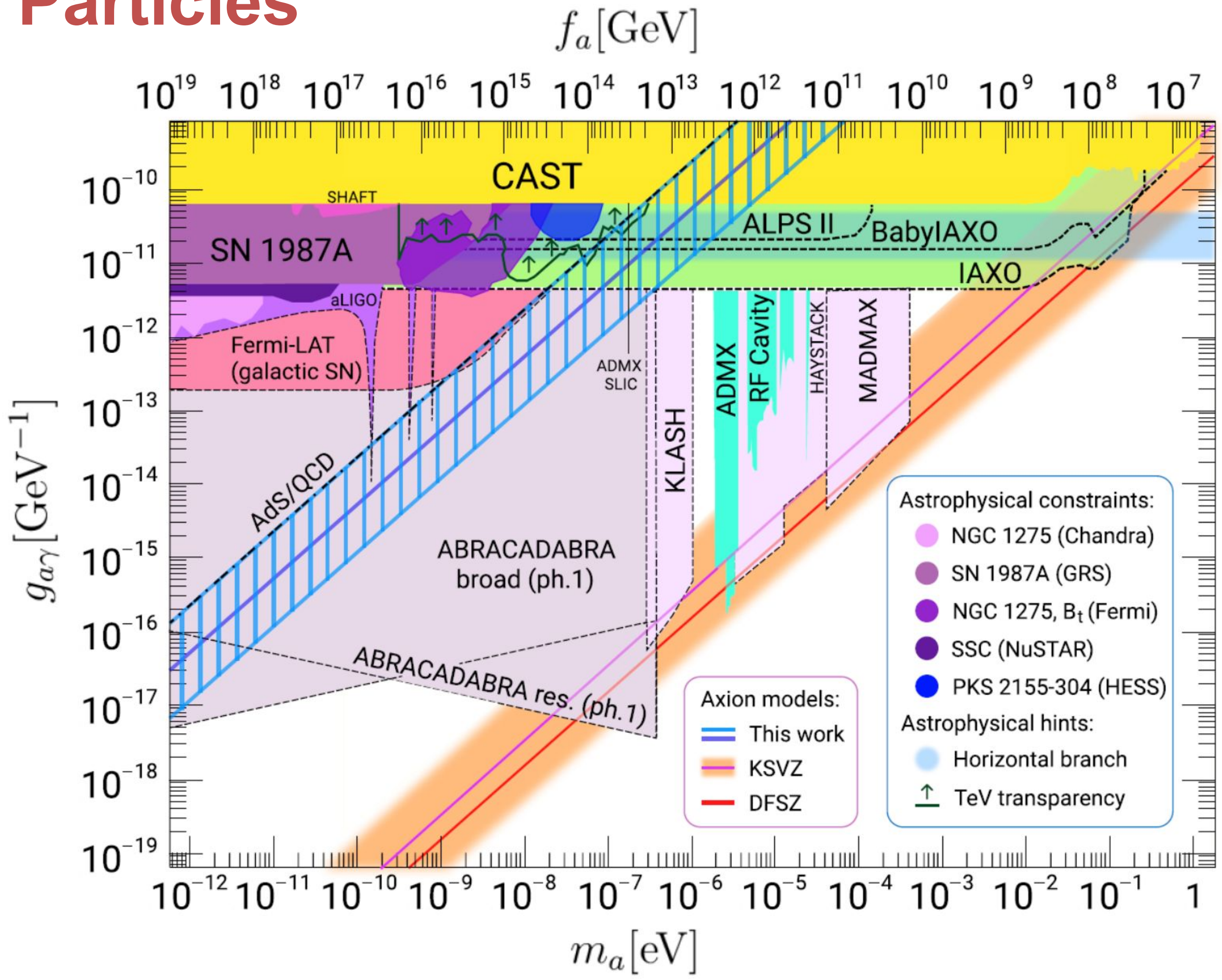

Sokolov-Ringwald: JHEP06(2021)123

Searching for Axion Dark Matter with a Dielectric Haloscope

Axions of Cosmic Origin

Axions as Cold Dark Matter

- pre-inflationary PQ-symmetry breaking scenario:
  - allows entire CDM to be cold axions with mass below ~ 500 µeV
- post-inflationary PQ-symmetry breaking scenario:
  - average of local variations in initial misalignment
  - complicated by topological defects, but nevertheless motivates a mass range:

    $26\ \mu\text{eV} < m_a < 1\ \text{meV}$
- a **window of opportunity** appears around **~ 100 µeV** to search for axion CDM from either scenario

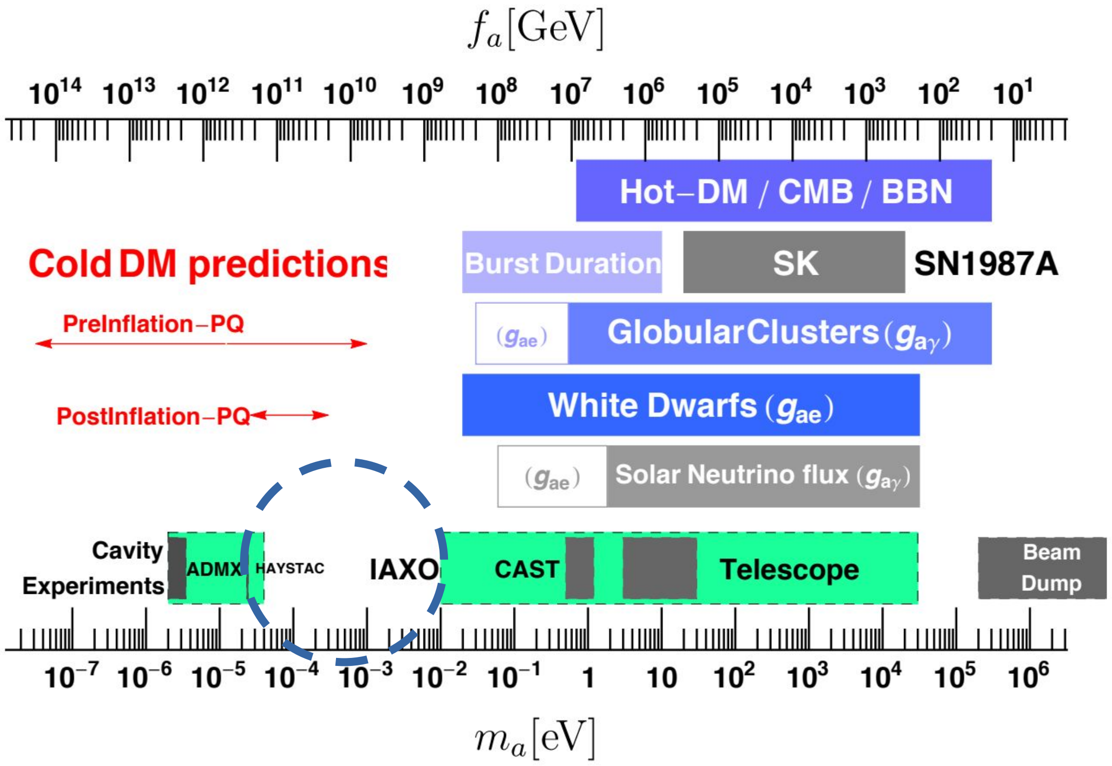

MADMAX Collaboration., Brun, P., Caldwell, A. *et al.* A new experimental approach to probe QCD axion dark matter in the mass range above 40µeV. *Eur. Phys. J. C* 79, 186 (2019).

MAgnetized Disk and Mirror Axion eXperiment

A Dielectric Haloscope

- generates an axion-induced electromagnetic wave from the **E-field discontinuity at the disk's dielectric boundary** in a magnetic field:

$$P_0 = 2.2 \times 10^{-27}\mathrm{W}\left(\frac{A}{1\ \mathrm{m}^2}\right)\left(\frac{B_e}{10\ \mathrm{T}}\right)^2\left(\frac{\rho_a}{0.3\ \mathrm{GeV/cm}^3}\right)C_{a\gamma}^2$$

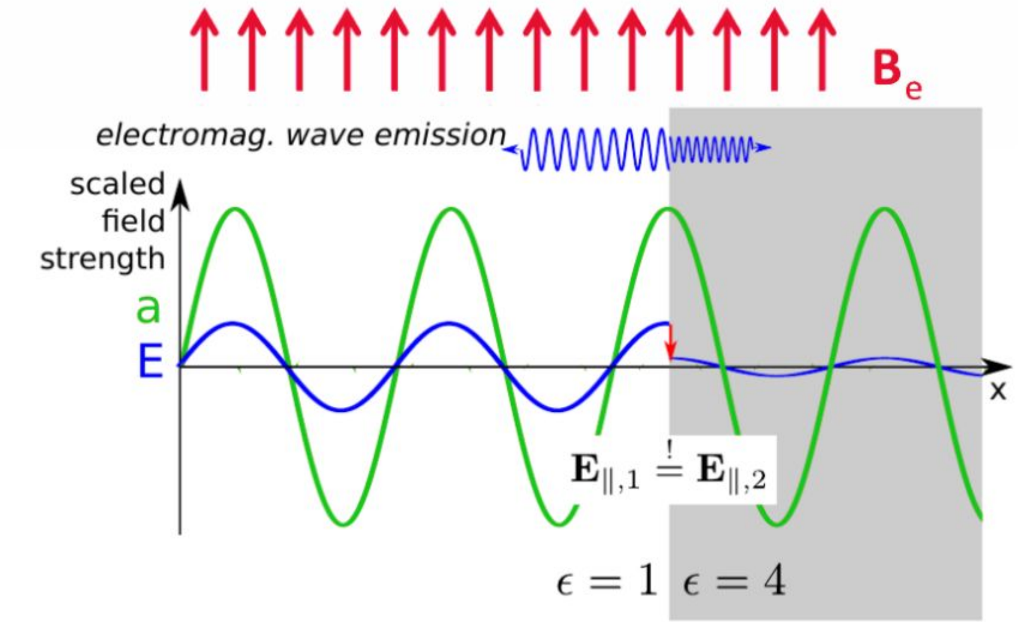

Egge, J., Knirck, S., Majorovits, B. et al. Eur. Phys. J. C 80, 392 (2020).

Graphic courtesy of Christoph Krüger

MAgnetized Disk and Mirror Axion eXperiment

A Dielectric Haloscope

- generates an axion-induced electromagnetic wave from the **E-field discontinuity at the disk's dielectric boundary** in a magnetic field:

$$P_0 = 2.2 \times 10^{-27}\mathrm{W} \left(\frac{A}{1\ \mathrm{m}^2}\right) \left(\frac{B_e}{10\ \mathrm{T}}\right)^2 \left(\frac{\rho_a}{0.3\ \mathrm{GeV/cm}^3}\right) C_{a\gamma}^2$$

- adding multiple dielectric media leads to a tunable "boost" factor, where the emissions from the different surfaces sum constructively:

$$P = P_0 \cdot \beta^2(\nu) = 1.1 \times 10^{-22}\ \mathrm{W} \left(\frac{\beta^2(\nu)}{5 \times 10^4}\right) \left(\frac{A}{1\ \mathrm{m}^2}\right) \left(\frac{B_e}{10\ \mathrm{T}}\right)^2 \left(\frac{\rho_a}{0.3\ \mathrm{GeV/cm}^3}\right) C_{a\gamma}^2$$

- boost factor tunable via the disk separations, in order to scan sensitivity to the axion dark matter mass

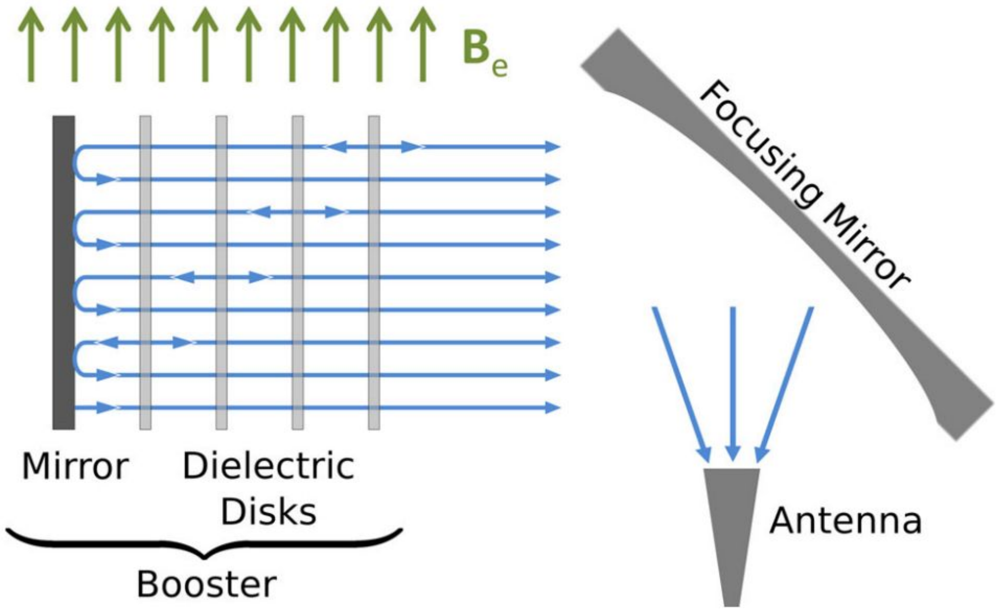

Egge, J., Knirck, S., Majorovits, B. et al. Eur. Phys. J. C 80, 392 (2020).

Graphic courtesy of Christoph Krüger

MAgnetized Disk and Mirror Axion eXperiment

MADMAX Design Concept

- arrangement of 80x 1.25 m diameter dielectric disks placed inside a purpose-built superconducting 9 T wide-bore magnet
- each dielectric disk (6 kg) need to be positioned to 10 µm accuracy to allow the electromagnetic fields to add coherently and optimize the boost factor
- entire detector is cryogenically cooled (4 K) to reduce background and improve sensitivity
- optimized to probe in the range of m_a ~ 100 µeV down to contemporary models

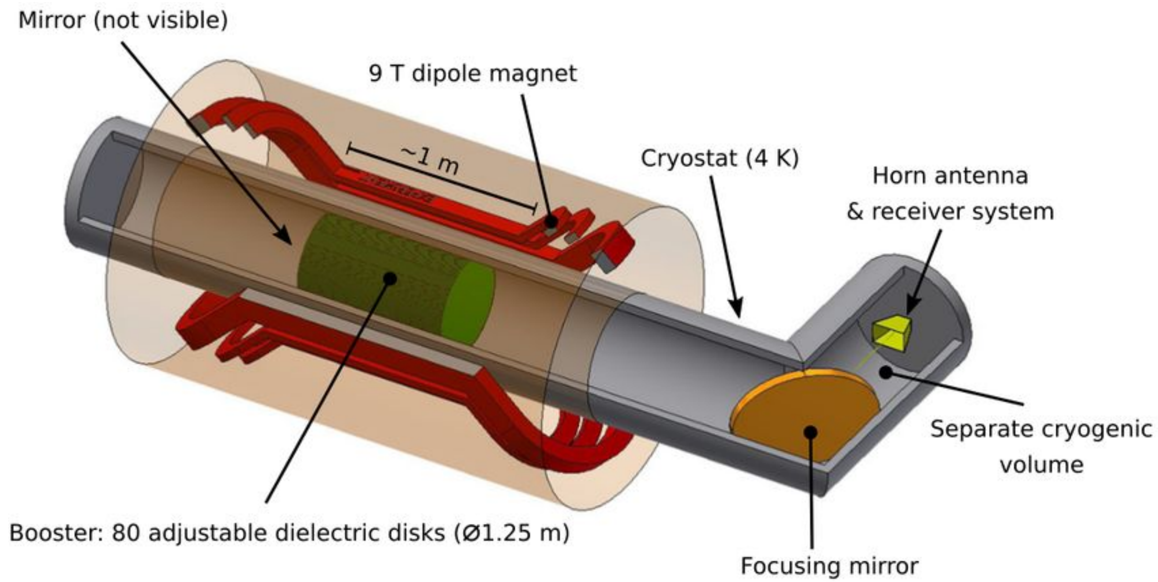

Xiaoyue Li and for the MADMAX Collaboration (2020) J. Phys.: Conf. Ser. 1468 012062

MAgnetized Disk and Mirror Axion eXperiment

MADMAX magnet

- custom cable-in-conduit conductor (CICC) design
  - coil design demonstrated acceptable quench velocity

    C. Lorin *et al.*, *IEEE Transactions on Applied Superconductivity*, vol. 33, no. 7, pp. 1-11, Oct. 2023
- HERA H1 detector iron yoke (pictured) to be repurposed for the MADMAX magnet

Site selection: HERA North Hall @ DESY

- dedicated “cryoplatform” under development
- adjacent to ALPS II site

- **Potential 2030 @ DESY**

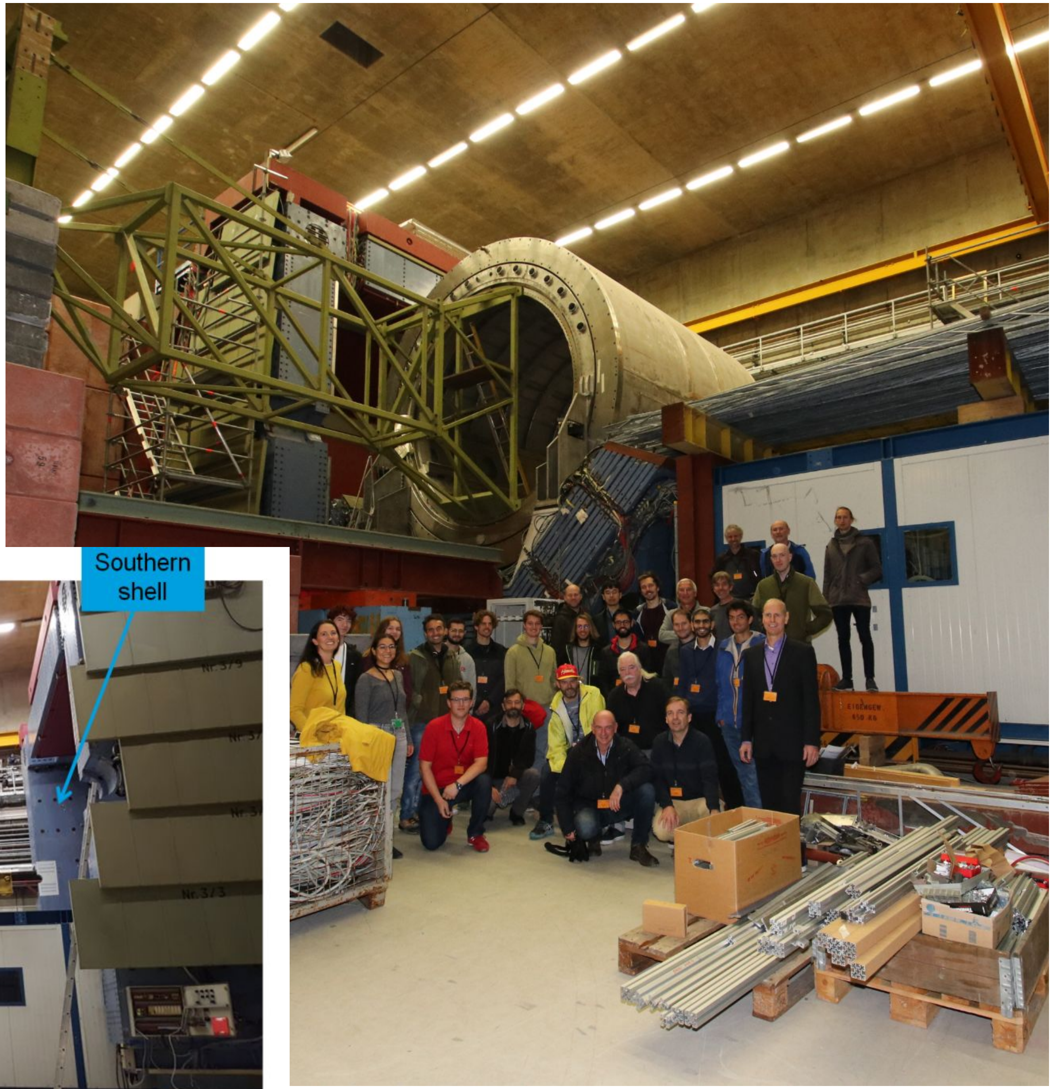

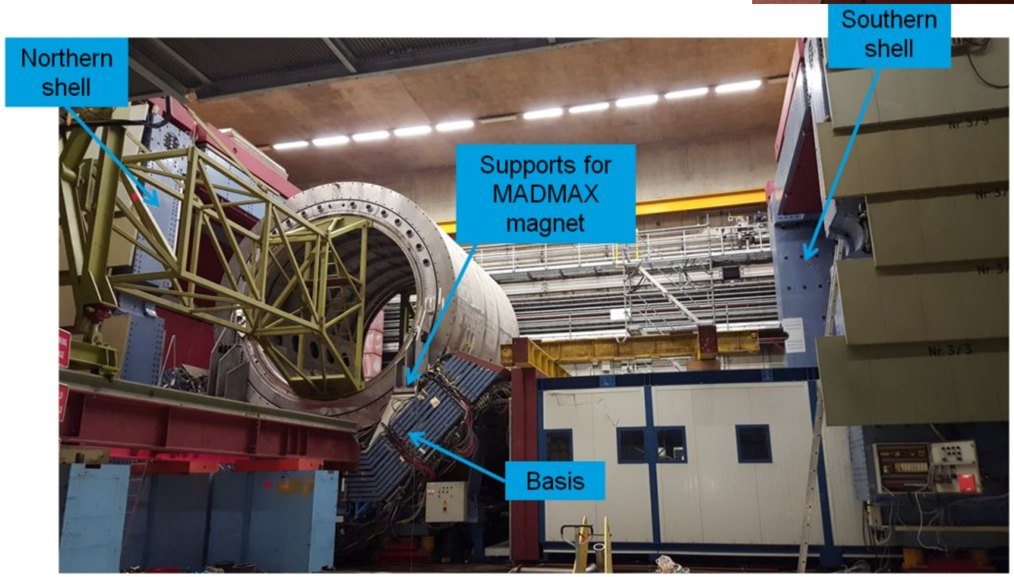

Phased Prototypes and R&D

Closed Boosters

- CB100: 3 x fixed ∅100mm Al_2O_3 disks
  - **initial measurements** in CERN MORPURGO magnet (pictured)
  - test read-out electronics, booster modeling, noise
- CB200: 3 x fixed ∅200mm Al_2O_3 disks
  - **under development** to investigate scaling

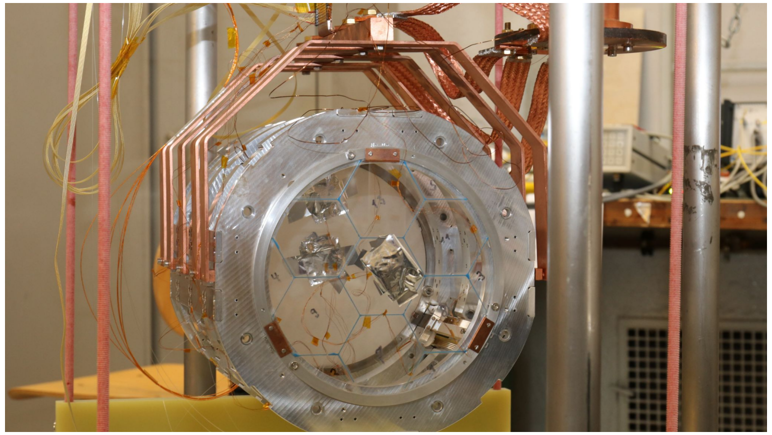

Open Boosters

- OB200: 2 x adjustable ∅200mm Al_2O_3 disks
  - testbed for mechanical disk positioners (pictured)
  - linear motors **successfully tested** in 5 K / 5.3 T / UHV @ DESY
- OB300: 3 x adjustable ∅300mm disks
  - under construction, room temp. end of year, cryo 2024-2025

E. Garutti *et al* 2023 *JINST* 18 P08011

MADMAX Prototype Cryostat

- Prototype liquid helium (4 K) cryostat
- ∅760mm large bore to accommodate all prototype booster designs
  - fits into MORPURGO magnet bore
- **to be delivered / commissioned @ DESY 2024**

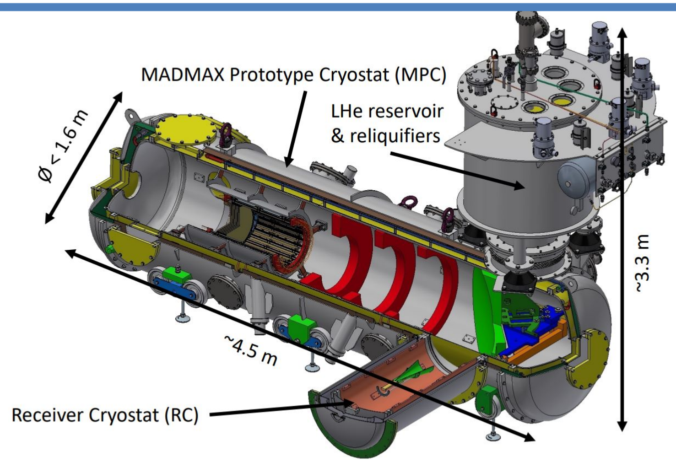

Measuring the solar axion flux with the Next-generation Helioscope

Solar Axion Origins

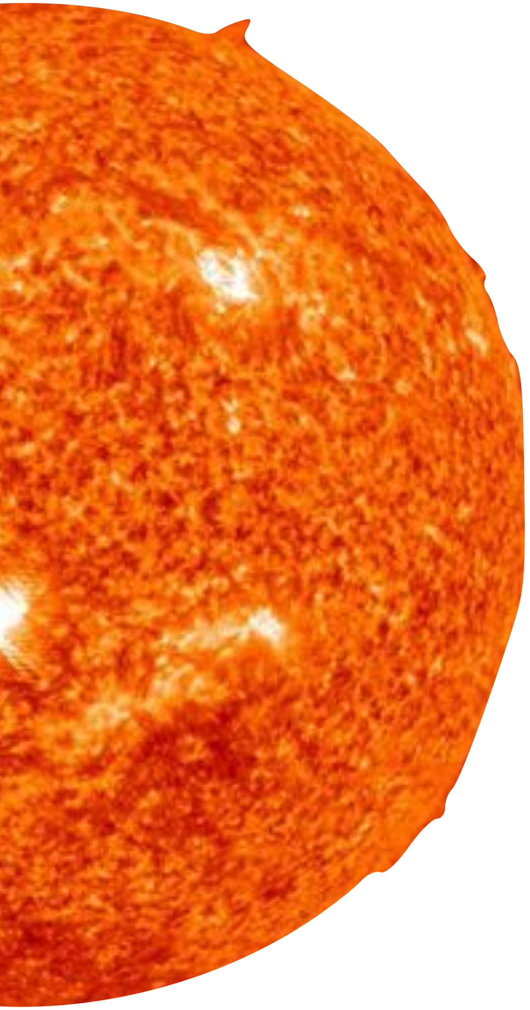

Primakoff Process

- classic axion production mechanism
- generates axions with solar core thermal (x-ray) spectrum

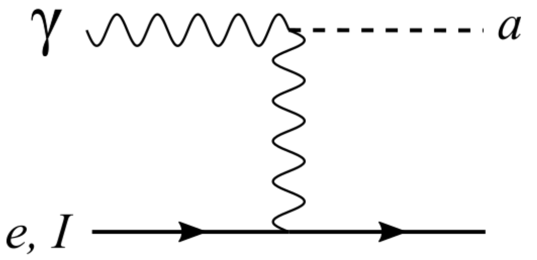

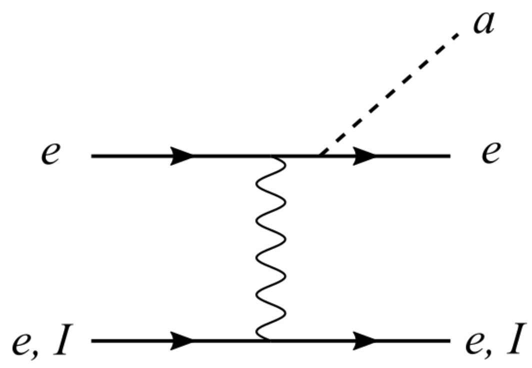

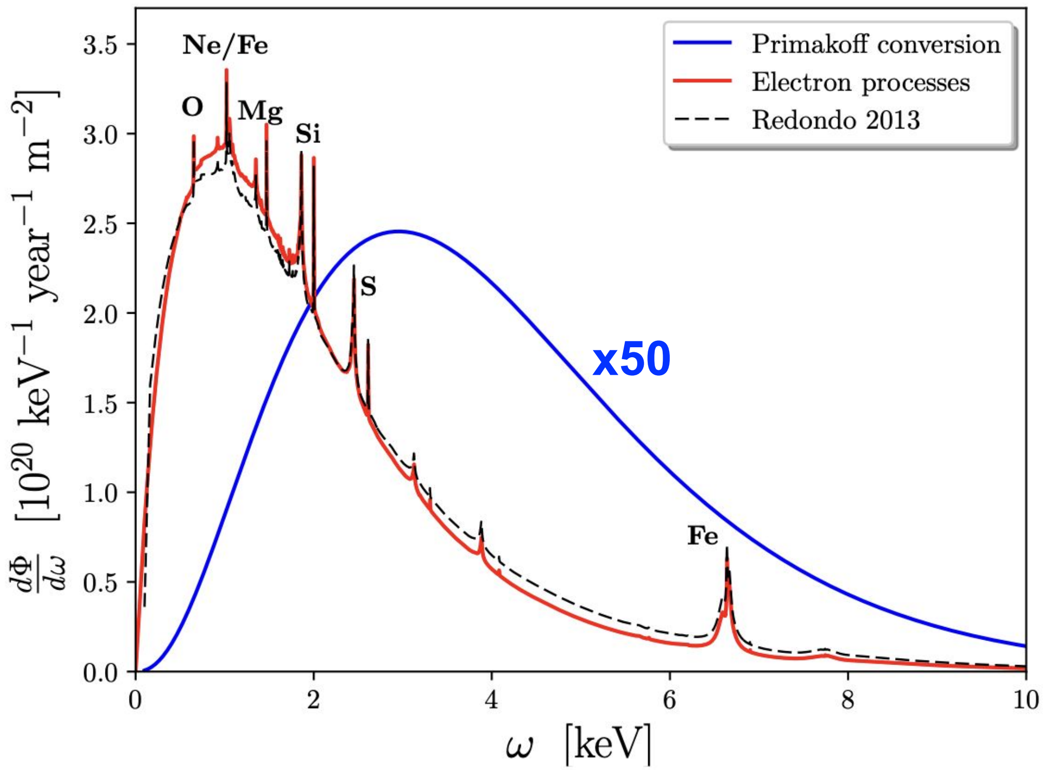

Phys. Rev. D 100, 123020

"ABC" solar axion production channels

- model dependent axion-electron coupling
- spectrum includes elemental features

Solar Axion Origins

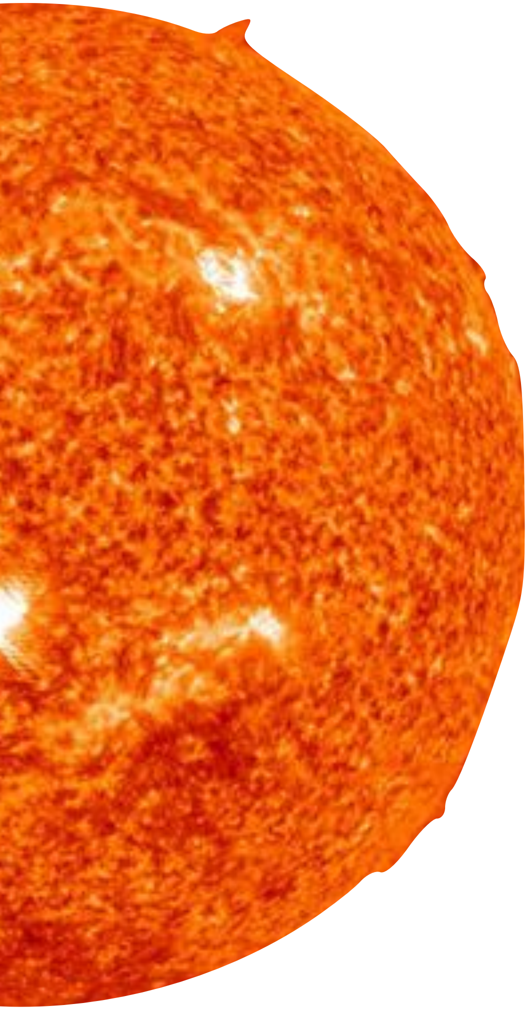

Primakoff Process

- classic axion production mechanism
- generates axions with solar core thermal (x-ray) spectrum

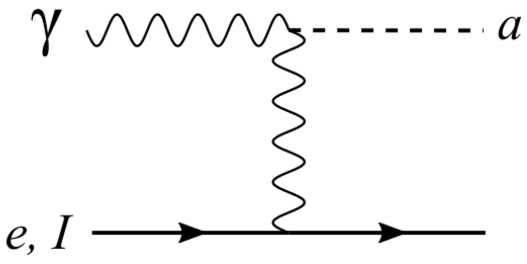

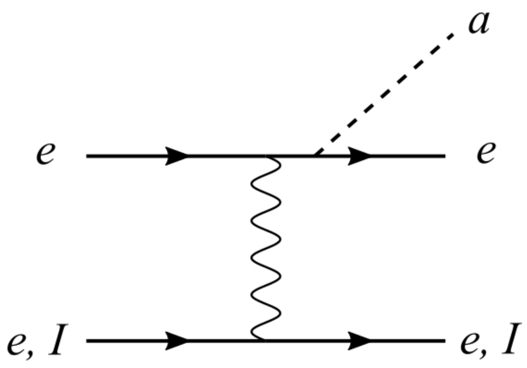

"ABC" solar axion production channels

- model dependent axion-electron coupling
- spectrum includes elemental features

Other solar axion production mechanisms

- axion-nucleon coupling (model dependent)
- axion production in the macroscopic solar magnetic field
- axion-plasmon conversion channels

[Phys. Rev. D 102, 123024](#)
[Phys. Rev. D 101, 123004](#)

Solar Axion Origins

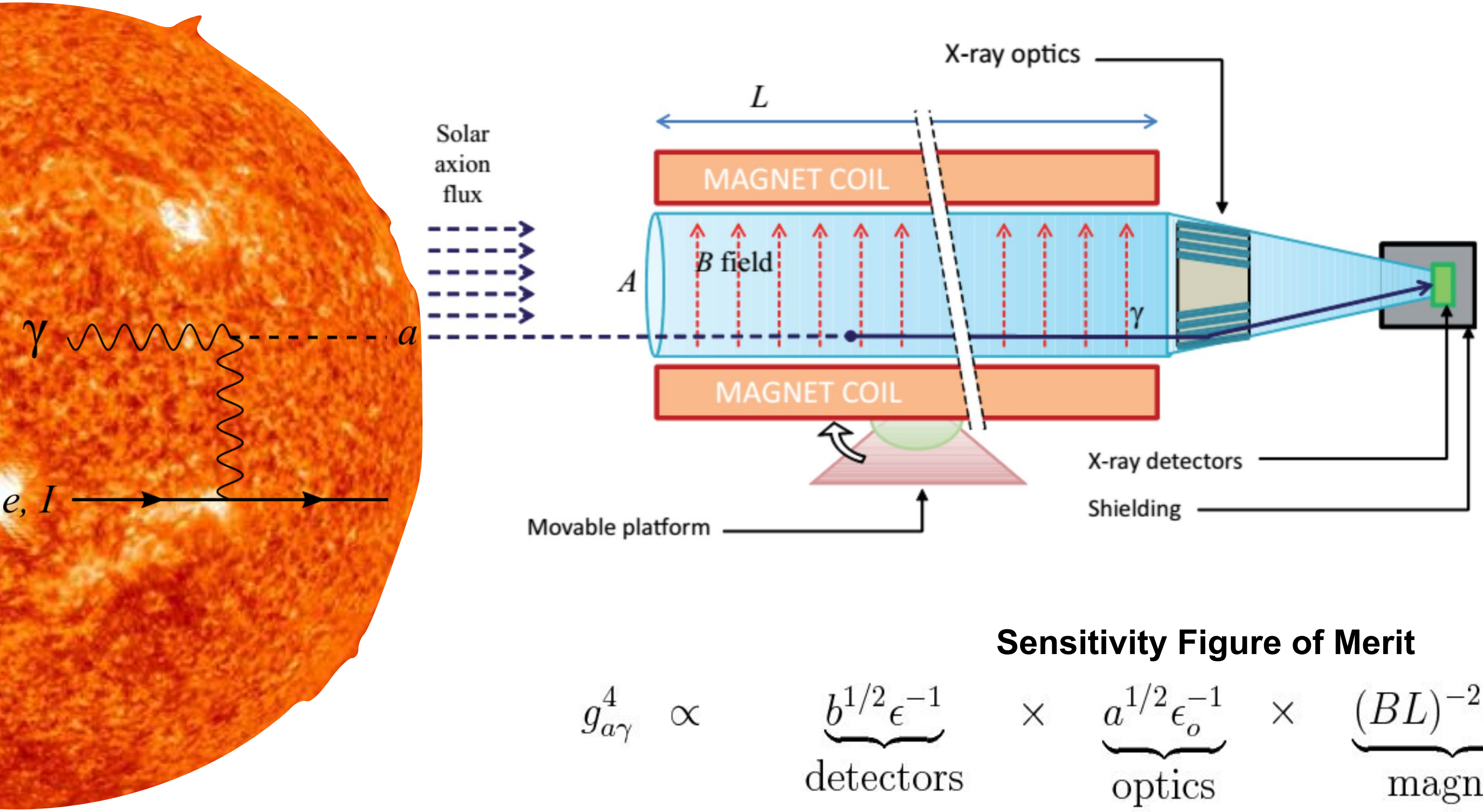

b → normalized detector background
a → detector focal spot size
B → magnetic field strength
L → magnetic field length
A → cross sectional area
ϵ, ϵ_o → detector, optics efficiencies

Sensitivity Figure of Merit

$$g^4_{a\gamma} \propto \underbrace{b^{1/2}\epsilon^{-1}}_{\text{detectors}} \times \underbrace{a^{1/2}\epsilon_o^{-1}}_{\text{optics}} \times \underbrace{(BL)^{-2}A^{-1}}_{\text{magnet}} \times \underbrace{t^{-1/2}}_{\text{exposure}}$$

Vogel, J.K., Irastorza, I.G. (2023). Solar Production of Ultralight Bosons. In: The Search for Ultralight Bosonic Dark Matter

International AXion Observatory

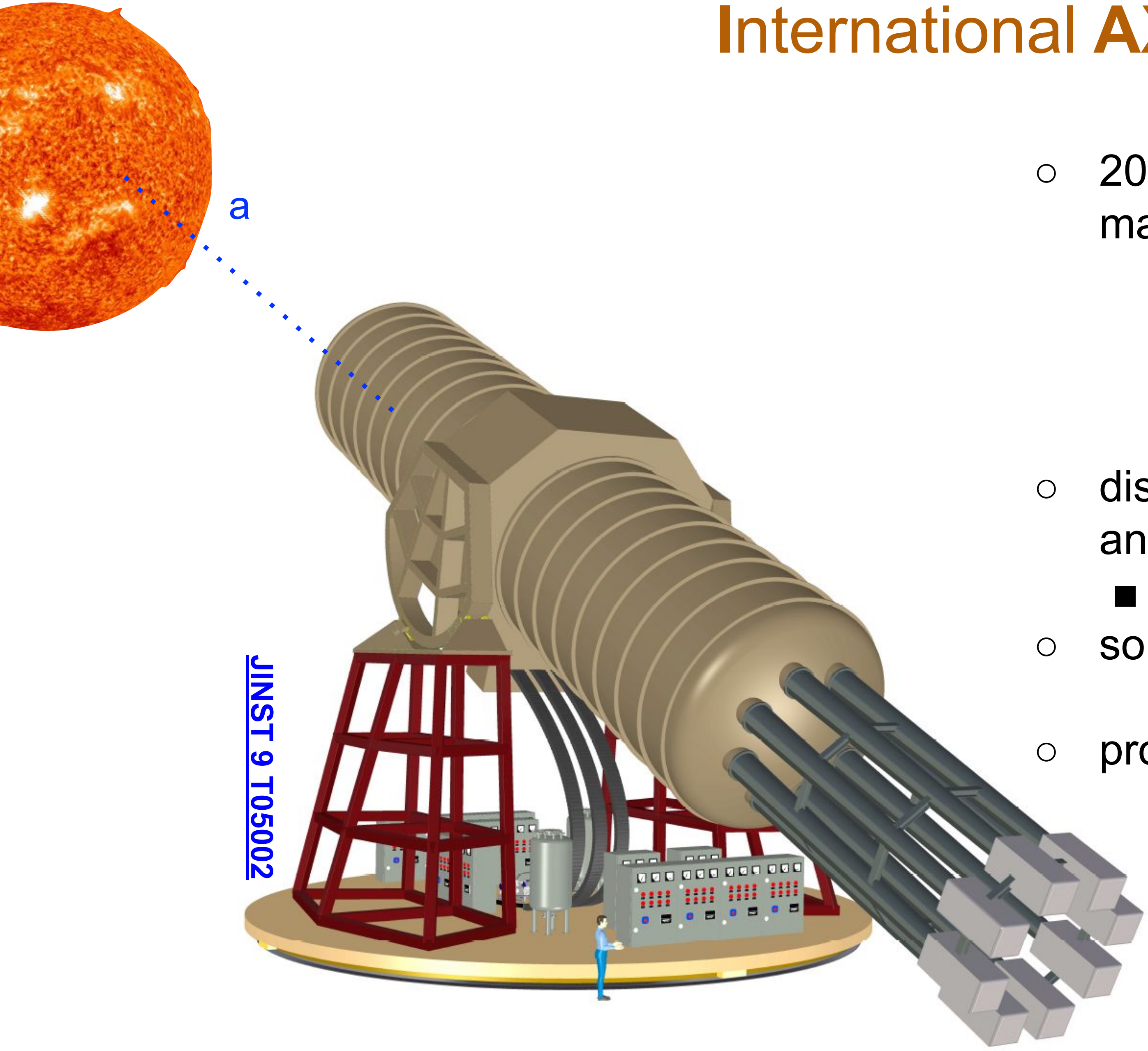

- 20 meter-long, purpose-built, superconducting magnets with 8 separate bores
  - **$B^2 L^2 A \sim 6200\ T^2 m^4$**
  - 300 times the value of CAST, the most sensitive axion helioscope in operation
    - see next talk by Serkant Cetin
- distinct detection lines allows parallel development and implementation of novel detector technology
  - yesterday’s talk by Loredana Gastaldo
- solar-tracking structure to allow for 50% duty cycle

- proposed construction site: **DESY, Hamburg**

BabyIAXO: a prototype with discovery potential

JHEP05(2021)137

- 10 meter superconducting magnet with two bores to support two separate detector lines
  - **$B^2 L^2 A \sim 325\ T^2 m^4$** (x 10 CAST)
- complementary detector development (need very high efficiency, ultra-low background): Micromegas TPC baseline + shielding + veto
- X-ray optics: 1 from ESA XMM Newton, 1 custom optic in development
- site preparation and in-situ background assessment already underway in the **HERA South Hall at DESY, Hamburg (pictured)**

BabyIAXO: a prototype with discovery potential

JHEP05(2021)137

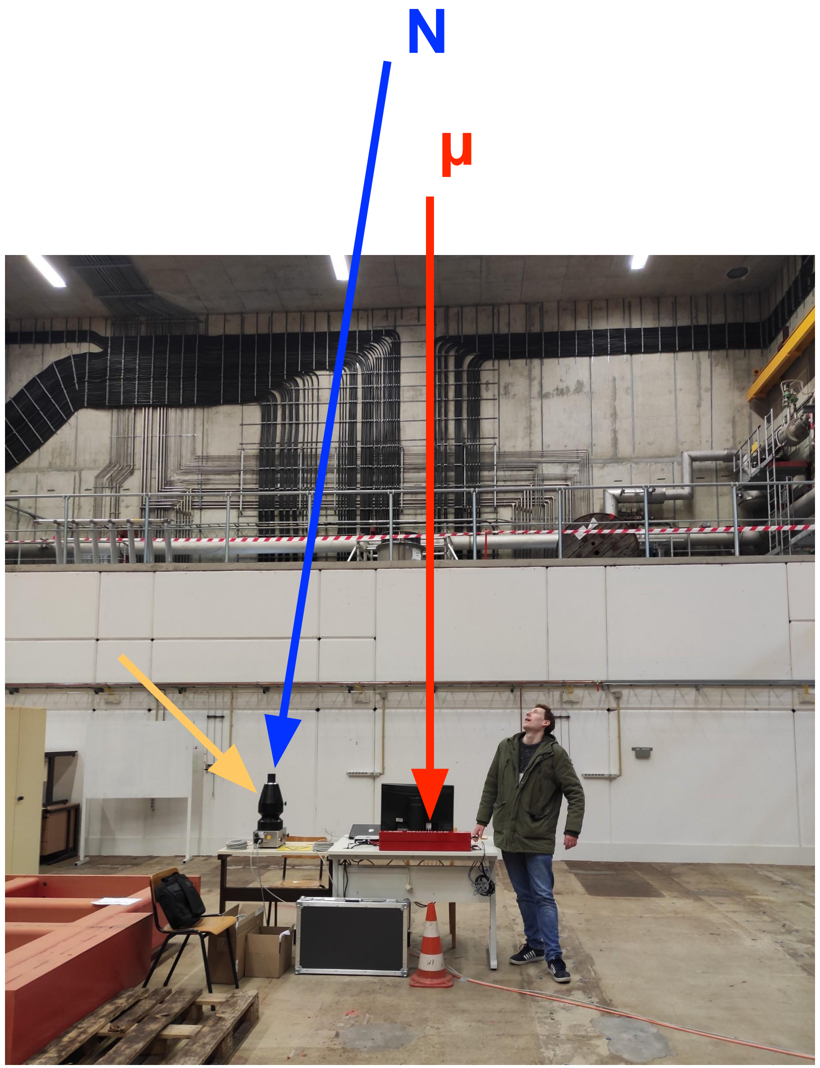

IAXO and BabyIAXO:

Broadband Searches of the Axion-Photon Parameter Space

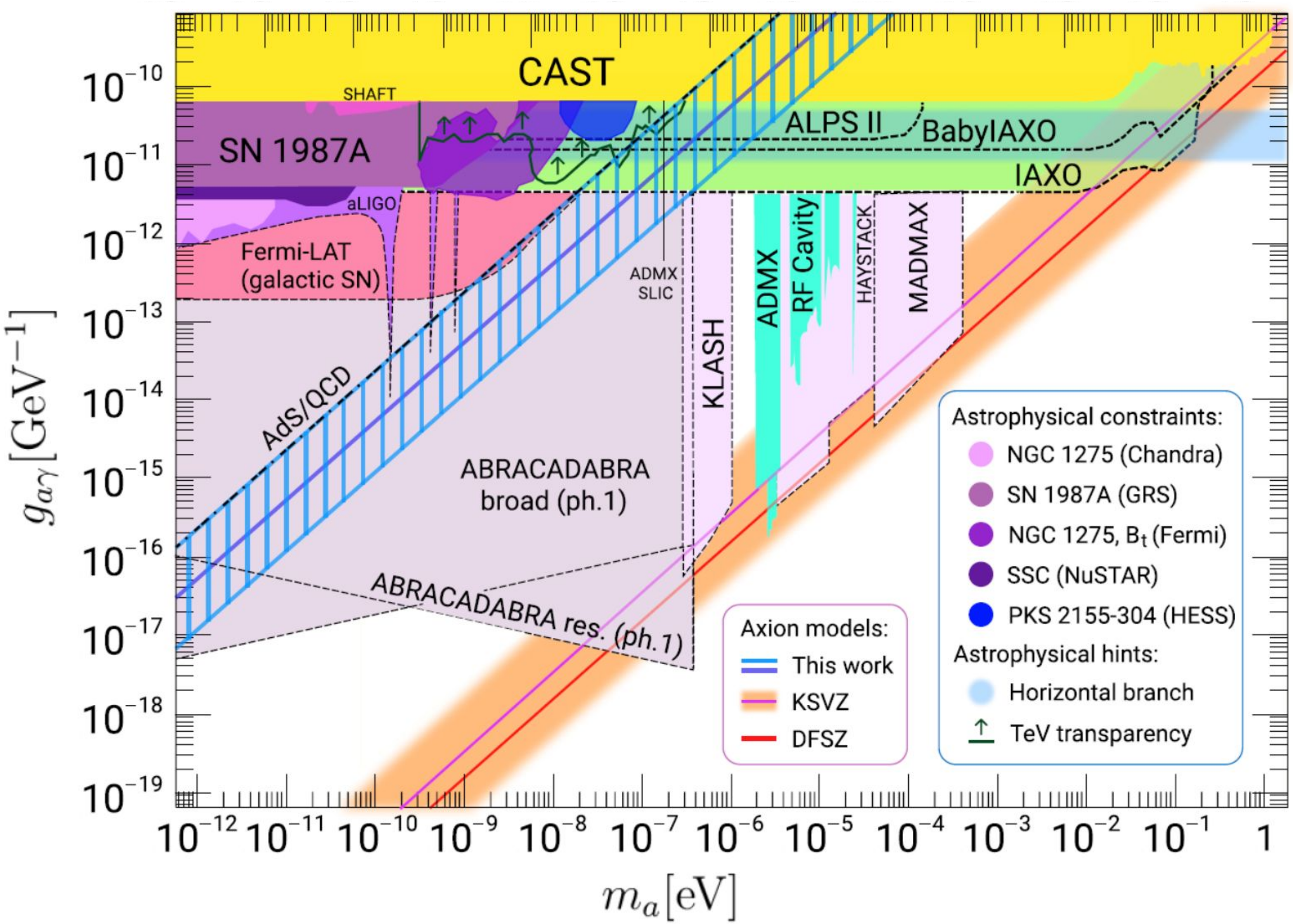

Sokolov-Ringwald: JHEP06(2021)123

ALPS II

A Resonantly Enhanced LSW Experiment

Light-Shining-Through-a-Wall Concept

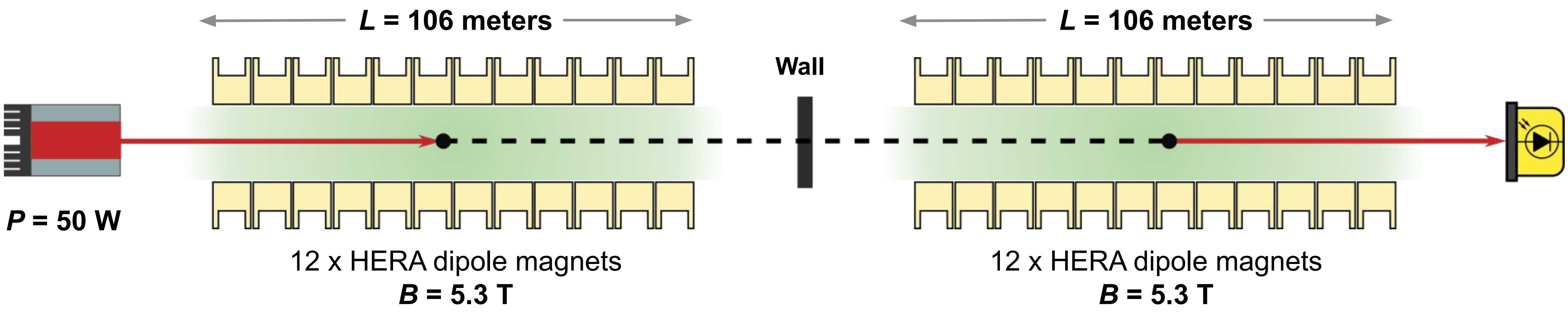

$$P_{\gamma\to a\to\gamma} \approx \frac{1}{16}(g_{a\gamma\gamma}BL)^4$$

$$n_{\text{signal}} \approx n_{\text{laser}}\frac{1}{16}(g_{a\gamma\gamma}BL)^4$$

$$n_{\text{signal}} \approx \frac{1\ \text{photon}}{115{,}000\ \text{yr}}\cdot\left(\frac{P_{\text{laser}}}{50\ \text{W}}\right)\left(\frac{g_{a\gamma\gamma}}{2\times10^{-11}\ \text{GeV}^{-1}}\right)^4\left(\frac{B}{5.3\ \text{T}}\right)^4\left(\frac{L}{106\ \text{m}}\right)^4$$

Design of the ALPS II Optical System (2022). *Physics of the Dark Universe, 35*: 100968. doi:10.1016/j.dark.2022.100968

ALPS II: a Resonantly Enhanced LSW Design

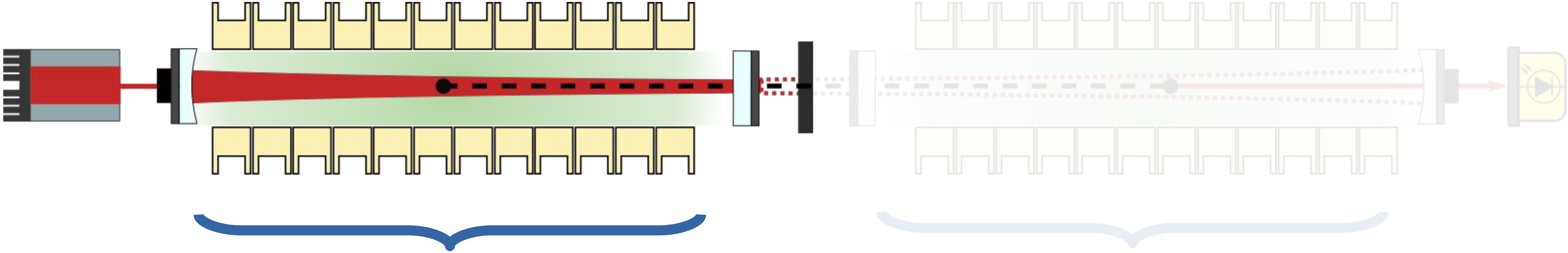

Production Cavity (PC)

- Builds up the power of the light circulating in the magnetic field
- Increases the flux of axion-like particles flowing through the wall

$$n_{\mathrm{laser}} \rightarrow n_{\mathrm{PC}}$$

Design objective: **150 kW circulating power (n_{PC} ~ 10^{24} /s)**

Regeneration Cavity (RC)

- Electromagnetic component of the ALP field is resonantly enhanced
- Improves the ALP-photon reconversion signal rate

$$n_{\mathrm{signal}} \rightarrow n_{\mathrm{signal}} \times \beta_{\mathrm{RC}}$$

Design objective: **β_{RC} > 10,000 power build-up**

ALPS II: a Resonantly Enhanced LSW Design

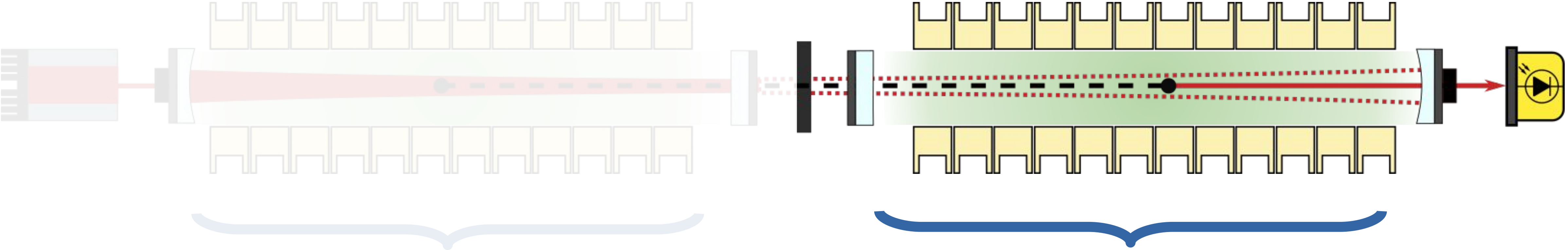

Production Cavity (PC)

- Builds up the power of the light circulating in the magnetic field
- Increases the flux of axion-like particles flowing through the wall

$$n_{\text{laser}} \rightarrow n_{\text{PC}}$$

Design objective: **150 kW circulating power (n_{PC} ~ 10^{24} /s)**

Regeneration Cavity (RC)

- Electromagnetic component of the ALP field is resonantly enhanced
- Improves the ALP-photon reconversion signal rate

$$n_{\text{signal}} \rightarrow n_{\text{signal}} \times \beta_{\text{RC}}$$

Design objective: **β_{RC} > 10,000 power build-up**

ALPS II: a Resonantly Enhanced LSW Design

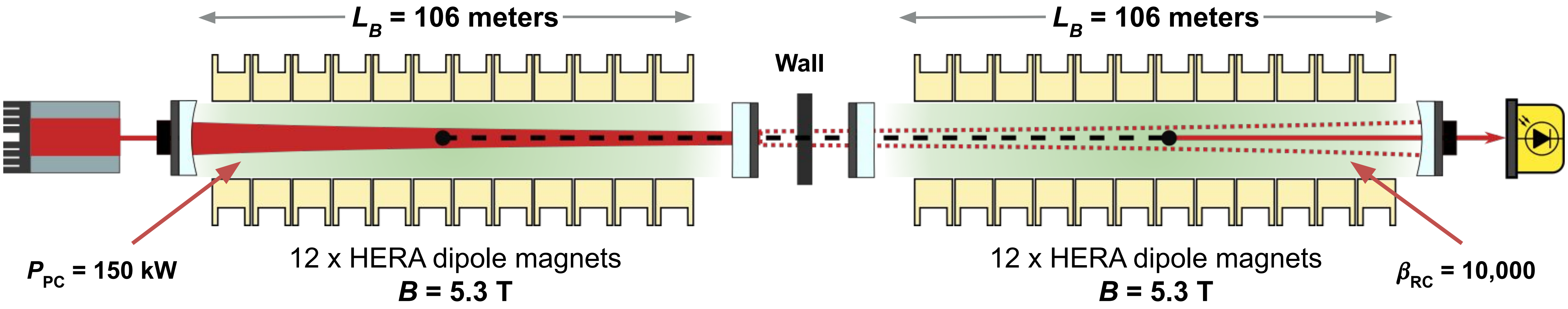

$$n_{\rm signal} \approx n_{\rm PC}\,\beta_{\rm RC}\,\frac{\eta}{16}\,(g_{a\gamma\gamma}BL)^4$$

For the ALPS II design parameters:

$$n_{\rm signal} \approx \frac{1\ \text{photon}}{37\ \text{hours}} \cdot \left(\frac{P_{\rm PC}}{150\ \text{kW}}\right)\left(\frac{\beta_{\rm RC}}{10{,}000}\right)\left(\frac{\eta}{0.9}\right)\left(\frac{g_{a\gamma\gamma}}{2\times10^{-11}\ \text{GeV}^{-1}}\right)^4\left(\frac{B}{5.3\ \text{T}}\right)^4\left(\frac{L}{106\ \text{m}}\right)^4$$

Design of the ALPS II Optical System (2022). *Physics of the Dark Universe, 35*: 100968. doi:10.1016/j.dark.2022.100968

ALPS II: a Resonantly Enhanced LSW Design

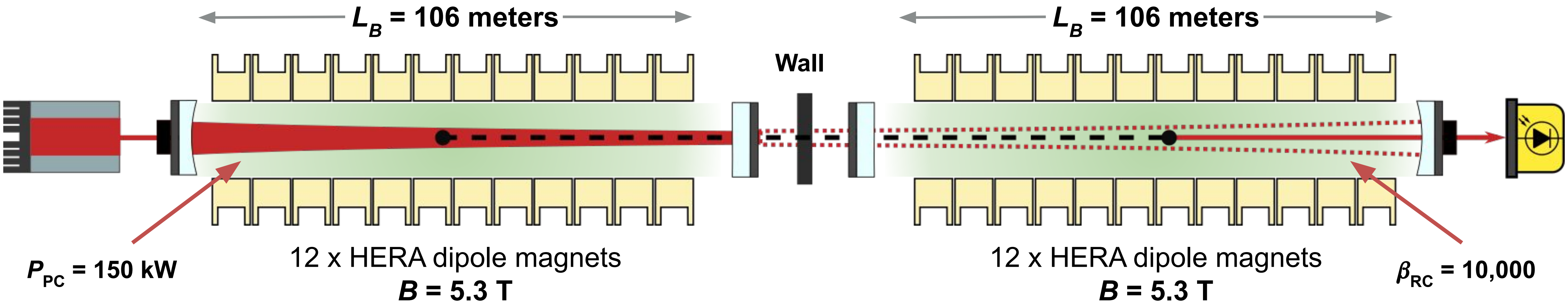

ALPS II Technology

1. Magnets and Infrastructure
2. Optical Systems
3. Control Systems
4. Ultra-low power Detector

$$n_{\text{signal}} \approx \frac{1\ \text{photon}}{37\ \text{hours}} \cdot \left(\frac{P_{\text{PC}}}{150\ \text{kW}}\right)\left(\frac{\beta_{\text{RC}}}{10{,}000}\right)\left(\frac{\eta}{0.9}\right)\left(\frac{g_{a\gamma\gamma}}{2\times10^{-11}\ \text{GeV}^{-1}}\right)^4\left(\frac{B}{5.3\ \text{T}}\right)^4\left(\frac{L}{106\ \text{m}}\right)^4$$

Design of the ALPS II Optical System (2022). *Physics of the Dark Universe, 35*: 100968. doi:10.1016/j.dark.2022.100968

From Ciaran O'Hare: https://cajohare.github.io/AxionLimits/

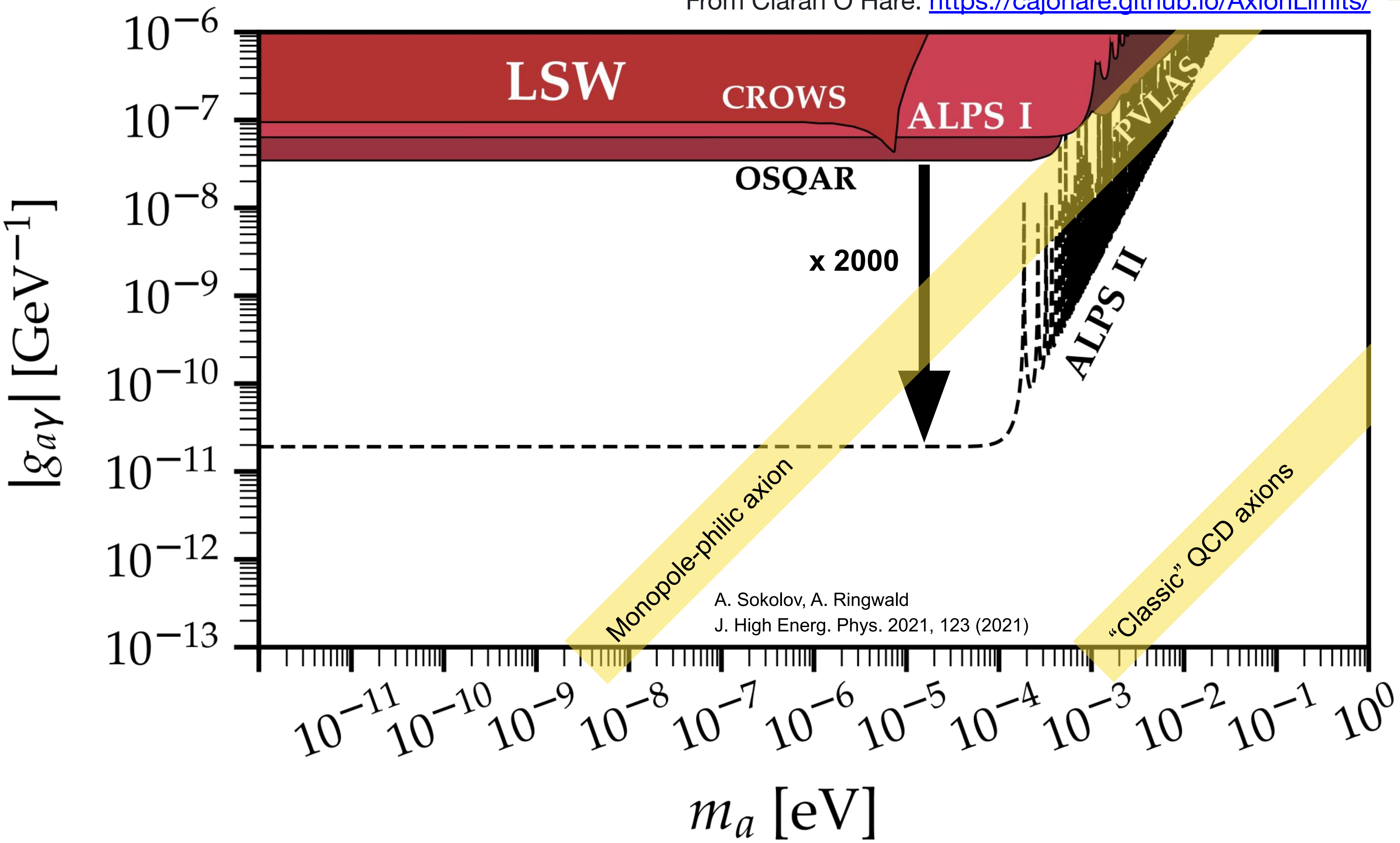

From Ciaran O'Hare: https://cajohare.github.io/AxionLimits/

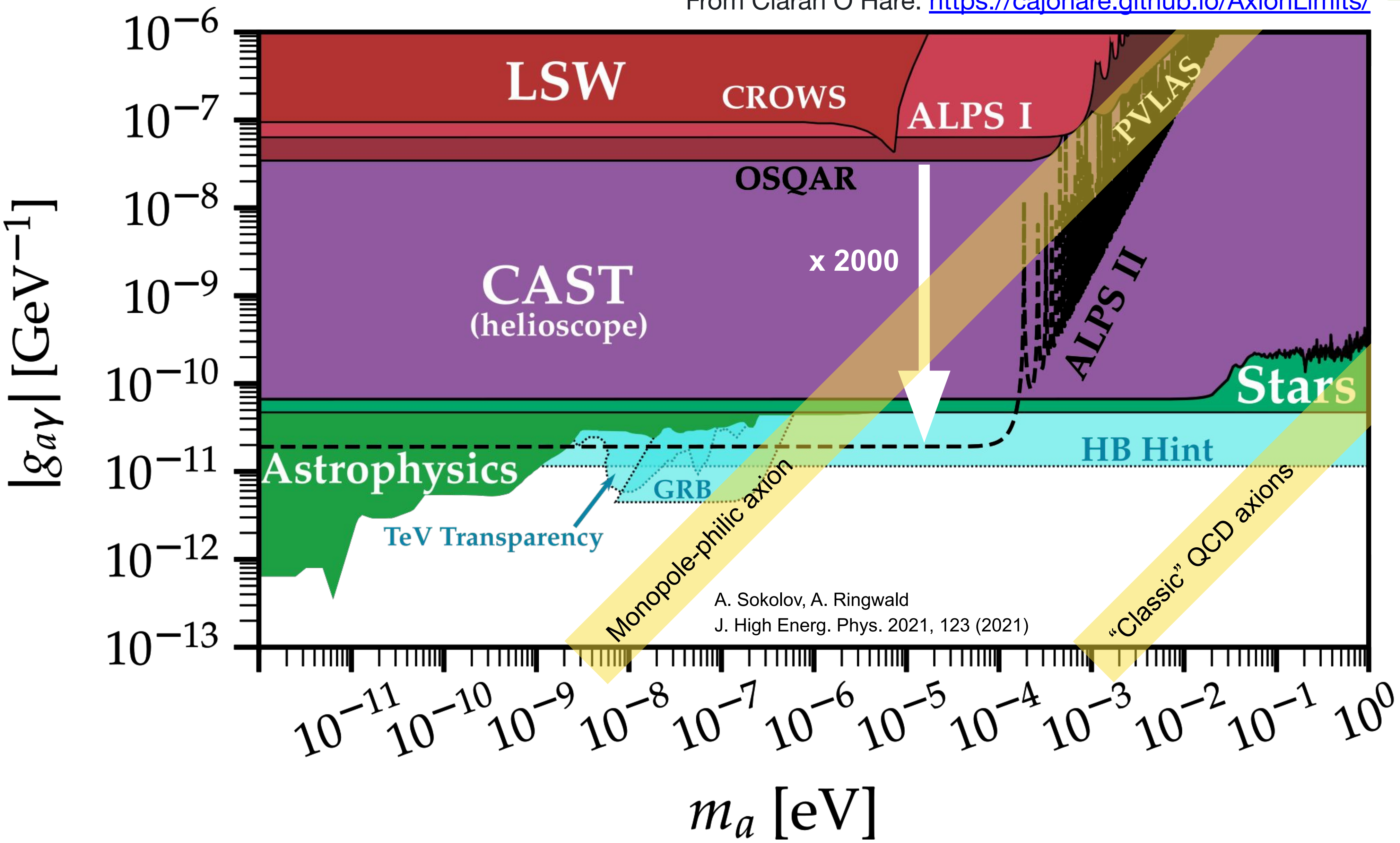

ALPS II Design for the First Science Run

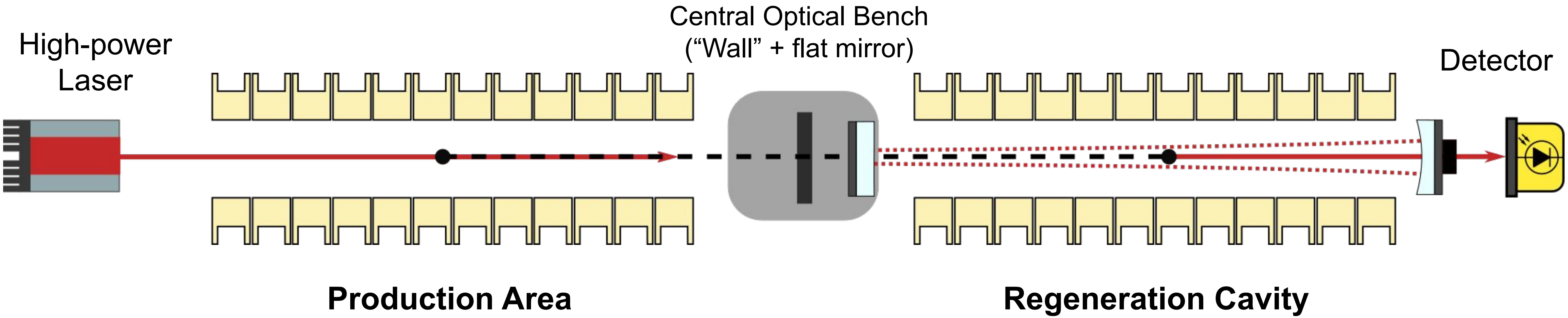

- simplified one-cavity design makes frequency and alignment control simpler for the initial science run
- 40x more incident HPL light on the COB to better identify stray light sources
- will nevertheless produce the most sensitive model-independent / laboratory-based ALP search

October 2020

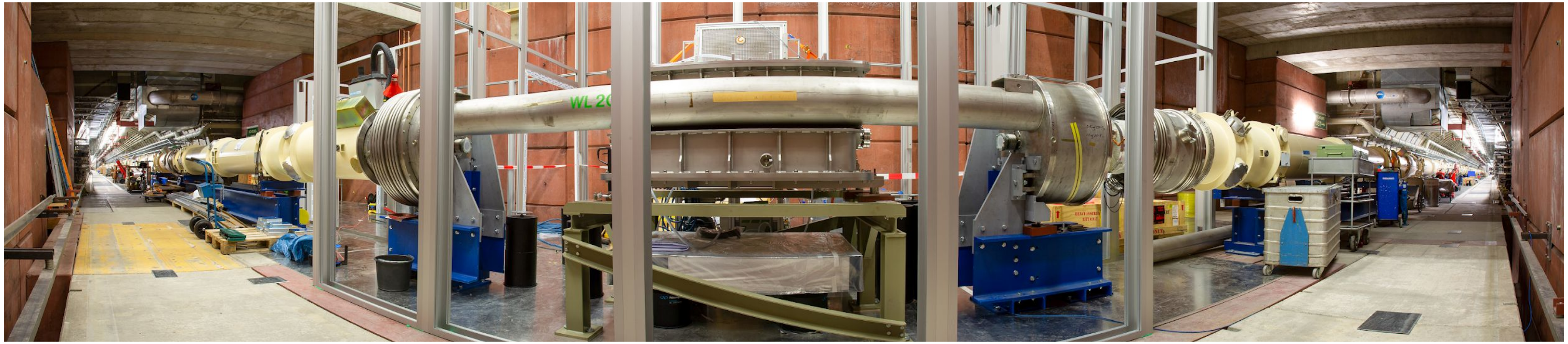

February 2021

Present

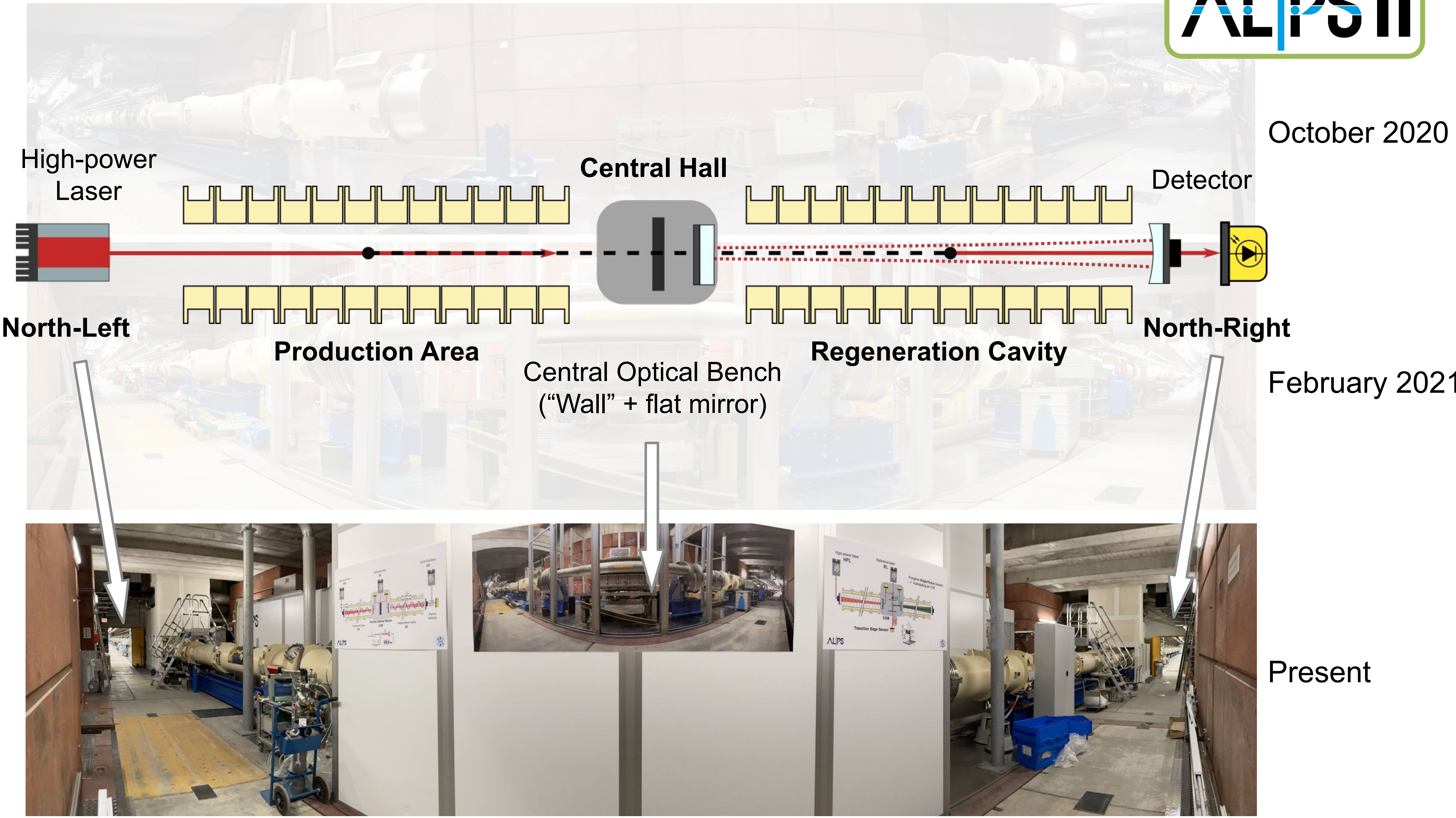
October 2020
High-power
Laser
Central Hall
Detector
North-Left
Production Area
Central Optical Bench
(“Wall” + flat mirror)
Regeneration Cavity
North-Right
February 2021
Present

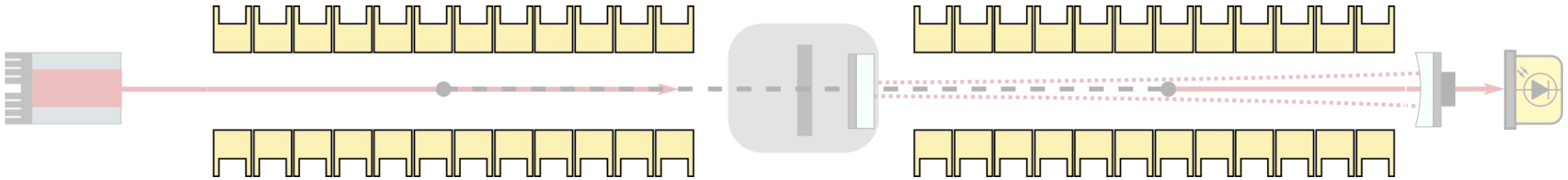

Magnets

- 24 (2 x 12) repurposed HERA dipole magnets successfully straightened, current- and quench-tested, aligned and operational
  - 5.3 T field strength at nominal 5700 A
  - Expanded beam tube aperture allows for longer optical cavities → improved sensitivity

Albrecht, C., Barbanotti, S., Hintz, H. *et al. EPJ Techn Instrum* 8, 5 (2021).

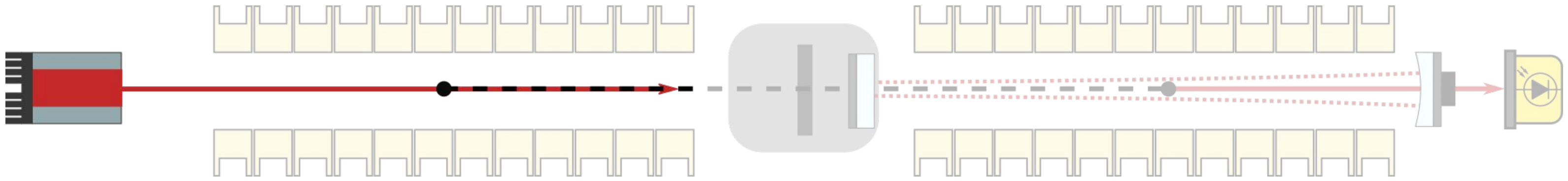

Optics

High Power Laser (HPL) System

- stable operation at 40 W of 1064 nm light

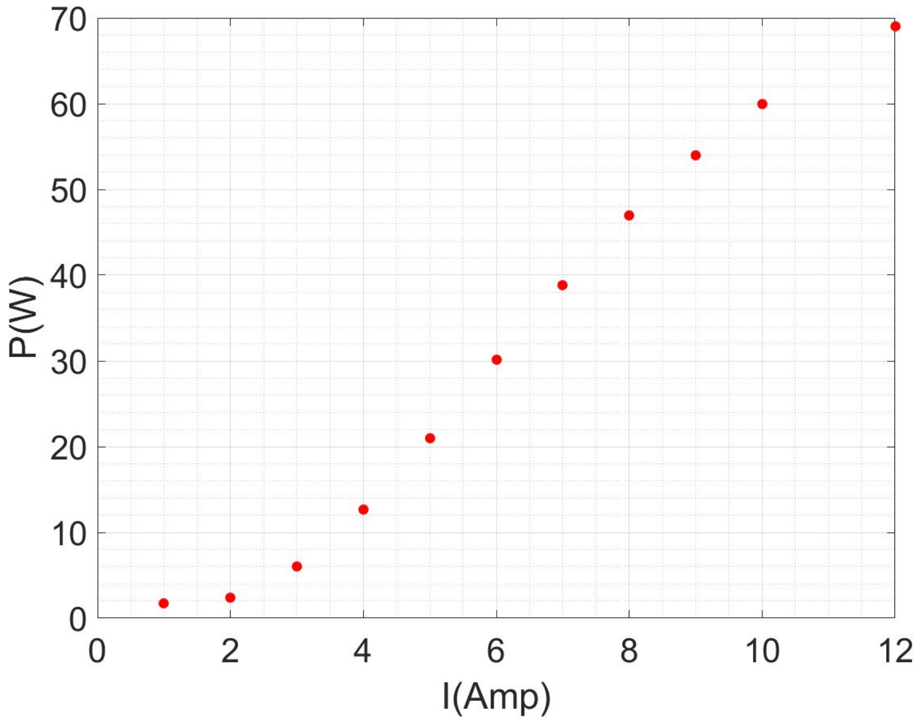

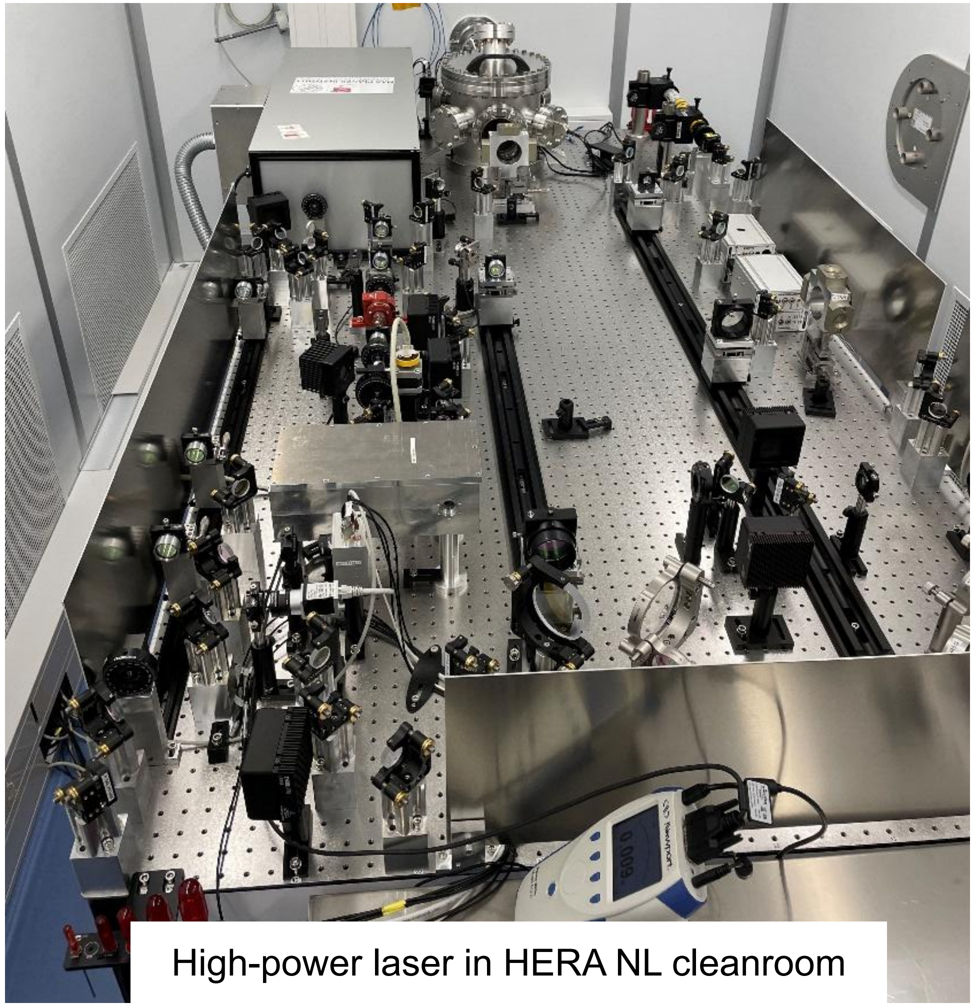

High-power laser in HERA NL cleanroom

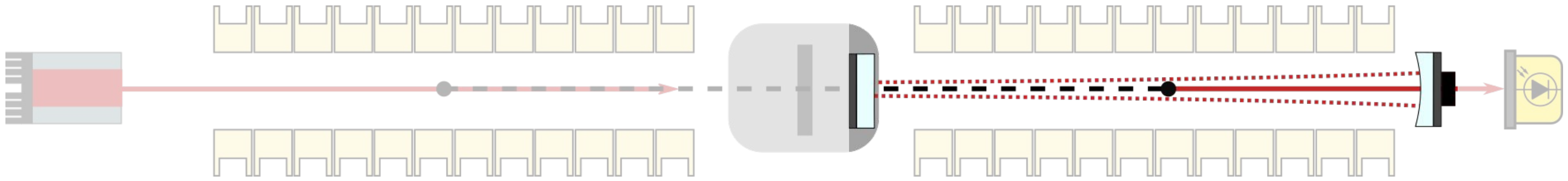

Optics

High Power Laser (HPL) System

- stable operation at 40 W of 1064 nm light

Regeneration Cavity

- Half-confocal, 122 meters long
- Cavity storage time: **7 ms (world record)**
  - **power build-up: 7,700**

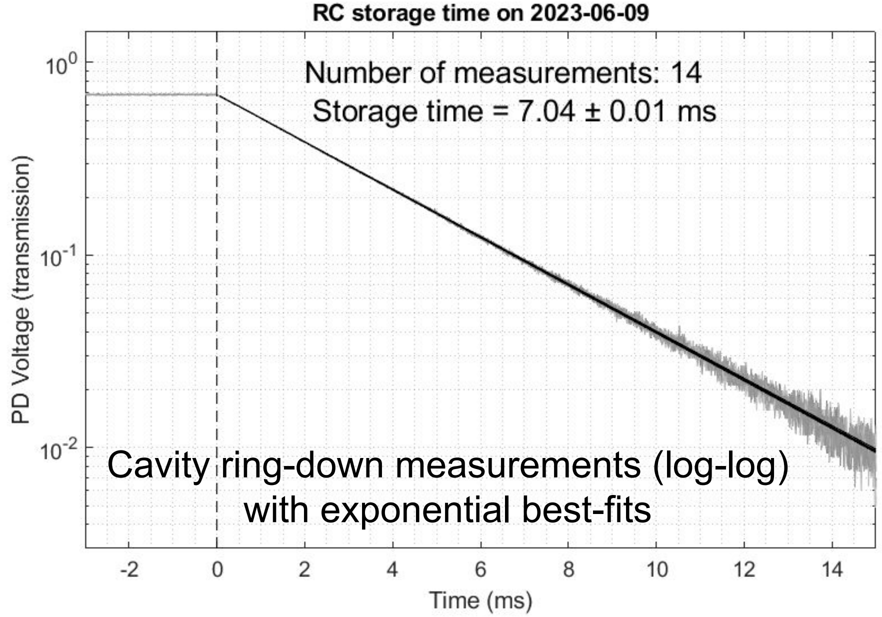

Cavity ring-down measurements (log-log) with exponential best-fits

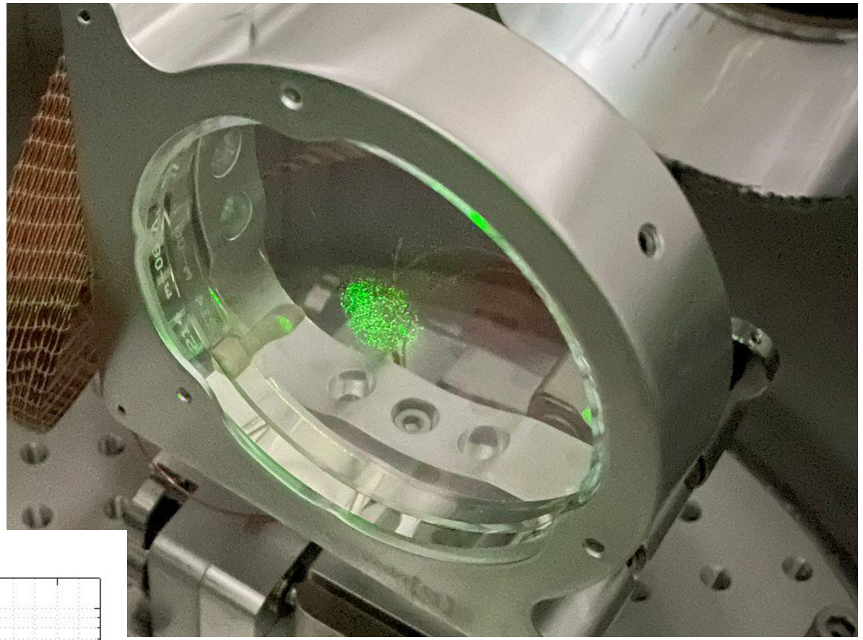
RC 3” curved end mirror in vacuum tank (illuminated by green alignment laser)

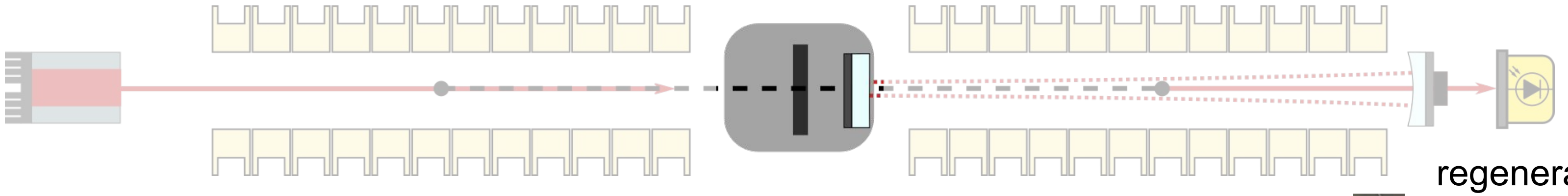

Optics

High Power Laser (HPL) System
- stable operation at 40 W of 1064 nm light

Regeneration Cavity
- Half-confocal, 122 meters long
- Cavity storage time: **7.04 ms (world record)**
  - **power build-up: 7,700**

Central Optical Bench
- Ensures passive alignment between PC and RC
- Light-tight housings to reduce stray light
- Remotely operable shutter serving as the “wall”

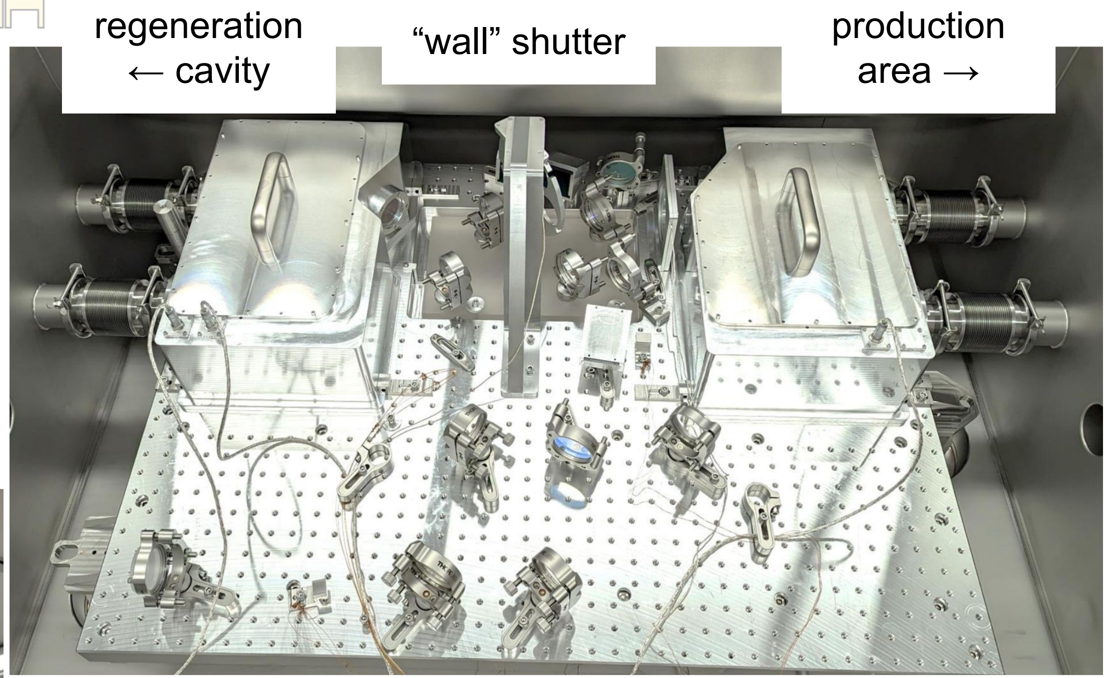

Installing pre-aligned COB into vacuum tank

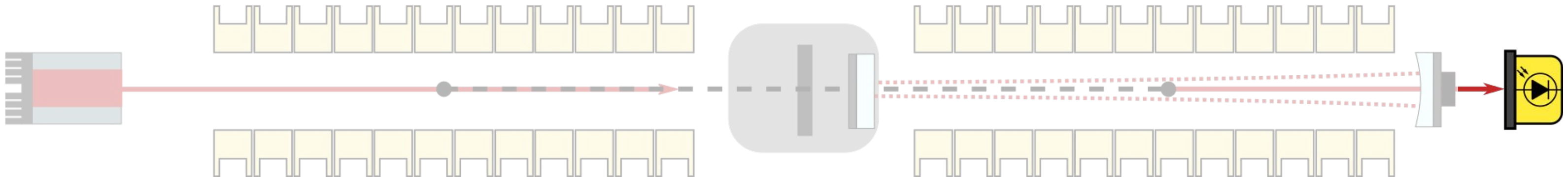

Optics

High Power Laser (HPL) System
- stable operation at 40 W of 1064 nm light

Regeneration Cavity
- Half-confocal, 122 meters long
- Cavity storage time: **7.04 ms (world record)**
  - **power build-up: 7,700**

Central Optical Bench
- Ensures passive alignment between PC and RC
- Light-tight housings to reduce stray light
- Remotely operable shutter serving as the “wall”

Heterodyne Interferometric Detector
- Coherent detection of extremely weak fields
- Relies on high relative phase stability over long periods

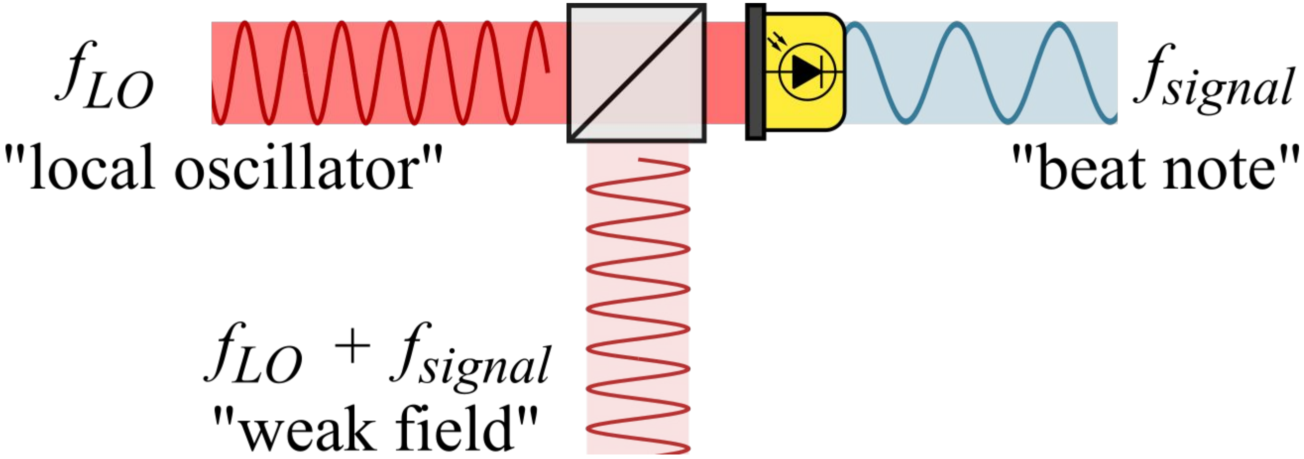

Frequency and Phase Control

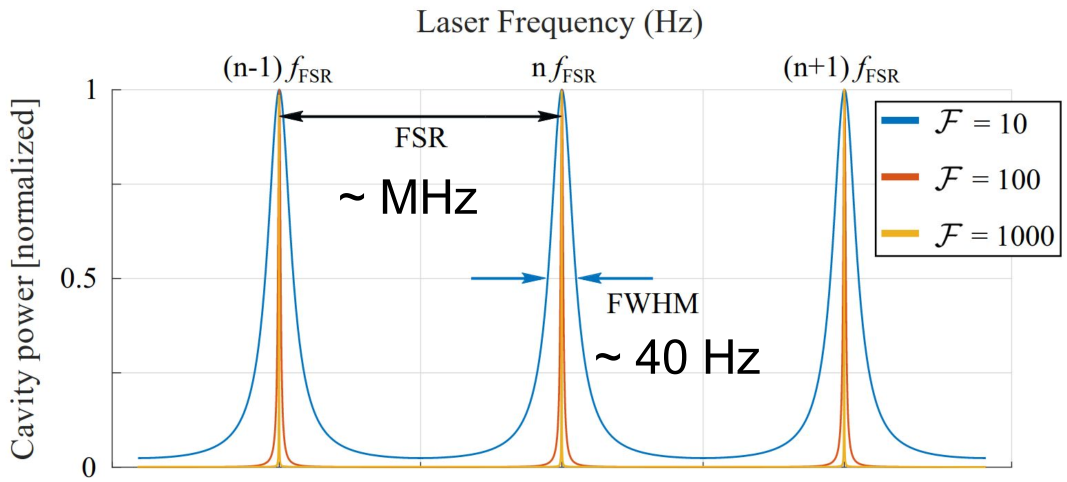

Resonant Enhancement

- Power build-up only when the HPL frequency is resonant within the RC
- Cannot directly interfere the HPL and LO fields → too much stray light! Need **blind control!**

$$\omega_{HPL} = \omega_{LO} + \Omega_{signal}$$

Production Area | **Regeneration Cavity**

$$\Omega_{signal} = n \times FSR$$

Frequency and Phase Control

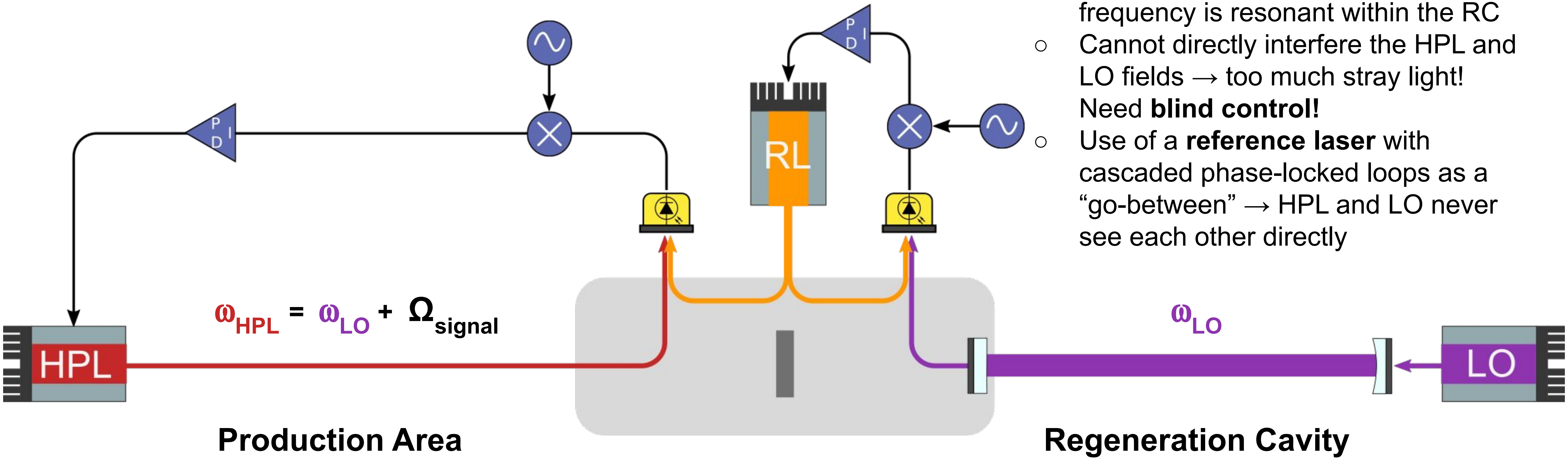

Resonant Enhancement

- Power build-up only when the HPL frequency is resonant within the RC
- Cannot directly interfere the HPL and LO fields → too much stray light! Need **blind control!**
- Use of a **reference laser** with cascaded phase-locked loops as a “go-between” → HPL and LO never see each other directly

Frequency and Phase Control

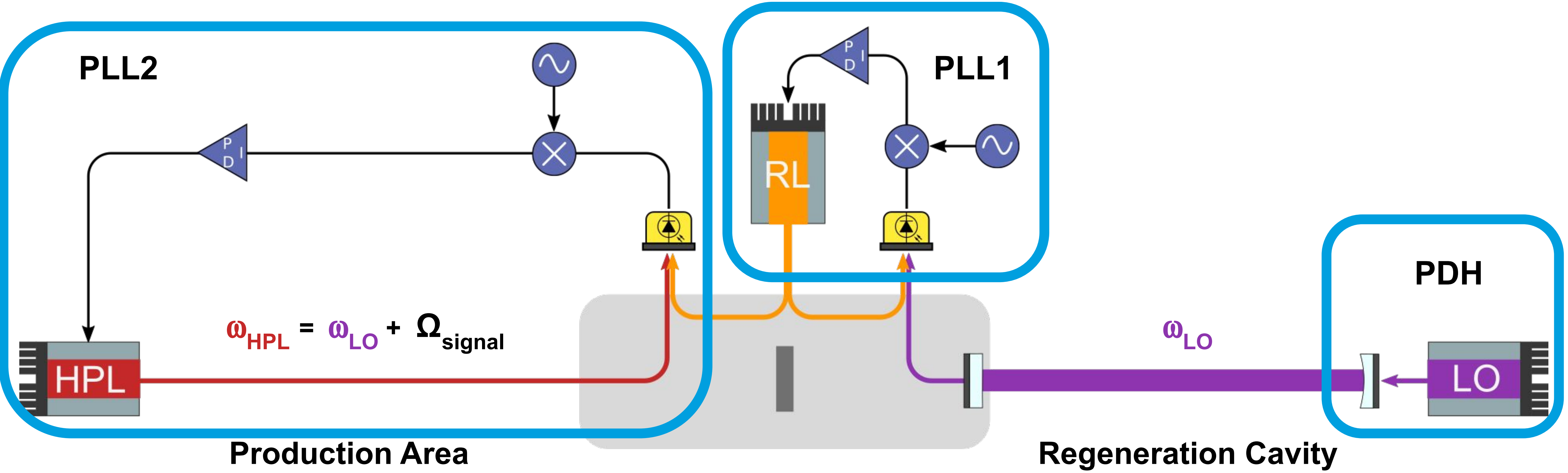

High-Power Laser ← PLL2 ← Reference Laser ← PLL1 ← Local Oscillator Laser ← PDH ← Regeneration Cavity

Frequency and Phase Control

Technical Achievements

- Local Oscillator stays locked to RC resonance for **day - week long periods**
- Reference Laser and High-Power Laser PLLs (PLL1&2) stay locked for **12+ hours**
- Overall control: high-power laser follows the local oscillator with a separation of 10’s of MHz to an accuracy of **sub-μHz** without directly seeing each other **over 2-week** measurement

$$\omega_{HPL} = \omega_{LO} + \Omega_{signal}$$

$$\Omega_{signal} = 24.45264600000(0)\ \text{MHz}$$

Frequency and Phase Control

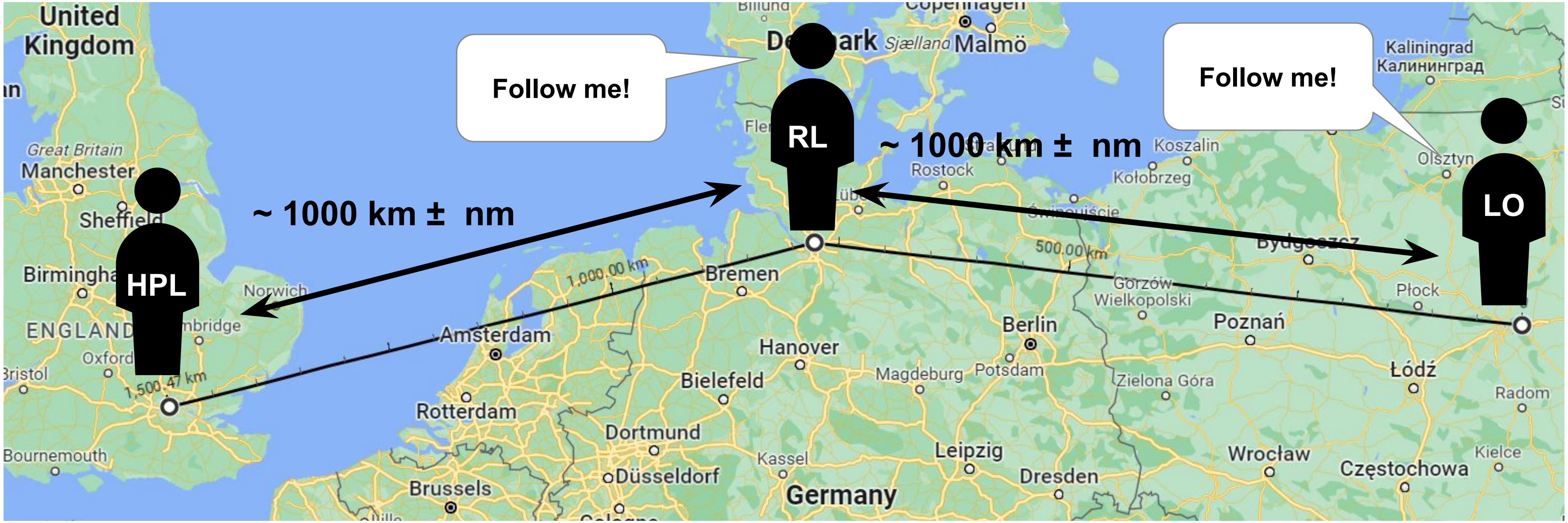

Frequency and Phase Control

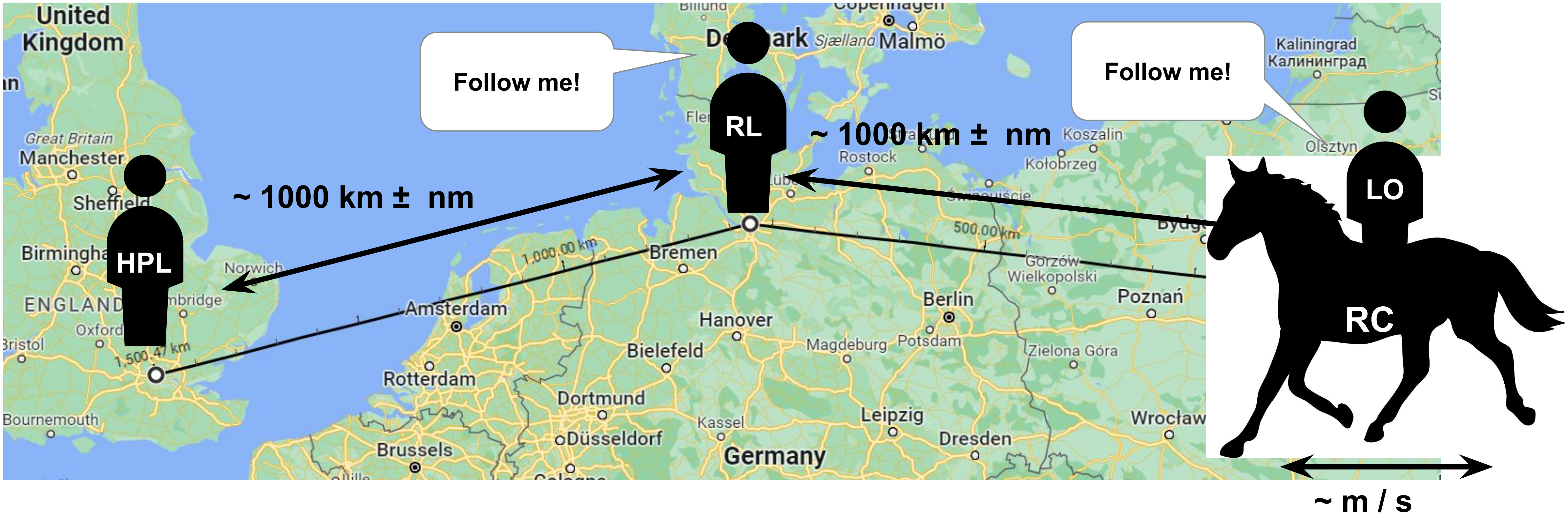

High-Power Laser ← PLL2 ← Reference Laser ← PLL1 ← Local Oscillator Laser ← PDH ← Regeneration Cavity

Frequency and Phase Control

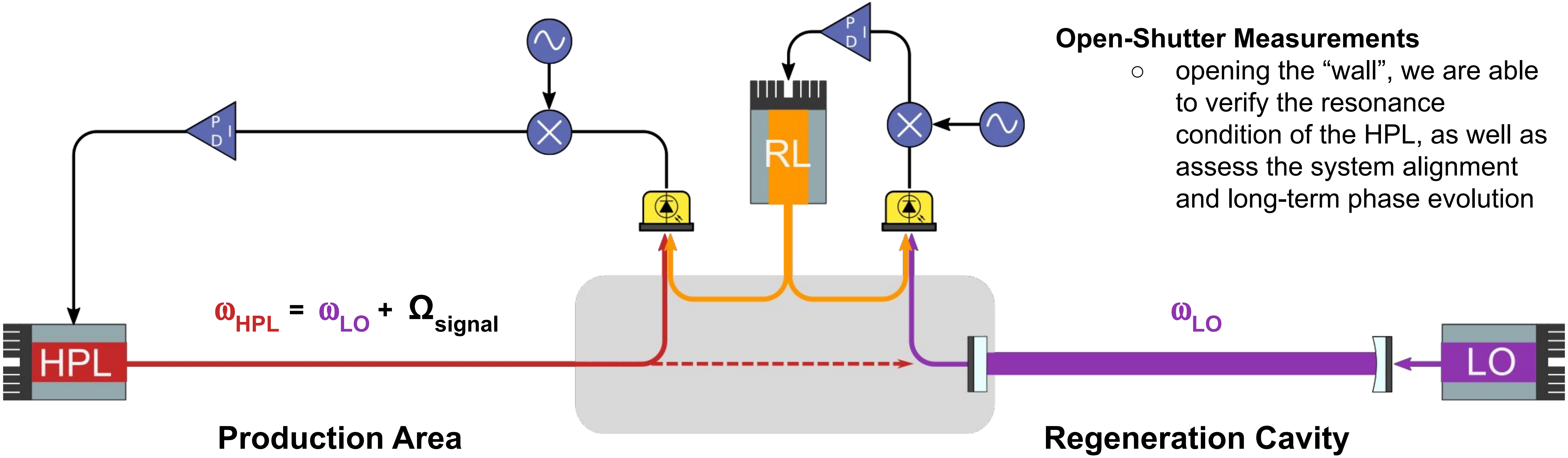

Open-Shutter Measurements

- opening the “wall”, we are able to verify the resonance condition of the HPL, as well as assess the system alignment and long-term phase evolution

Frequency and Phase Control

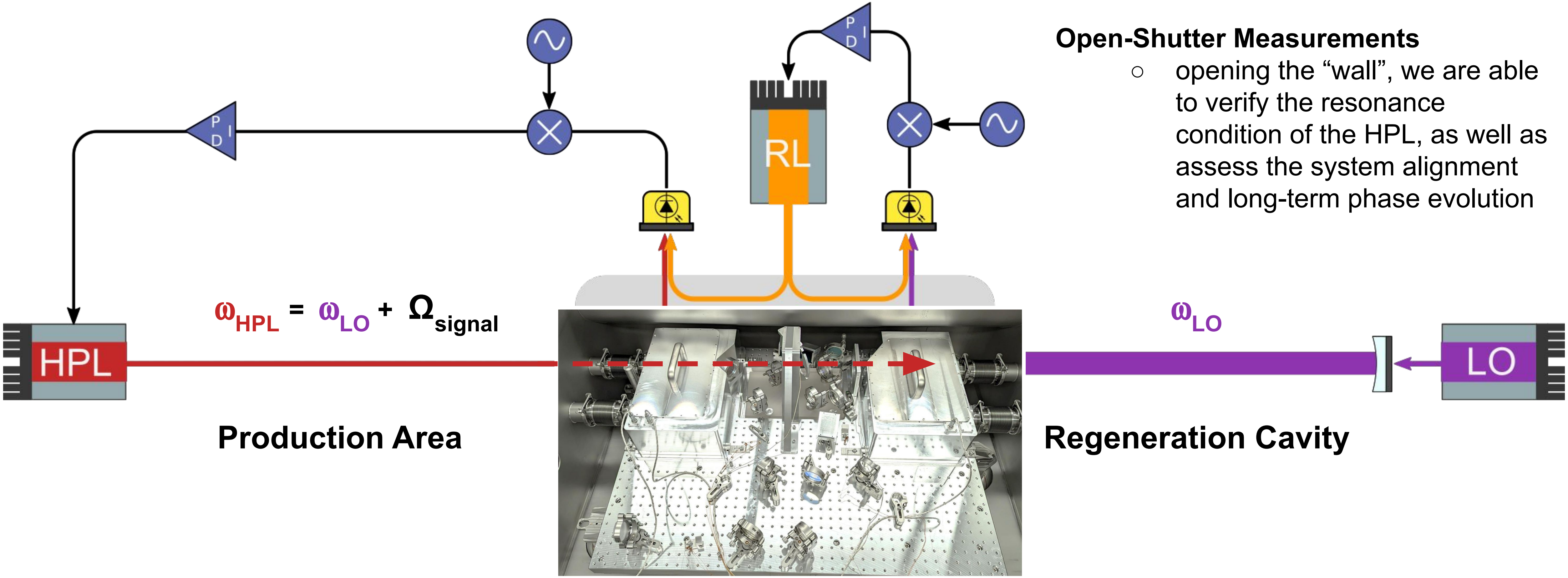

Open-Shutter Measurements

- opening the “wall”, we are able to verify the resonance condition of the HPL, as well as assess the system alignment and long-term phase evolution

Heterodyne Interferometric Detection

Heterodyne Interferometry

- interference beat-note between:
  1. *weak field* (regenerated photons from axions)
  2. strong *local oscillator* (additional laser)

  on a photodetector

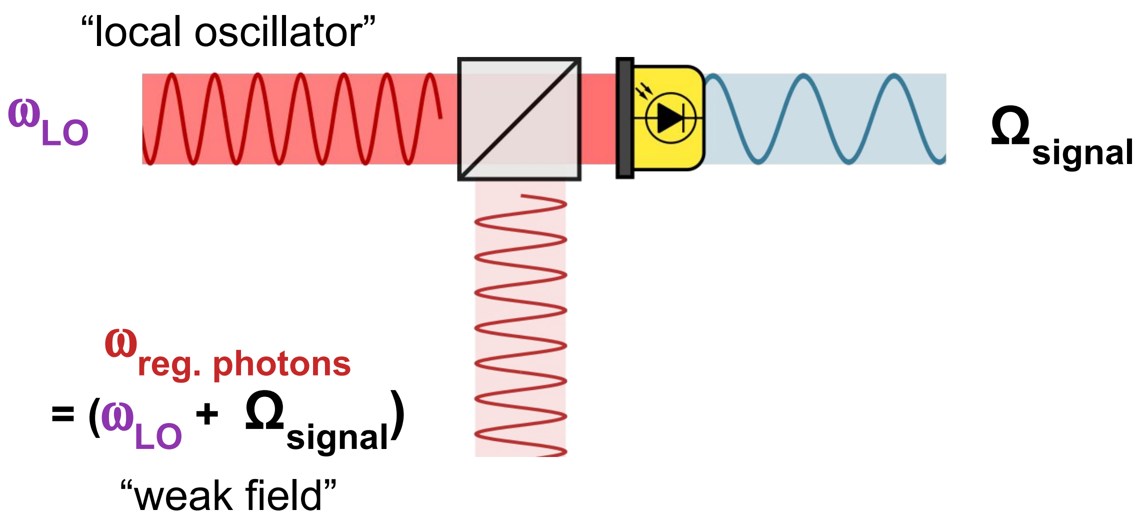

$$\left|\sqrt{P_{LO}}e^{i\omega_{LO}t} + \sqrt{P_{reg.\ photons}}e^{i[(\omega_{LO}+\Omega_{signal})t+\phi]}\right|^2$$

$$= \underbrace{P_{LO} + P_{reg.\ photons}}_{\text{D.C. terms}} + \underbrace{2\sqrt{P_{LO}P_{reg.\ photons}}\cos(\Omega_{signal}t + \phi)}_{\text{RF beatnote}}$$

Heterodyne Interferometric Detection

Heterodyne Interferometry

- interference beat-note between:
    1. *weak field* (regenerated photons from axions)
    2. strong *local oscillator* (additional laser)

  on a photodetector

- with *fixed frequency and phase offset*, detection is **coherent** and **noise integrates away**
    - only stray light is present as a background
        - even stray light demonstrates (slow) phase evolution

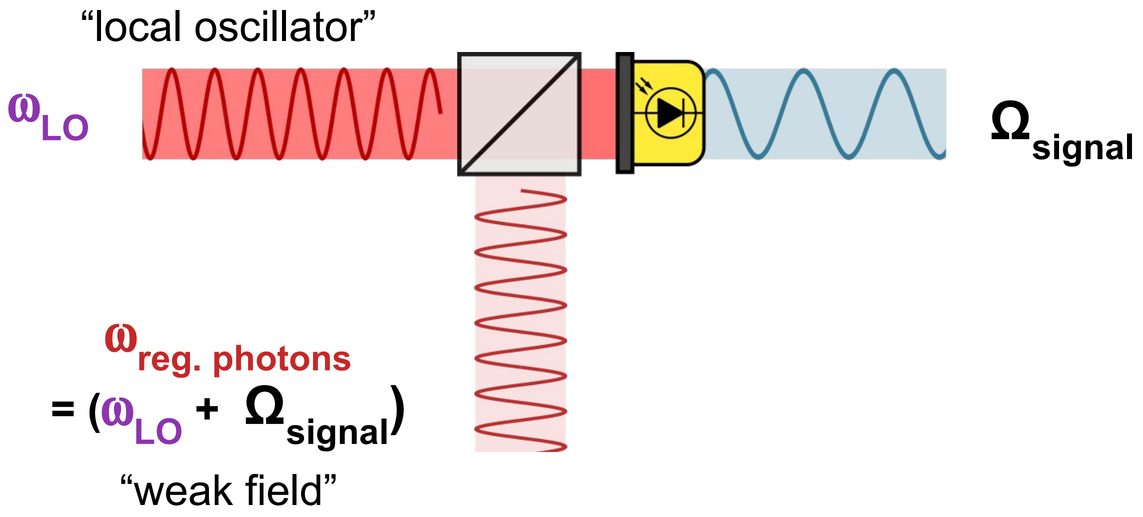

$$\left|\sqrt{P_{LO}}e^{i\omega_{LO}t} + \sqrt{P_{reg.\ photons}}e^{i[(\omega_{LO}+\Omega_{signal})t+\phi]}\right|^2$$

$$= \underbrace{P_{LO} + P_{reg.\ photons}}_{\text{D.C. terms}} + \underbrace{2\sqrt{P_{LO}P_{reg.\ photons}}\cos(\Omega_{signal}t+\phi)}_{\text{RF beatnote}}$$

Heterodyne Interferometric Detection

Heterodyne Interferometry

- interference beat-note between:
  1. *weak field* (regenerated photons from axions)
  2. strong *local oscillator* (additional laser)

  on a photodetector

- with *fixed frequency and phase offset*, detection is **coherent** and **noise integrates away**
  - only stray light is present as a background
    - even stray light demonstrates (slow) phase evolution

SIMULATION

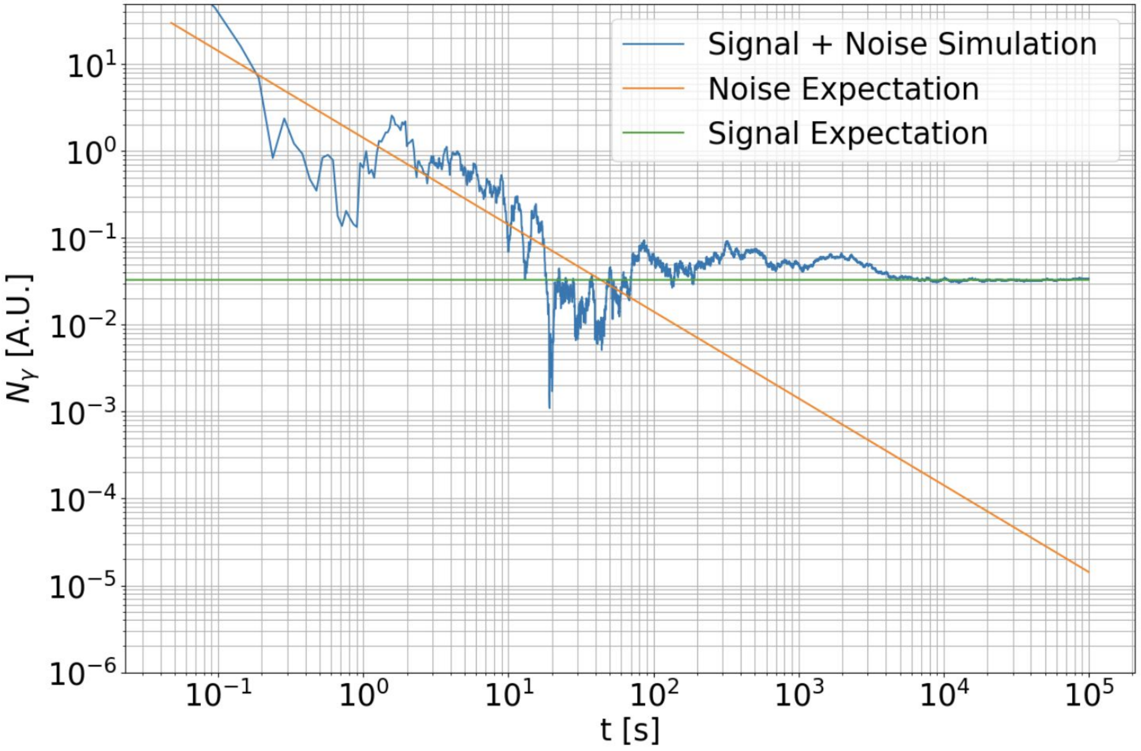

Heterodyne Interferometric Detection

Heterodyne detection in ALPS II

- MHz beat-note formed between the LO (~mW) and regenerated photons in reflection of the RC on the **science detector**
- background rate dominated by stray light from the HPL on the COB
- **Veto detector** also measures the heterodyne beatnote before the cavity to assess stray light background live during the measurement

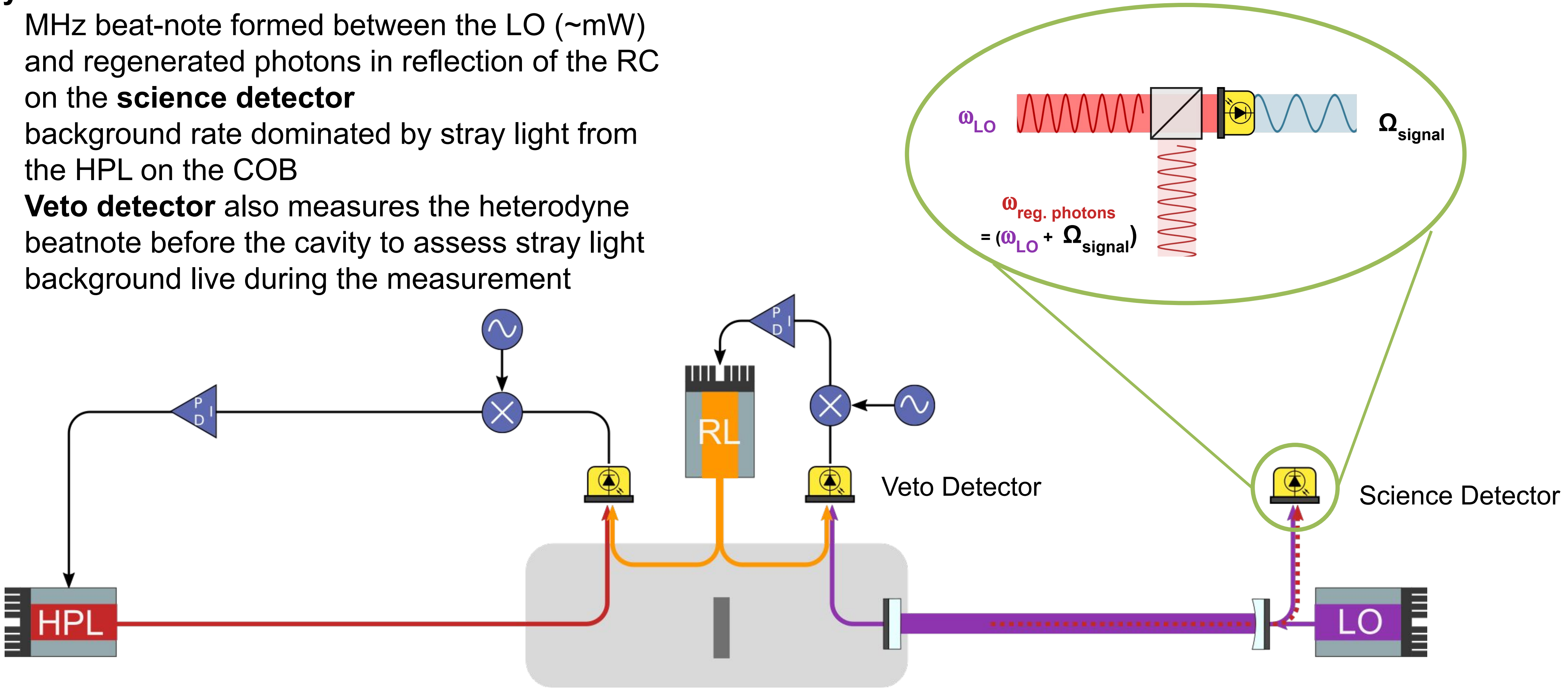

ALPS II Initial Science Run

First measurement performed from 23. to 31. May

- good overall stability and alignment performance
- ~ 45 hours of “system locked” science data acquired with magnets on
- operated with laser light polarization oriented for a “scalar” ALP search

- Open-shutter periods:
  - reconstruct the long term phase evolution of the system
  - monitor the alignment and calibration mid-measurement for calibration
- Closed-shutter periods:
  - **the “science” data**

Evaluating "Open Shutter" Periods

A. Spector, PATRAS 2023

Step 1: demodulate recorded signal to generate in-phase and quadrature components of the raw heterodyne function

Step 2: used to calibrate raw heterodyne data in terms of a regenerated photon rate

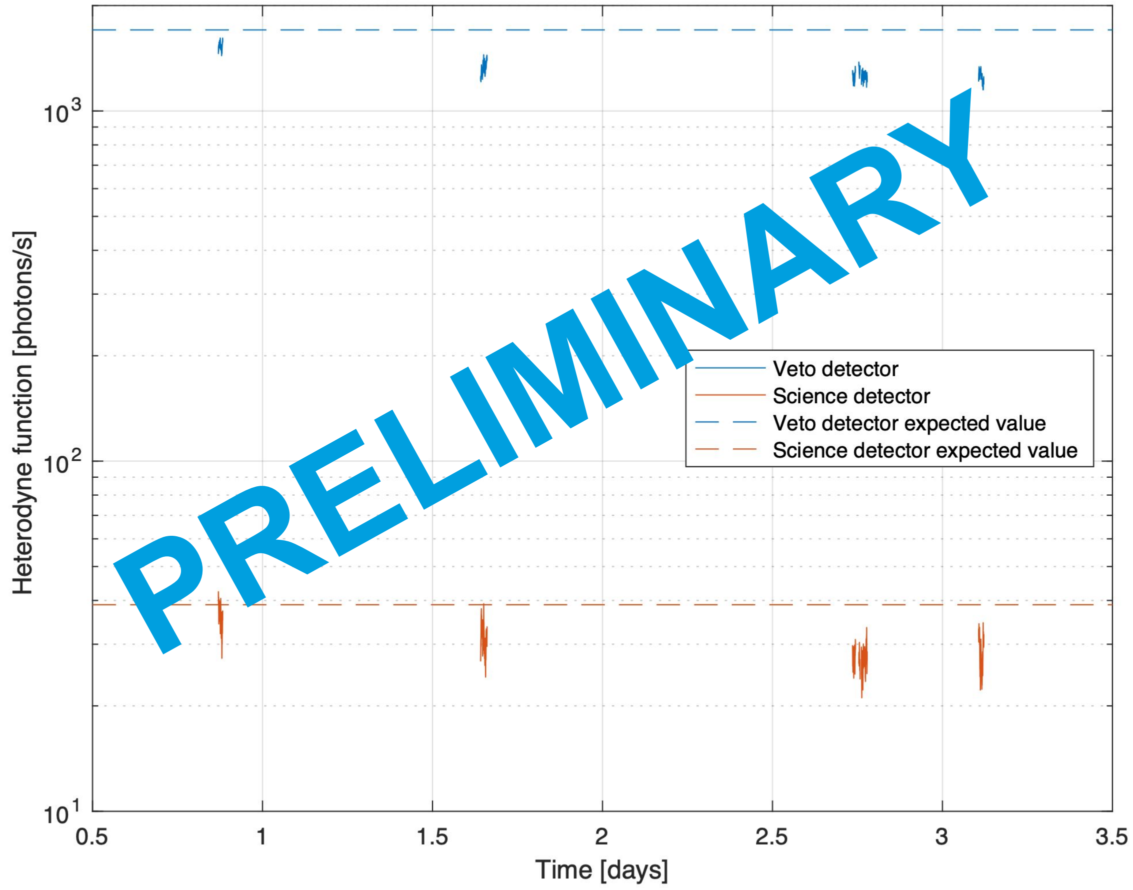

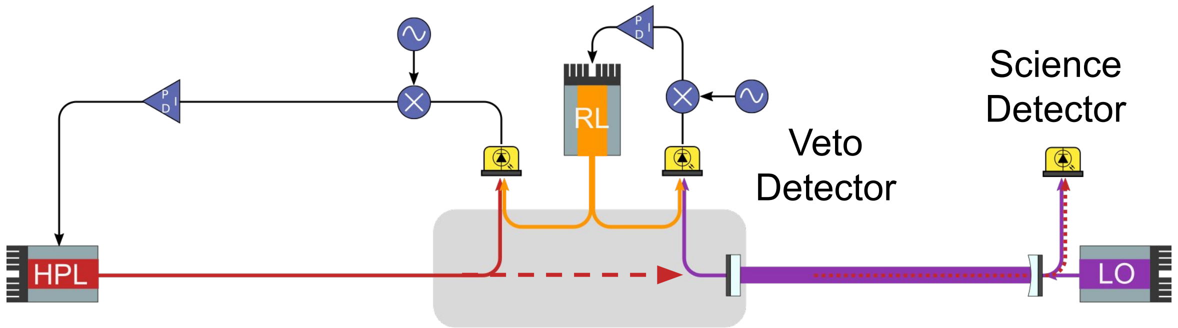

Evaluating "Closed Shutter" Periods

Generating the Heterodyne function

- combine closed shutter data sets
- calibrate heterodyne signal in terms of photon rate

$$n_{\mathrm{signal}} \approx n_{\mathrm{HPL}}\,\beta_{\mathrm{RC}}\,\frac{1}{16}\left(g_{a\gamma\gamma}\cdot B\cdot L\right)^4$$

Calibrate to a sensitivity in $g_{a\gamma\gamma}$ (GeV^{-1}):

Using measured values for:

- cavity power build-up (β_{RC})
- high power laser power (n_{HPL})
- magnetic field ($B \times L$)

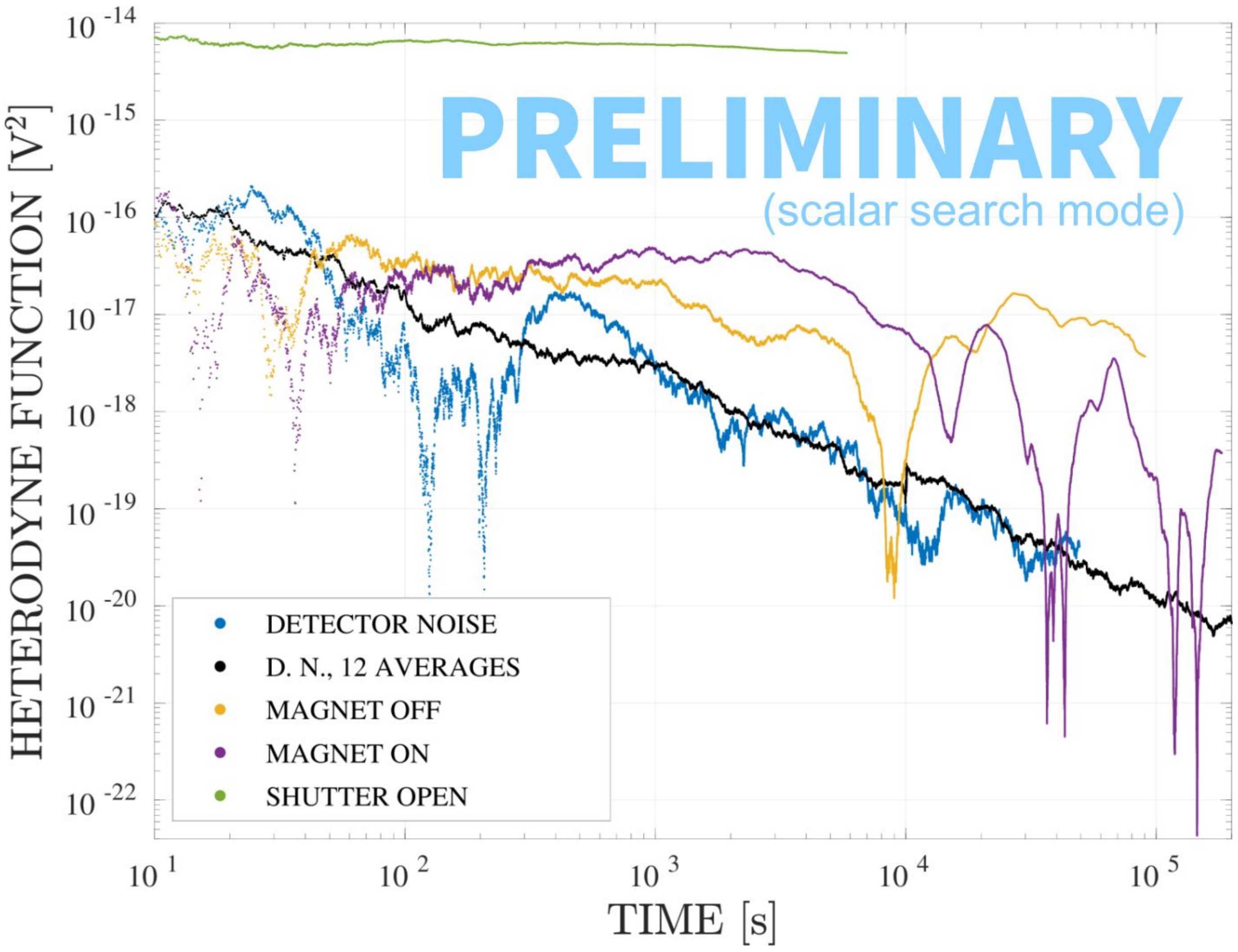

From Ciaran O'Hare: https://cajohare.github.io/AxionLimits/

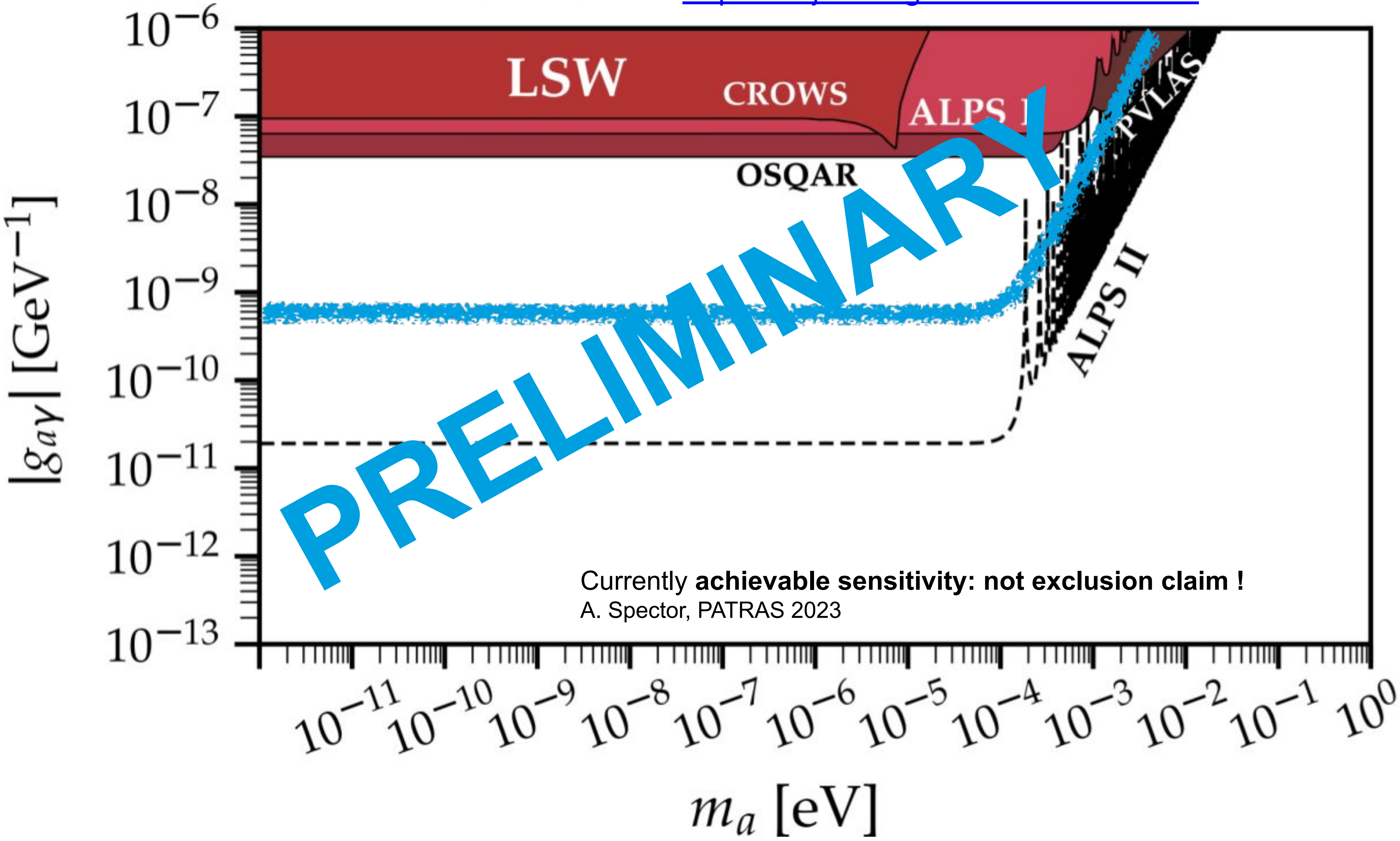

ALPS II

End 2023

Final preparation for the Initial Science Run

- automation
- '1 million seconds' of magnets-on, closed-shutter data

Early 2024

Upgraded cavity optics

2024

Production Cavity commissioning

2025 +

Beyond ALPS

- vacuum magnetic birefringence (VMB)
- high-frequency gravitational waves

Conclusion: Three Approaches, Three Experiments

MADMAX: Axion Haloscope

- Proposal for a dielectric haloscope to probe axion cold dark matter
- R&D on open and closed boosters, magnet, and precision positioning systems underway
- outlook: **prototype @ DESY 2024; MADMAX @ DESY 2030**

IAXO: Axion Helioscope

- A next-generation axion haloscope to perform unprecedented broadband searches
- Prototype version, babyIAXO, already in initial construction phase; no major roadblocks
- outlook: **data-taking by the end of the decade with babyIAXO @ DESY**

ALPS II: Laboratory Axion Search

- **Currently operating** in “initial science run” mode, collecting data
- Noteworthy technical achievements in the optics, controls, magnets and detector
- Currently sensitive enough to begin claiming new lab-based exclusions (**coming soon!**)

Thank you!

Todd Kozlowski

todd.kozlowski@desy.de

ALPS II

Back-up Slides

Heterodyne Interferometric Detection

Two-stage Digital Demodulation Signal Extraction

- local oscillator and regenerated photon fields form signal at frequency Ω_{signal}
- first demodulation on-board FPGA lock-in amplifier instrument to an intermediate frequency
- second demodulation performed “offline”

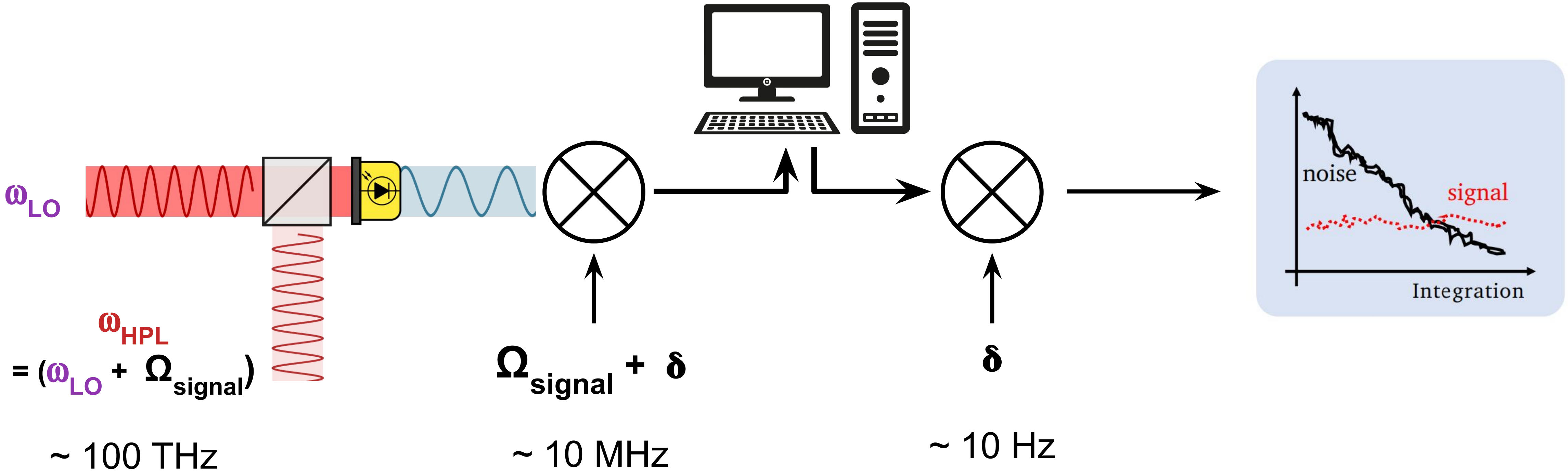

Heterodyne Interferometric Detection

Heterodyne Interferometry

- interference beat-note between:
  - a *weak field* (regenerated photons from axions)
  - a strong *local oscillator* (additional laser)

  on a photodetector

- with *fixed frequency and phase offset*, detection is **coherent** and **noise integrates away**
  - only stray light is present as a background
  - phase evolution of the stray light background also allows us to integrate it away over long (million second) measurement periods

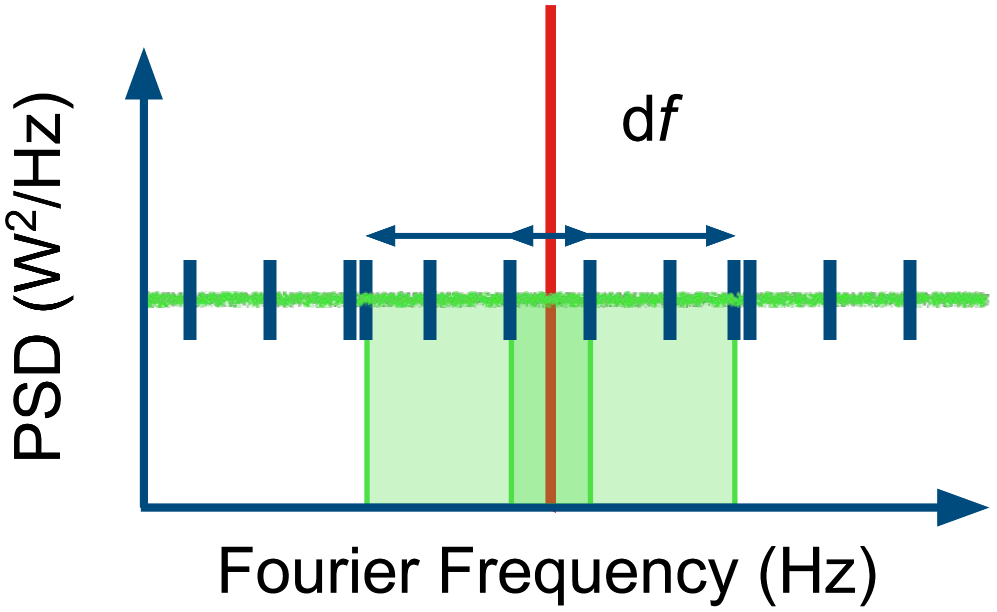

Graphic courtesy of Aaron Spector

Heterodyne Interferometric Detection

Heterodyne Interferometry

- interference beat-note between:
  - a *weak field* (regenerated photons from axions)
  - a strong *local oscillator* (additional laser)

  on a photodetector

- with *fixed frequency and phase offset*, detection is **coherent** and **noise integrates away**
  - only stray light is present as a background
  - phase evolution of the stray light background also allows us to integrate it away over long (million second) measurement periods

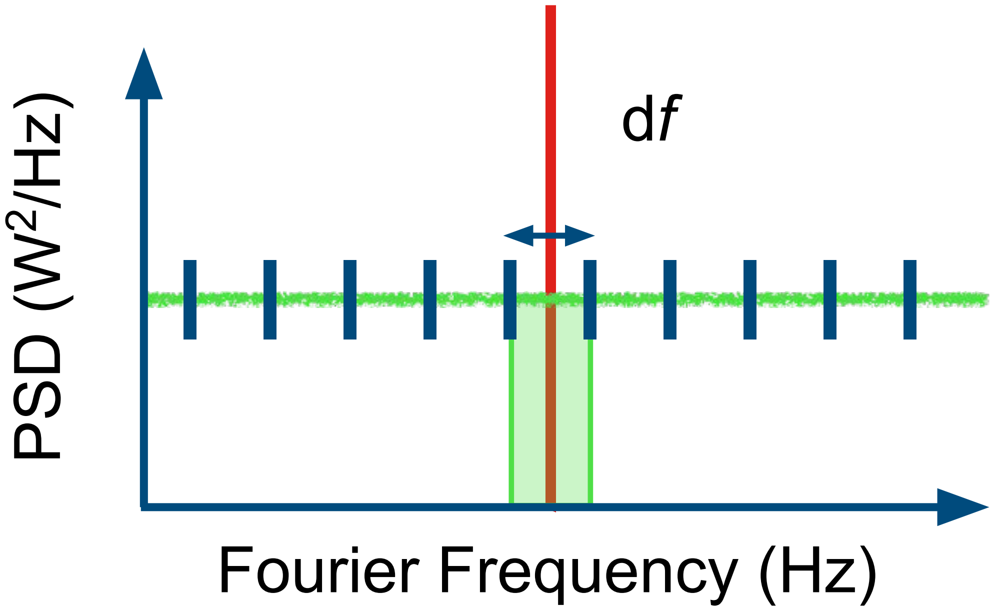

Graphic courtesy of Aaron Spector

VMB Effect and Magnitude

- prediction of QED: in a magnetic field, the vacuum acts like a birefringent medium

$$\Delta n^{(\mathrm{VMB})} = n_{\|}^{(\mathrm{VMB})} - n_{\perp}^{(\mathrm{VMB})} = 3A_e B_{\mathrm{ext}}^2$$

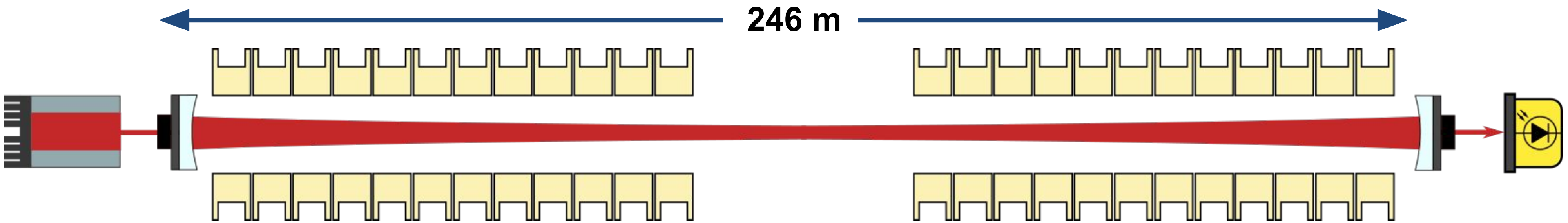

- scale of the effect in **ALPS II** (B^2 = 28 T^2, L = 212m, λ = 1064nm, N ~ 10,000)

$$\Delta L \sim 2.1 \times 10^{-20}\mathrm{m}$$

$$\Gamma(L) = 3.159 \times 10^{-9} \left(\frac{B_{\mathrm{ext}}}{5\mathrm{T}}\right)^2 \left(\frac{\mathcal{F}}{40,000}\right) \left(\frac{L}{212\mathrm{m}}\right) \quad \mathrm{radian}$$

VMB Measurement Concepts

1. Classic transmission polarimetry
   - experience from contemporary VMB experiments (PVLAS, BMV)

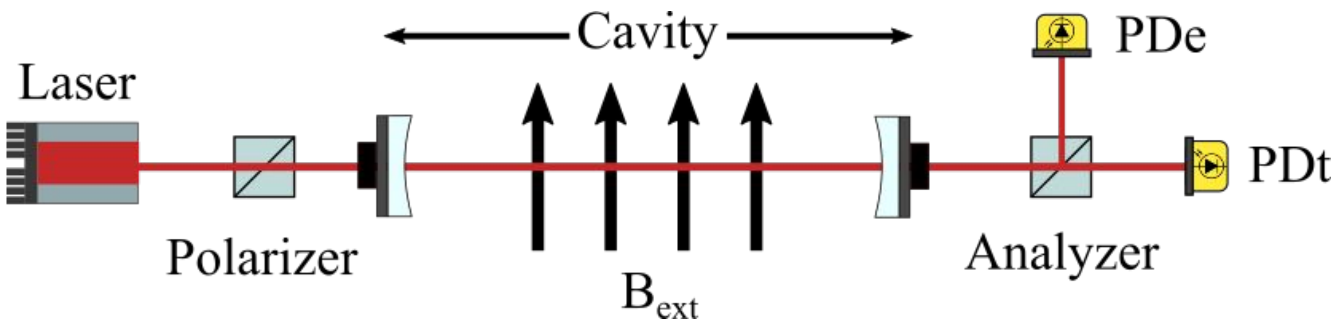

- currently only option for modulation is ramping the magnet current:
  - 20 minutes up / down
    - 0.04 mHz
  - 5.3 T full modulation amplitude

Siu Au Li at the 2015 DESY VMB workshop (link)

VMB Measurement Concepts

2. **“Hall approach”** - based on Fermilab P877 / J.Hall et al. Phys. Rev A 62, 013815 (2000)
   - lock two orthogonal polarization states separately to the cavity
   - measure the relative frequency splitting induced by VMB
   - difference in cavity resonance frequencies read out in the two PDH control signals

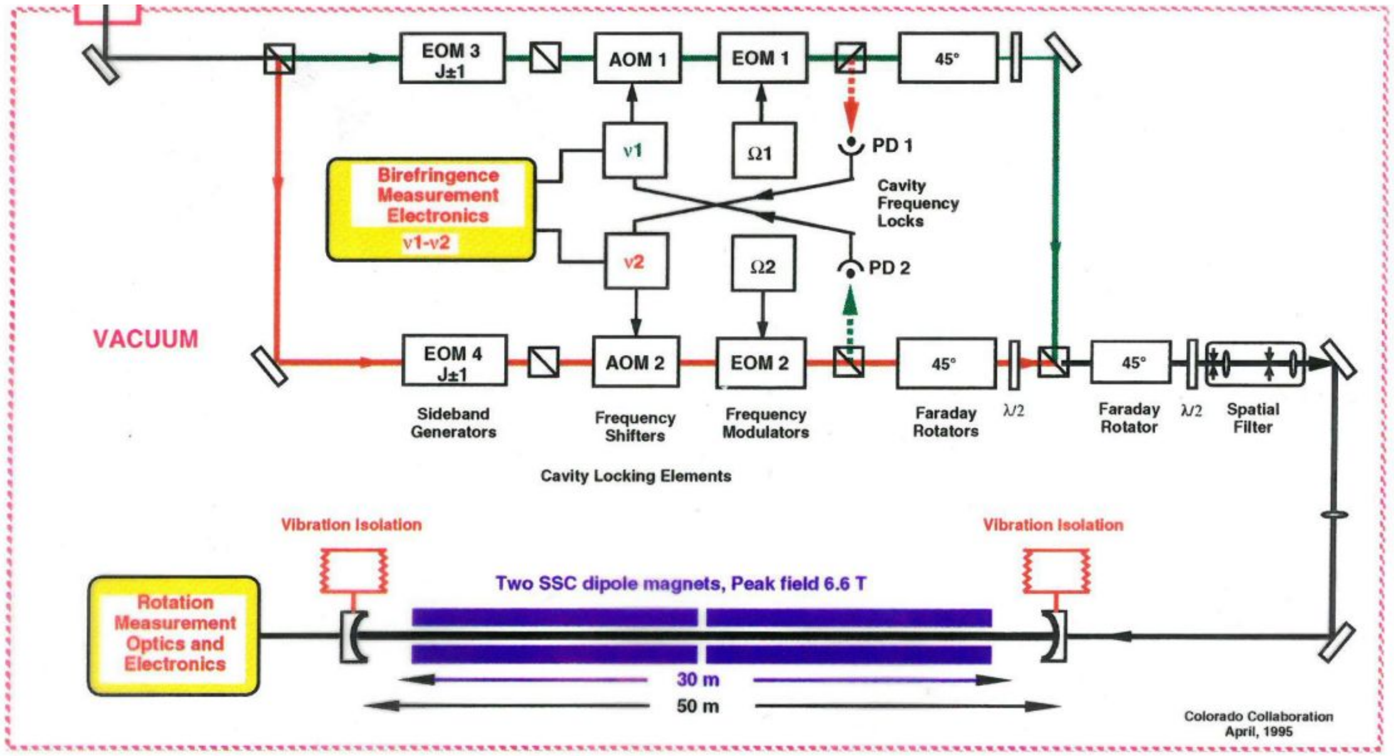

from Siu Au Li at the 2015 DESY VMB workshop (link)

VMB Measurement Concepts

3. Heterodyne Birefringence Readout
   - lock three fields to cavity resonance: one “p-pol” field, and two “s-pol” lasers, one at an FSR above and an FSR below the “p-pol” laser frequency
   - using a fourth field as a **local oscillator**, read out the relative frequency differences between the upper and lower s-pol fields in reflection and transmission
   - frequency difference between the p-pol resonance and the “simulated” s-pol resonance at the p-pol FSR can be computed from the resultant beat-notes:

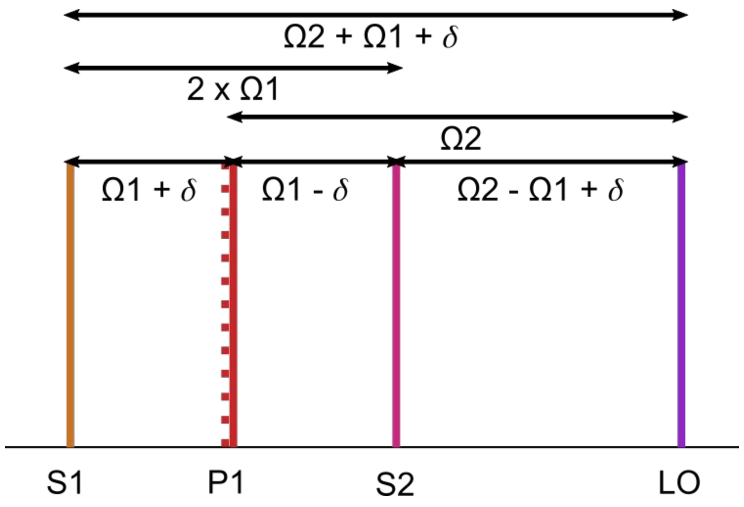

$$\frac{1}{2}\Big((LO \,\&\, S2) + (LO \,\&\, S1)\Big) - (LO \,\&\, P1)$$
$$= \frac{1}{2}\Big((\Omega_2 - \Omega_1 + \delta) + (\Omega_2 + \Omega_1 + \delta)\Big) - \Omega_2$$
$$= \delta$$

   - set up is effectively immune to absolute length changes / FSR changes

from Siu Au Li at the 2015 DESY VMB workshop (link)

Noise Sources to Consider

- mirror coating thermal noise
  - the suspected limiting noise source preventing shot-noise limited detection in contemporary experiments. [Ejlli et al '20] found:

$$L(\nu) = 2 \times 10^{-18}\ \mathrm{m}/\sqrt{\nu}$$

  - Coating thermal noise is inversely proportional with beam size
  - ALPS II cavity would have a 10x larger beam spot size
    - factor 100 lower mirror coating thermal noise for the same power.
    - At our modulation frequency and for our larger beam,

$$L(0.4\ \mathrm{mHz}) = 1.8 \times 10^{-18}\mathrm{m}/\sqrt{\mathrm{Hz}}$$

  - assuming this is our dominant noise source @ 0.4 mHz, and a signal strength of $\Delta L \sim 2.1 \times 10^{-20}\mathrm{m}$
    - potential to resolve VMB effect after 200,000 seconds of integration time

- additional noise sources to consider:
  - PDH sensing noise / residual amplitude modulation noise
  - noise in phase-lock loops
  - magnet modulation-related length / alignment / pointing noise
  - relative power noise
  - stray light

Summary and Prospect

- The ALPS II experiment, with its 24 HERA dipole magnets (**B^2L = 6000**) can produce the largest magnitude VMB effect of any contemporary experiment
- ALPS II experimental site is very well suited for VMB studies:
  - Long-baseline, high-finesse cavities
  - Class 10 optical clean rooms and related support infrastructure
  - well-studied long-term seismic stability of the HERA tunnel
  - well-characterized control and readout systems / DAQ
  - group expertise measuring weak optical signals using high-resolution heterodyne interferometry techniques

Most importantly, it all comes practically for free with ALPS II

- VMB@ALPS concept is still in its conceptual infancy
- we have multiple readout concepts currently being studied with a 20-meter prototype cavity
  - supported by PIER research grant
- VMB will not be implemented into the ALPS II program until after all experimental goals achieved - outlook 3-4 years
  - smaller scale R&D on-going in that time, will start a dedicated working group within the collaboration to advance this goal

Evaluating “Open Shutter” Periods

A. Spector, PATRAS 2023

Step 1: demodulate recorded signal to generate in-phase and quadrature components of the raw heterodyne function

Step 2: calibrate raw heterodyne data in terms of photon rate

Step 3: divide by expected signal to determine field overlap / coupling efficiency

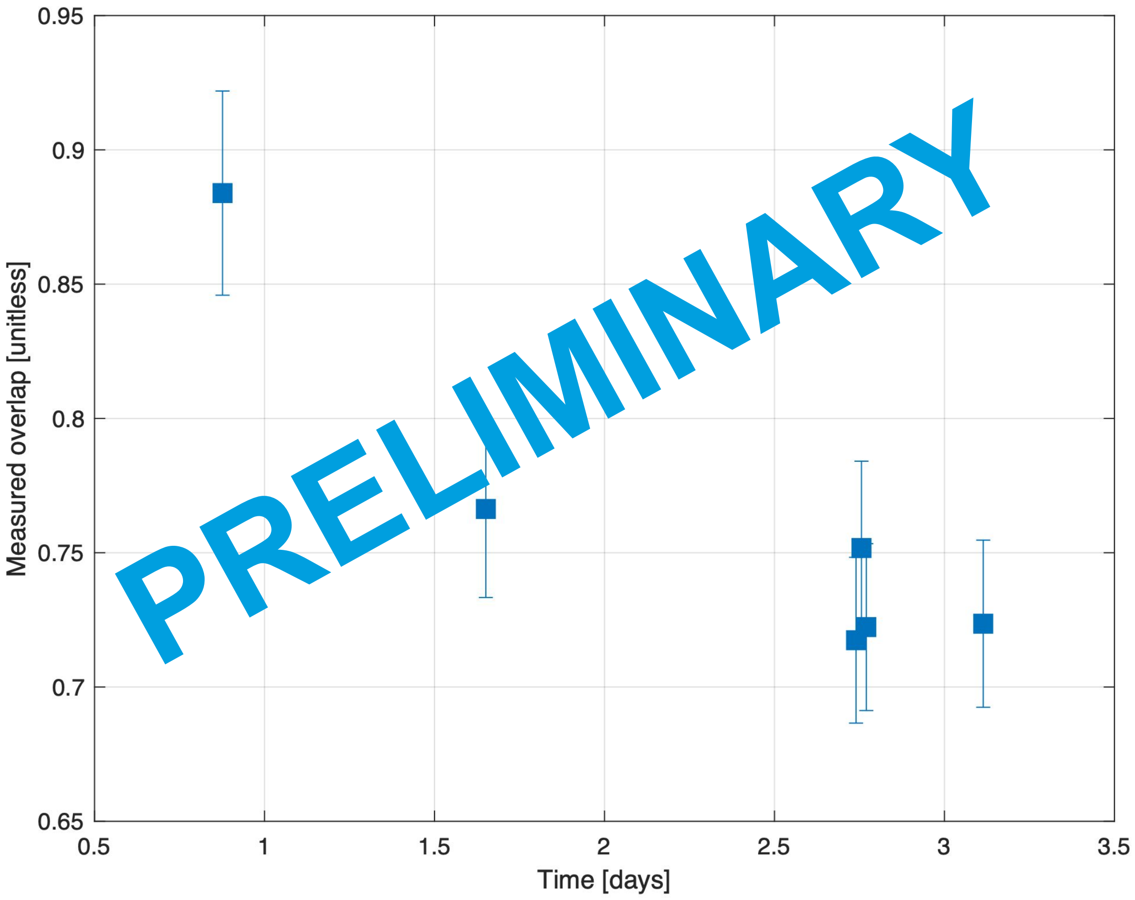

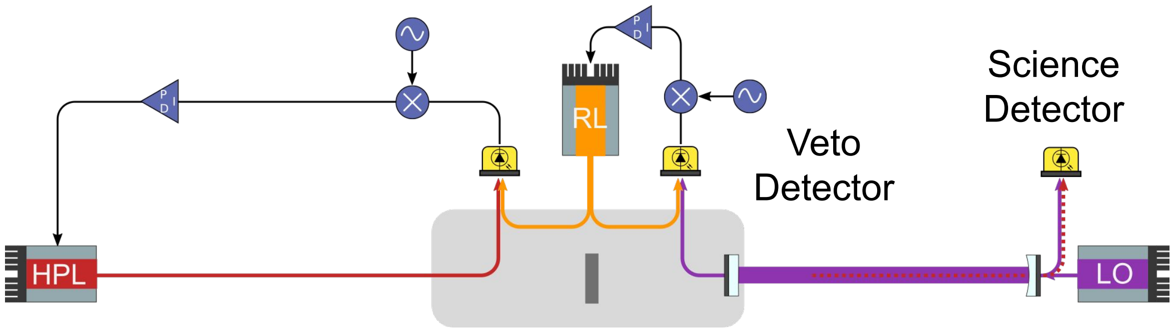

Evaluating "Open Shutter" Periods

A. Spector, PATRAS 2023

Step 1: demodulate recorded signal to generate in-phase and quadrature components of the raw heterodyne function

Step 2: calibrate raw heterodyne data in terms of photon rate

Step 3: divide by expected signal to determine field overlap / coupling efficiency

Step 4: assess phase evolution with and without manual phase correction

- linear phase trend present due to different frequency resolutions between devices
- μHz frequency drift on MHz signals: all our devices need equal frequency resolution beyond **15 digits!**

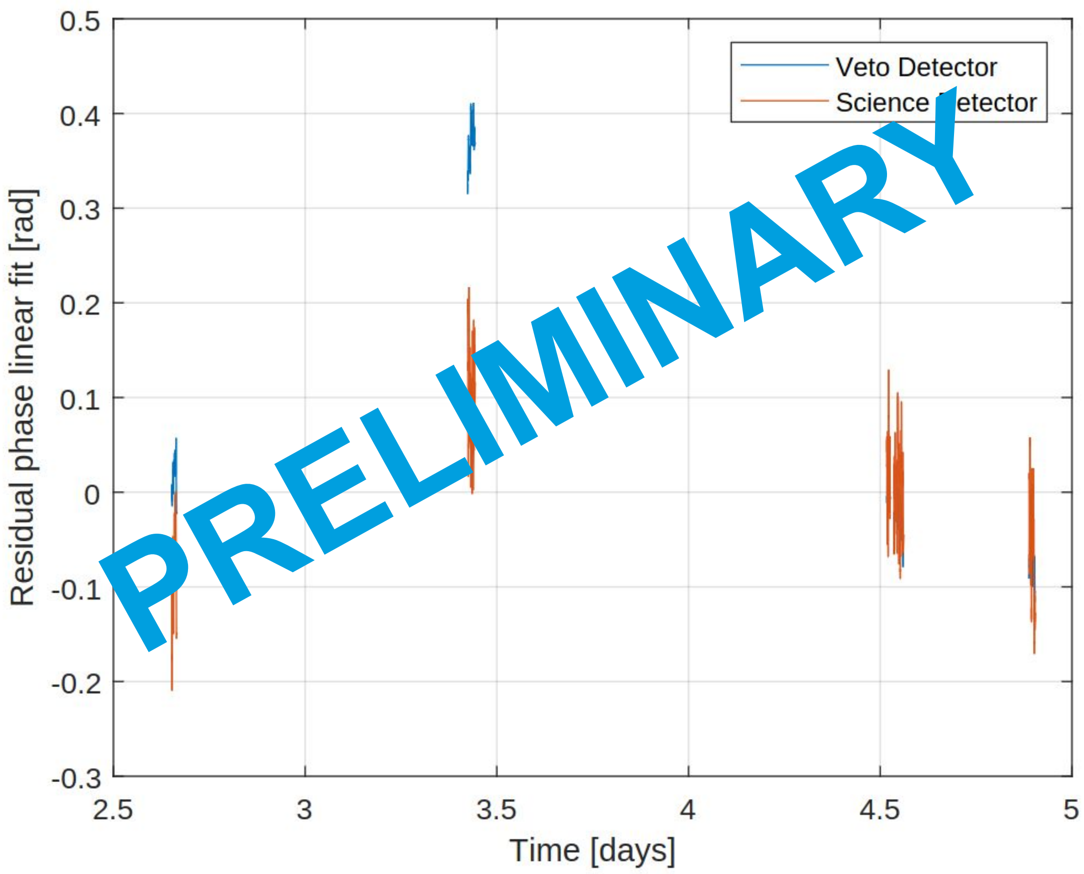

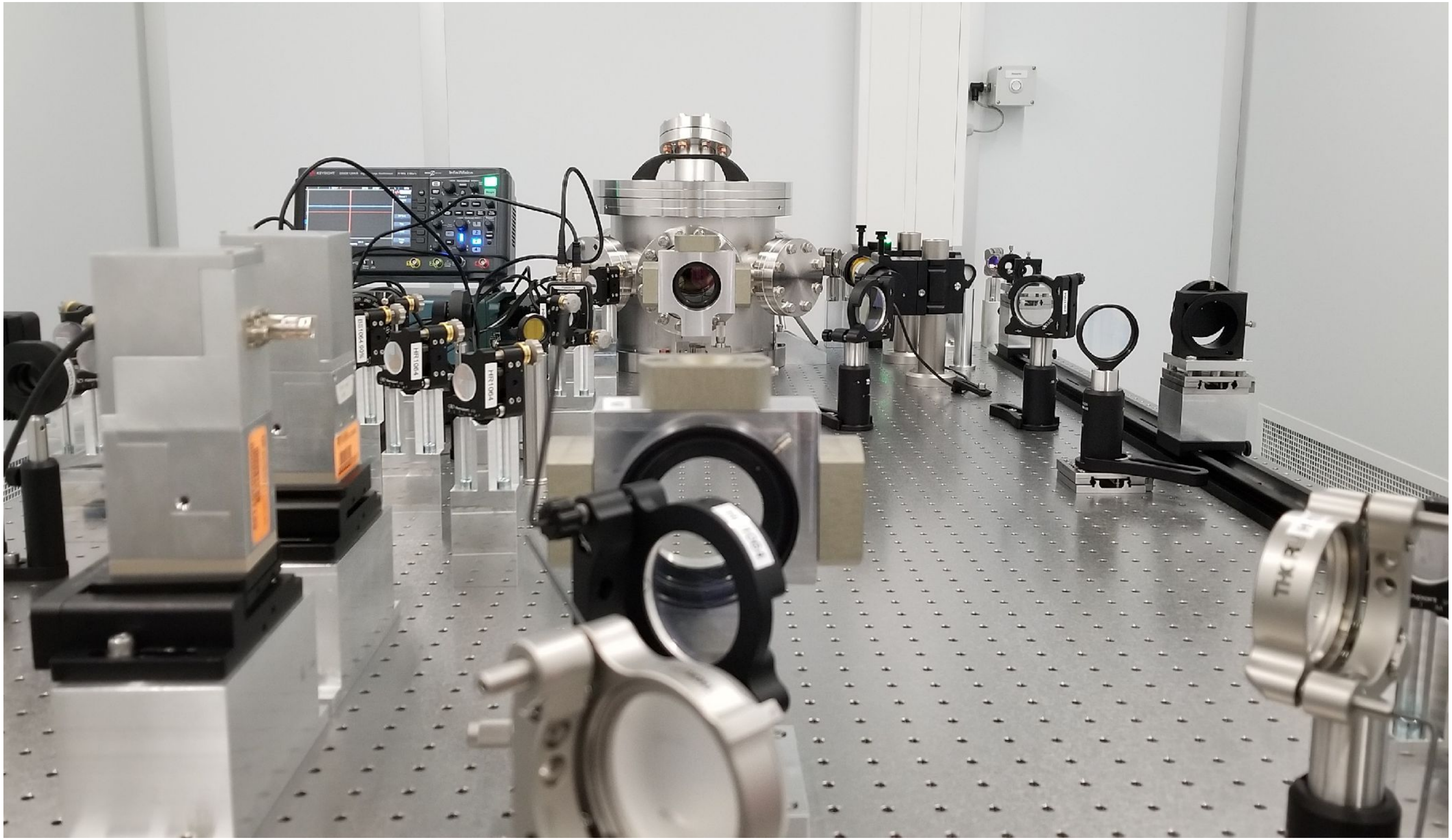

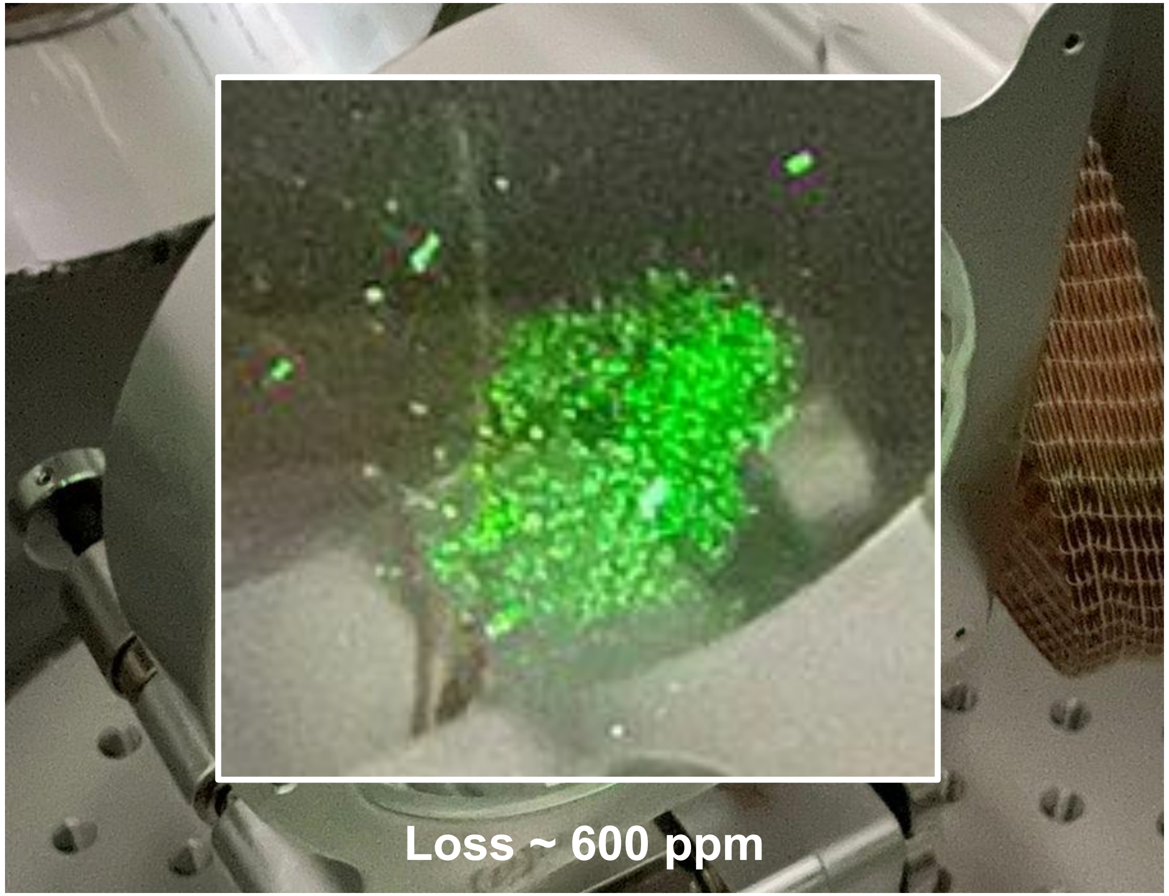
Loss ~ 600 ppm

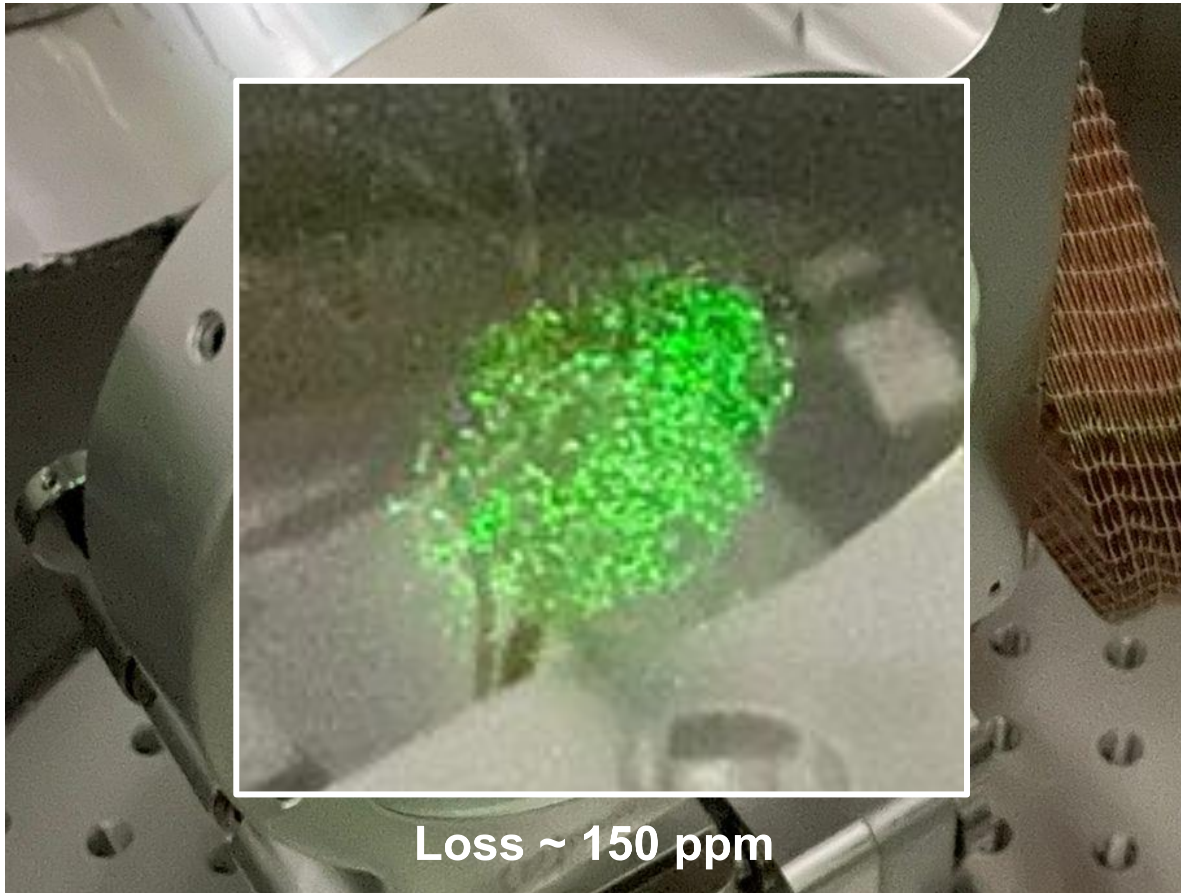
Loss ~ 150 ppm

(Very) preliminary sensitivity measurement performed with sub-optimal, non-optimized 250m cavity:

- no active pointing stabilization of cavity eigenmode or input alignment
- no power stabilization
- very crude ellipsometer/polarization monitor consisting of just a waveplate, off-the-shelf cube beamsplitter, and a high-gain differential photodetector
- low cavity finesse (~4,000)

- approx. 5 orders of magnitude away from expected signal with this “toy detector”

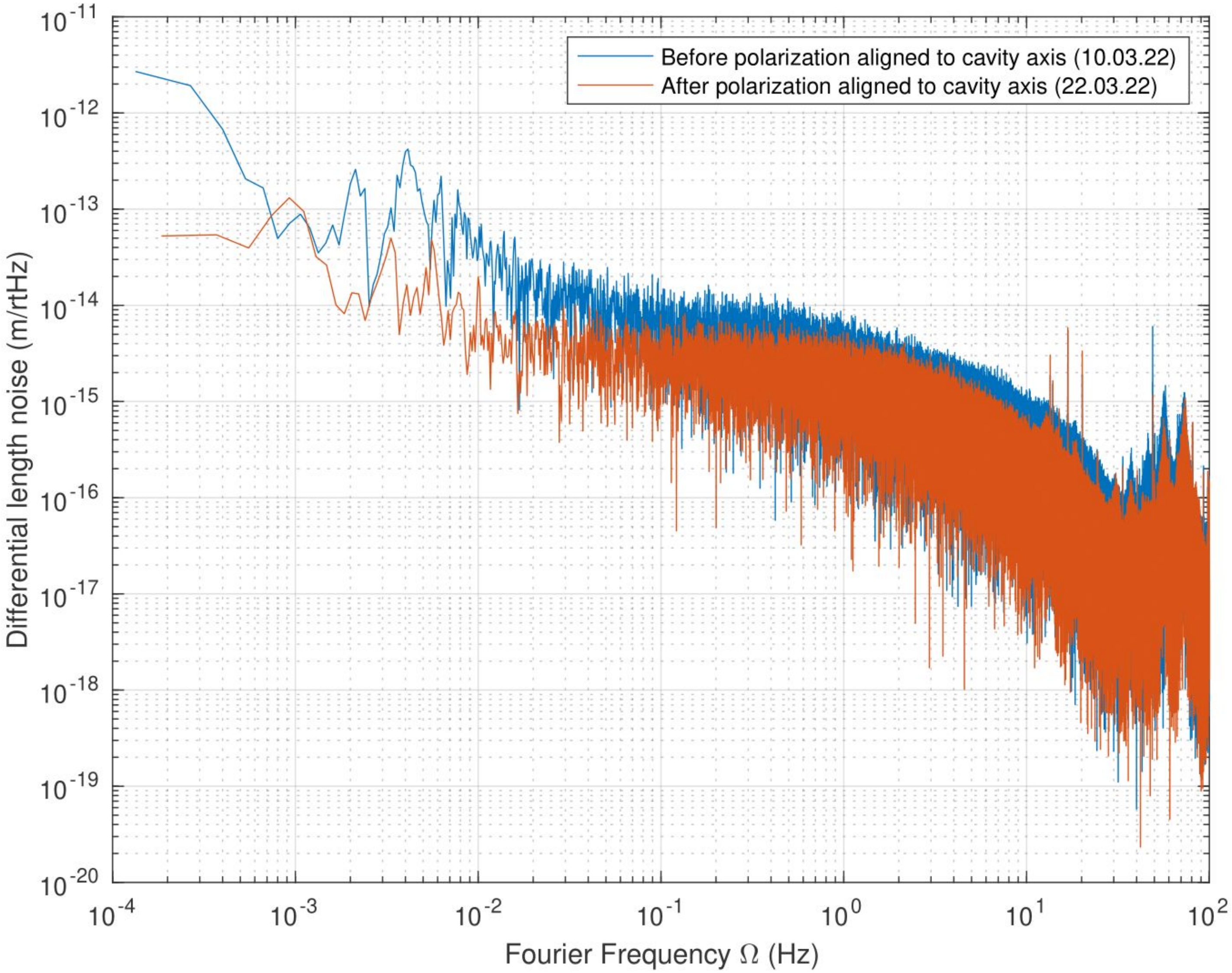

Sikivie Process

- Axion / axion-like particle Lagrangian contains an interaction term with the EM field
- axion - photon oscillations possible in a background magnetic field with coupling strength ($g_{a\gamma\gamma}$)
- process exploited by some direct searches

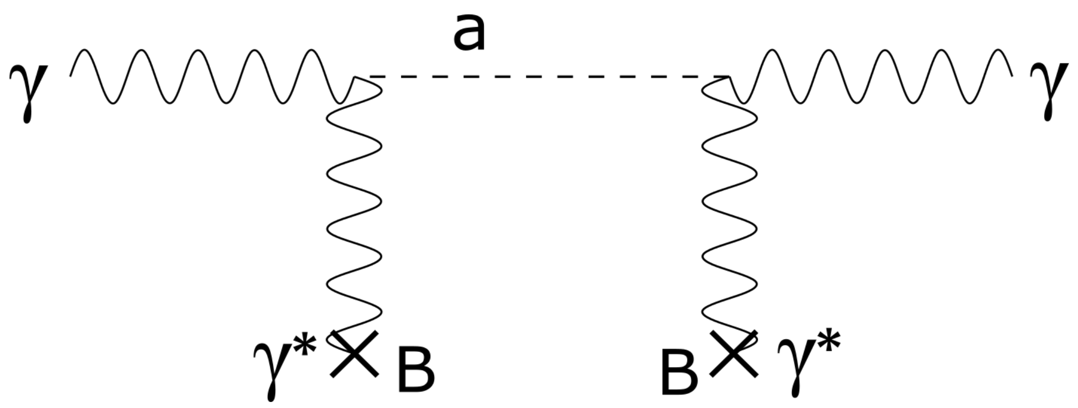

$$\mathcal{L}_{a\gamma} = -\frac{1}{4} g_{a\gamma\gamma} a F_{\mu\nu} \tilde{F}^{\mu\nu} = g_{a\gamma\gamma} a \mathbf{E} \cdot \mathbf{B}$$

Astrophysical hints (e.g. stellar cooling) motivate ALPS search parameters:
$g_{a\gamma\gamma} \sim 2 \times 10^{-11}$ GeV^{-1}
for masses < 0.1 meV

$$n_{\text{signal}} \approx n_{\text{PC}} \beta_{\text{RC}} \frac{\eta}{16} (g_{a\gamma\gamma} BL)^4$$

For the ALPS II design parameters:

$$n_{\text{signal}} \approx \frac{1 \text{ photon}}{37 \text{ hours}} \cdot \left(\frac{P_{\text{PC}}}{150 \text{ kW}}\right) \left(\frac{\beta_{\text{RC}}}{10{,}000}\right) \left(\frac{\eta}{0.9}\right)$$

A Resonantly Enhanced LSW Design

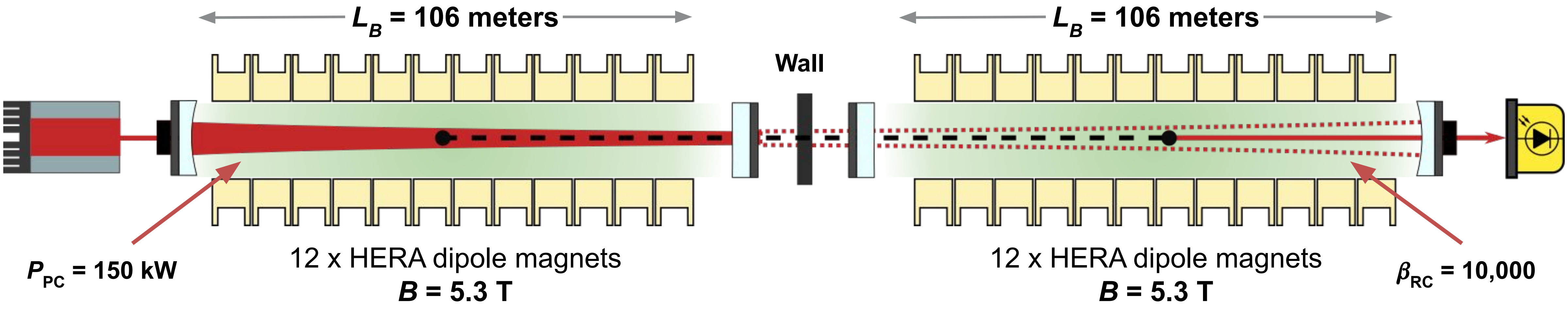

$$n_{\mathrm{signal}} \approx n_{\mathrm{PC}} \beta_{\mathrm{RC}} \frac{\eta}{16} (g_{a\gamma\gamma} BL)^4$$

For the ALPS II design parameters:

$$n_{\mathrm{signal}} \approx \frac{1 \text{ photon}}{37 \text{ hours}} \cdot \left(\frac{P_{\mathrm{PC}}}{150 \text{ kW}}\right)\left(\frac{\beta_{\mathrm{RC}}}{10{,}000}\right)\left(\frac{\eta}{0.9}\right)\left(\frac{g_{a\gamma\gamma}}{2\times10^{-11} \text{ GeV}^{-1}}\right)^4\left(\frac{B}{5.3 \text{ T}}\right)^4\left(\frac{L}{106 \text{ m}}\right)^4$$

Design of the ALPS II Optical System (2022). *Physics of the Dark Universe, 35*: 100968. doi:10.1016/j.dark.2022.100968

Heterodyne Interferometric Detection

Heterodyne Interferometry

- measurement of the interference beat-note between an ultra-weak signal field and a strong local oscillator on a shot-noise-limited photodetector
- double-stage demodulation:
  - first stage on-board a high-frequency, low-noise FPGA (Liquid Instruments Moku)
  - second demodulation performed offline in Matlab to avoid spurious electronic pickup
  - In-phase and quadrature demodulation performed to extract signal amplitude and phase:

$$z[N] = \frac{(\sum_i^N I[n])^2 + (\sum_i^N Q[n])^2}{N^2}$$

Number of photons

$$N_\gamma = \frac{z[N]}{G^2 P_{LO} h\nu}$$

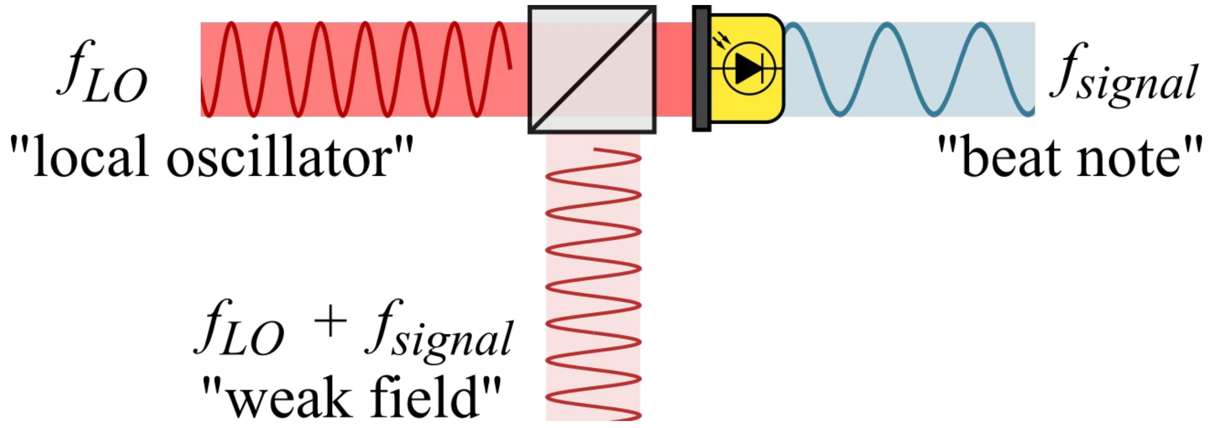

$$\left| \sqrt{P_{\rm LO}}\; e^{i(2\pi f_{\rm LO} t + \phi_{\rm LO})} + \sqrt{P_{\rm signal}}\; e^{i(2\pi (f_{\rm LO} + f_{\rm signal}) t + \phi_{\rm signal})} \right|^2 =$$

$$P_{\rm LO} + P_{\rm signal} + 2\sqrt{P_{\rm LO} P_{\rm signal}} \cos(2\pi f_{\rm signal} t + \Delta\phi)$$

Photo credit: D. Reuther, M. Mayer, A. Spector

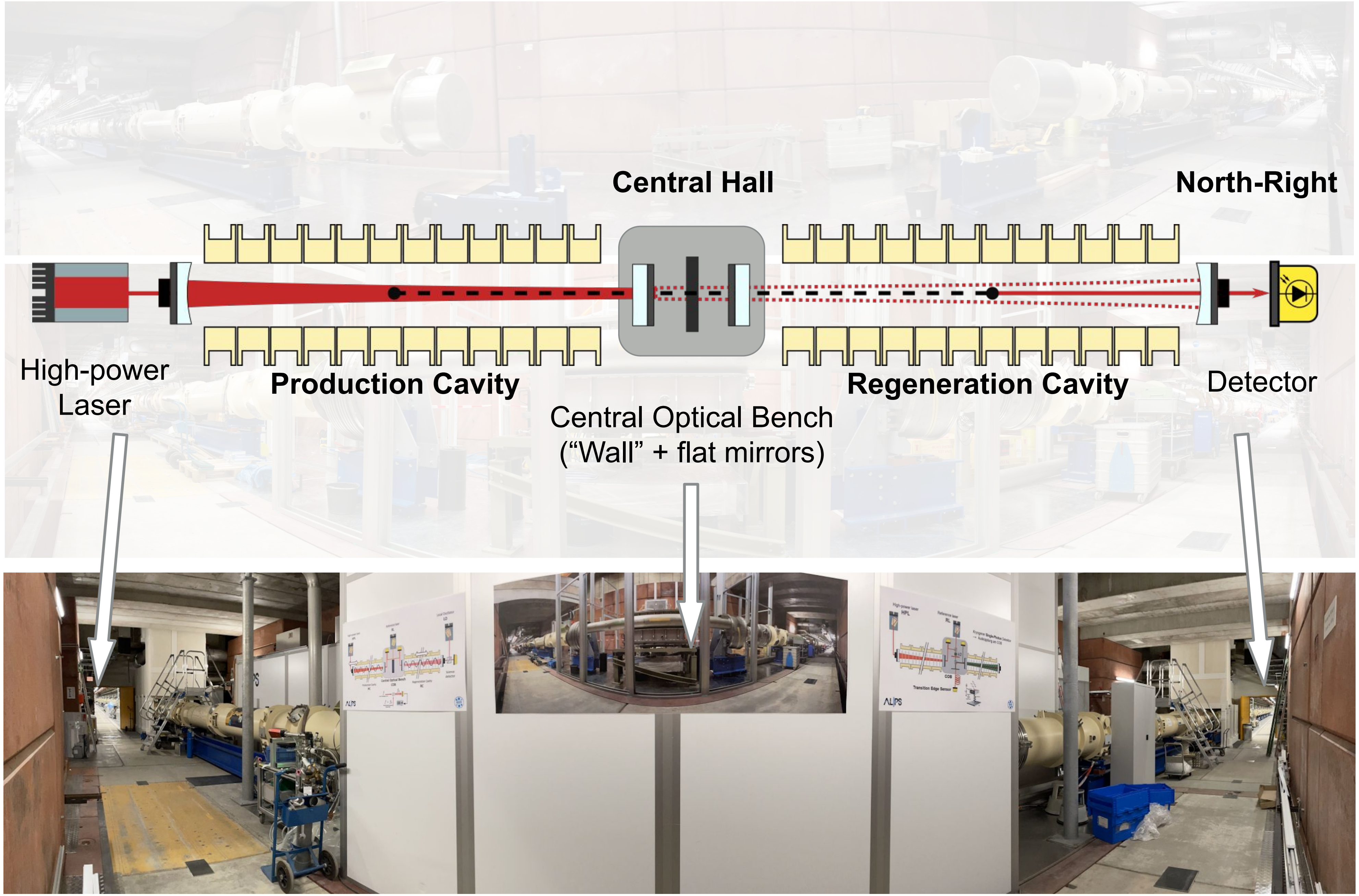

October 202

February 20

Present

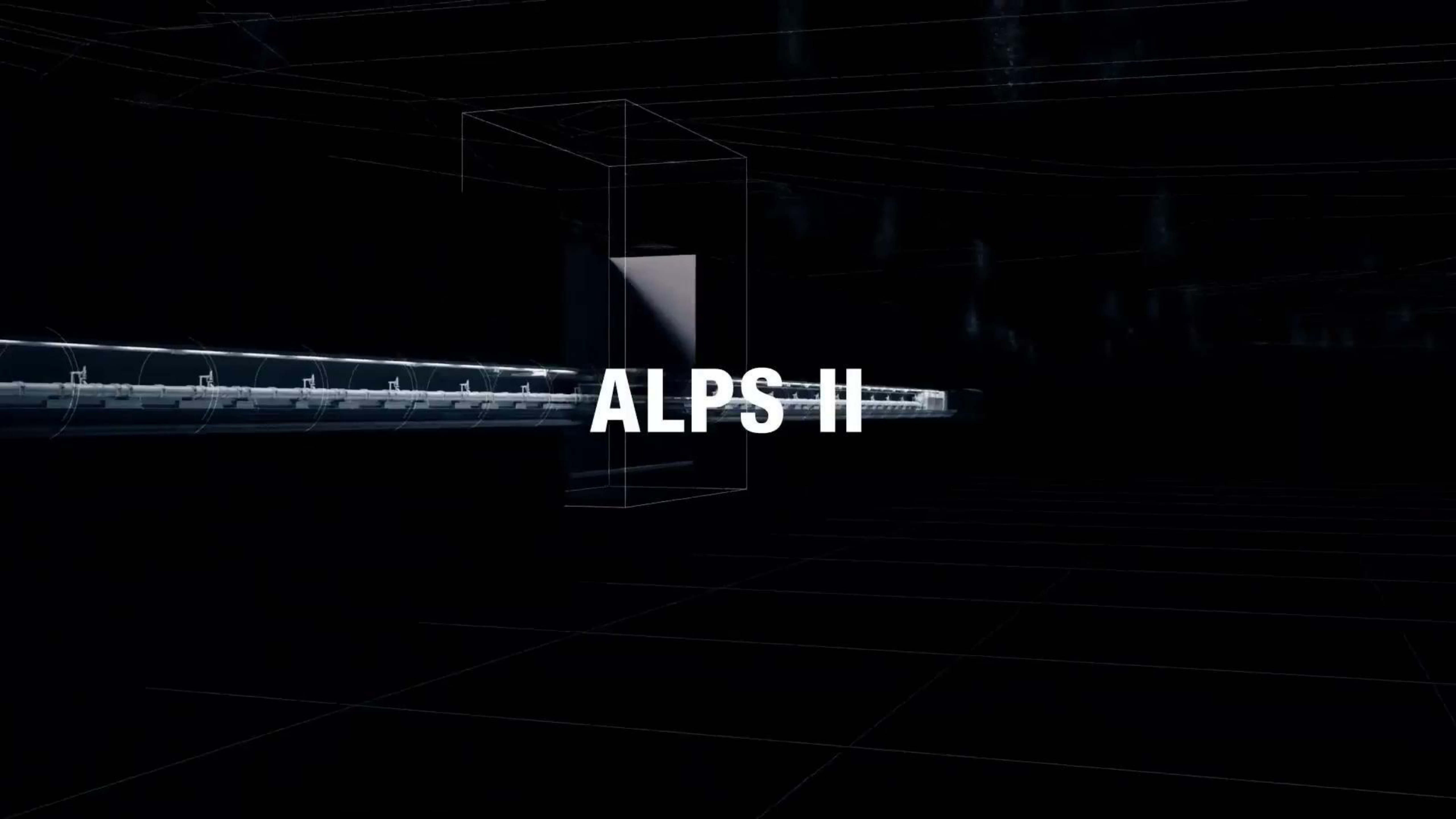
ALPS II

Image credits: D. Reuther, L. Wei, DESY MVS

Magnets

- All 24 magnets successfully straightened, current- and quench-tested, aligned and running
  - 5.3 T field strength at nominal 5700 A
  - Expanded beam tube aperture allows for longer optical cavities → improved sensitivity

Albrecht, C., Barbanotti, S., Hintz, H. *et al.* Straightening of superconducting HERA dipoles for the any-light-particle-search experiment ALPS II. *EPJ Techn Instrum* 8, 5 (2021).

Optics

Regeneration Cavity

- Half-confocal, 122 meters long
- Cavity storage time: **7.04 ms (world record)**
  - equivalent to 3.52 ms decay time
  - finesse: ~27,000
  - round-trip losses: ~120 ppm
  - **power build-up: ~ 8,000** (design goal 10,000)

- Very good long-term stability:
  - week-long periods of local oscillator (LO) frequency stabilization (PDH) with all-digital control
  - minimal re-alignment required over a 122 meter-long baseline (*when weather is good*)
  - input mode-matching > 92% even without active auto-alignment
  - fully remote operation to not perturb the set-up with vibrational or thermal disturbances

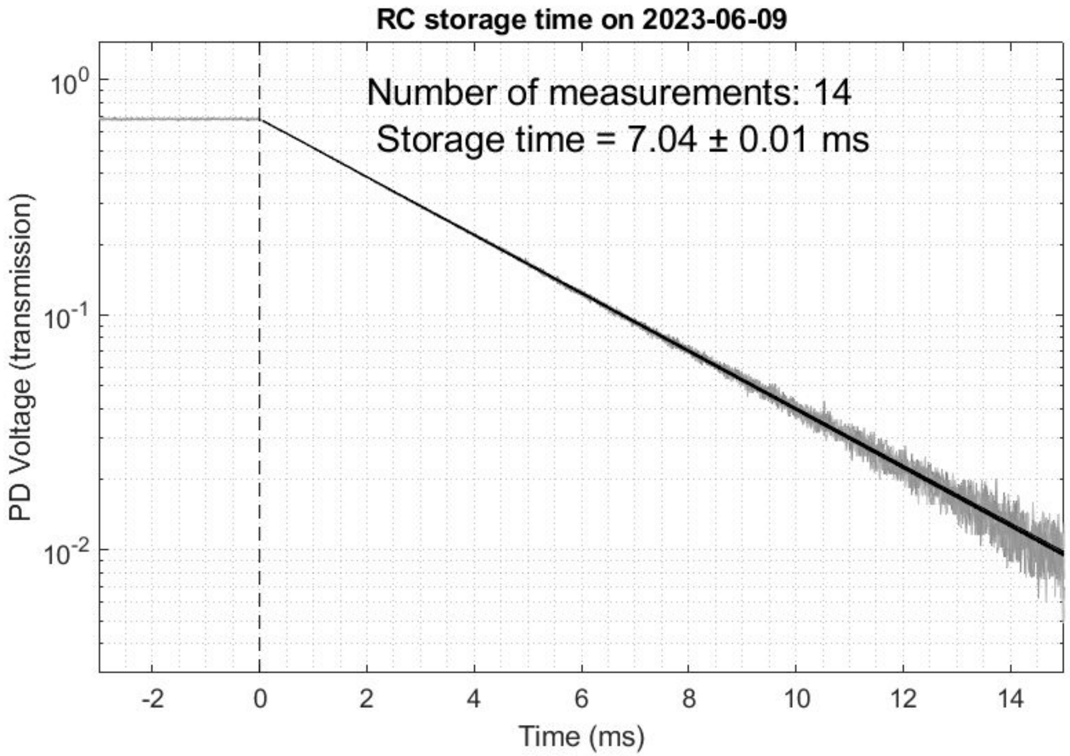

$$\beta \approx \frac{4T_{\rm in}}{(T_{\rm in} + T_{\rm out} + {\rm Loss})^2}$$

Optics

Central Optical Bench

- intermediate reference laser (RL) is used to phase-lock the HPL frequency to the LO transmitted field **without direct interference**
  - PLL1 between RL and LO
  - PLL2 between HPL and RL
  - sum of offset frequencies equal to integer number of RC FSR's
- Ultra-low expansion (ULE) plate inserts minimize phase drift
- Optics on COB must be pre-aligned before insertion into vacuum
- Quadrant photodiode position sensors to monitor beam pointing

High Power laser

- > 35 W of stable 1064 nm laser light injected through the Production Area
- urad alignment precision and stability

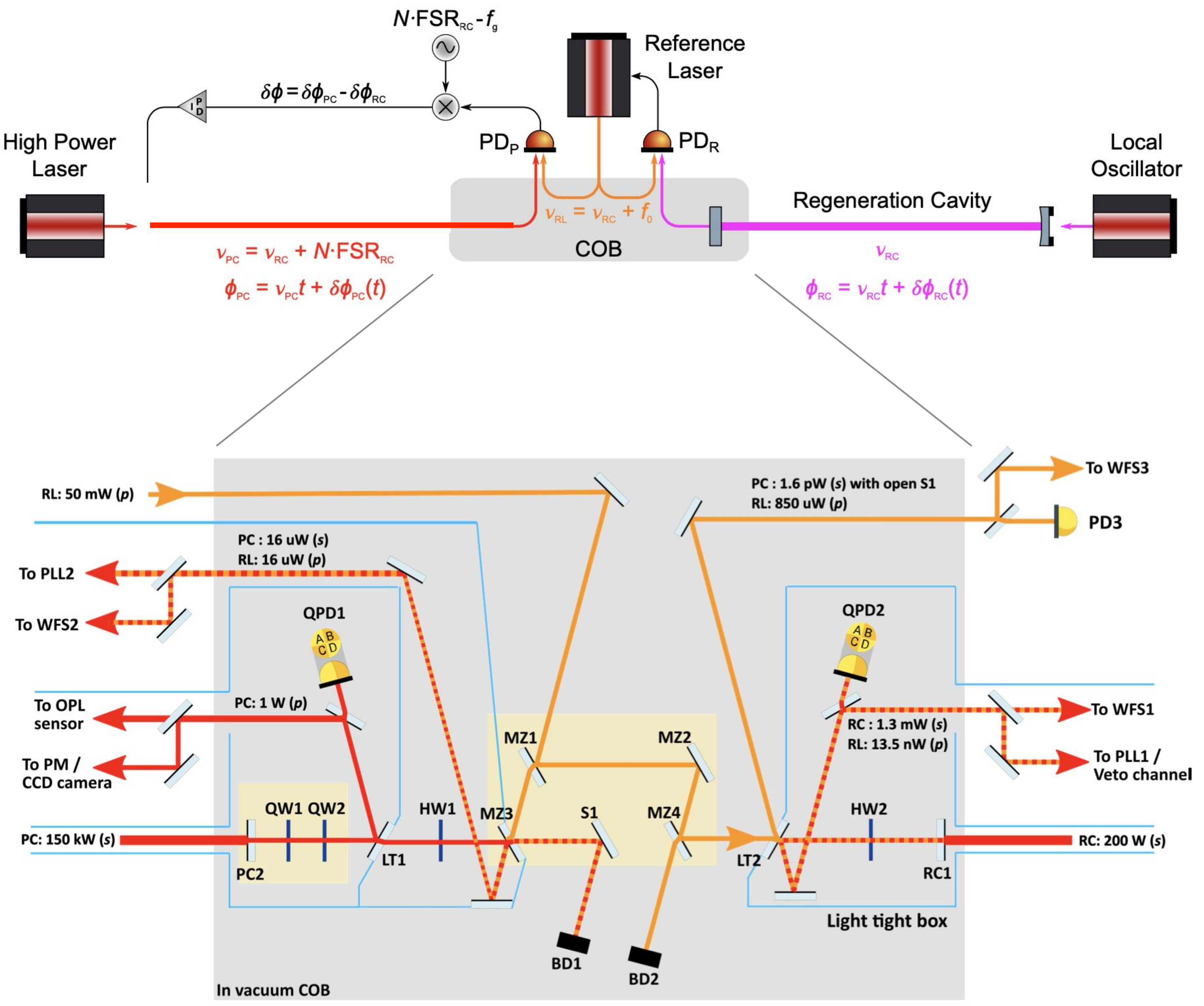

Optics

Central Optical Bench

- intermediate reference laser (RL) is used to phase-lock the HPL frequency to the LO transmitted field **without direct interference**
    - PLL1 between RL and LO
    - PLL2 between HPL and RL
    - sum of offset frequencies equal to integer number of RC FSR's
- Ultra-low expansion (ULE) plate inserts minimize phase drift
- Optics on COB must be pre-aligned before insertion into vacuum
- more than 40 hours of "good data" collected over a week - 30% duty cycle on first science run

High Power laser

- > 35 W of stable 1064 nm laser light injected through the Production Area
- urad alignment precision and stability

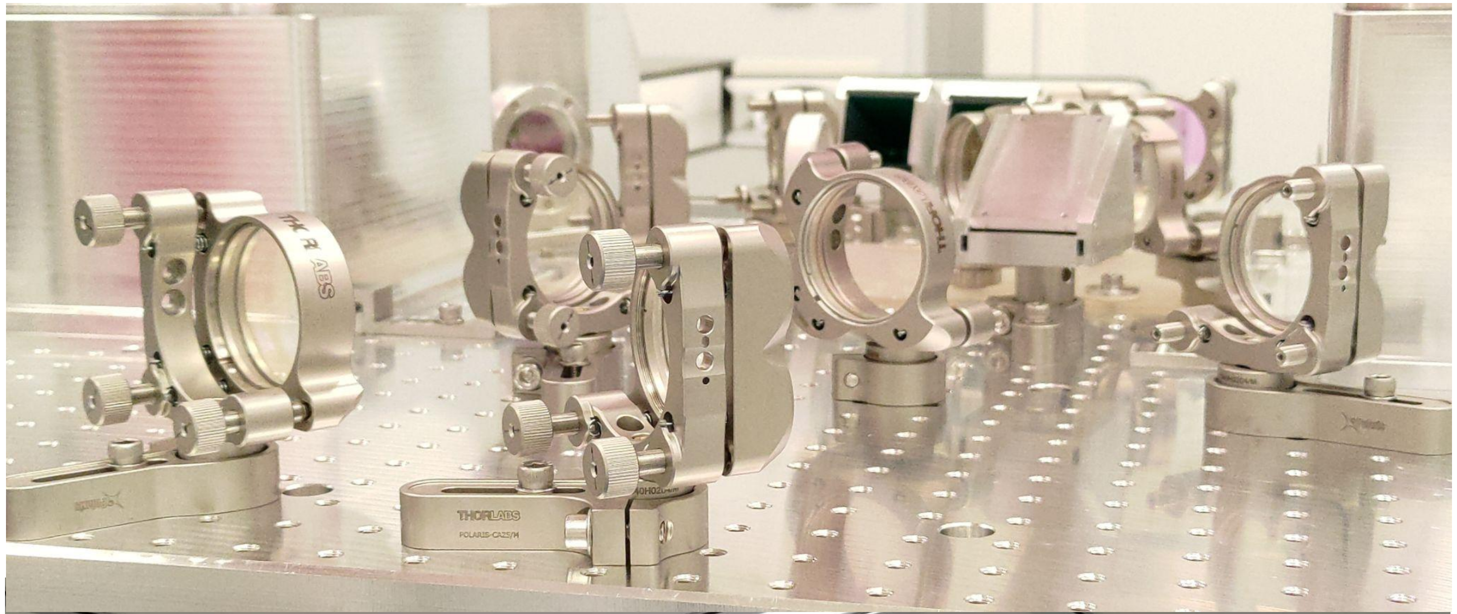

Detector

$$\left| \sqrt{P_{\rm LO}}\; e^{i(2\pi f_{\rm LO} t + \phi_{\rm LO})} + \sqrt{P_{\rm signal}}\; e^{i(2\pi (f_{\rm LO} + f_{\rm signal}) t + \phi_{\rm signal})} \right|^2 =$$

$$P_{\rm LO} + P_{\rm signal} + 2\sqrt{P_{\rm LO} P_{\rm signal}} \cos(2\pi f_{\rm signal} t + \Delta\phi)$$

Heterodyne Interferometry

- measurement of the interference beat-note between an ultra-weak signal field and a strong local oscillator on a shot-noise-limited photodetector
- double-stage demodulation:
  - first stage on-board a high-frequency, low-noise FPGA (Liquid Instruments Moku)
  - second demodulation performed offline in Matlab to avoid spurious electronic pickup
  - In-phase and quadrature demodulation performed to extract signal amplitude and phase:

$$z[N] = \frac{(\sum_i^N I[n])^2 + (\sum_i^N Q[n])^2}{N^2}$$

Number of photons

$$N_\gamma = \frac{z[N]}{G^2 P_{LO} h\nu}$$

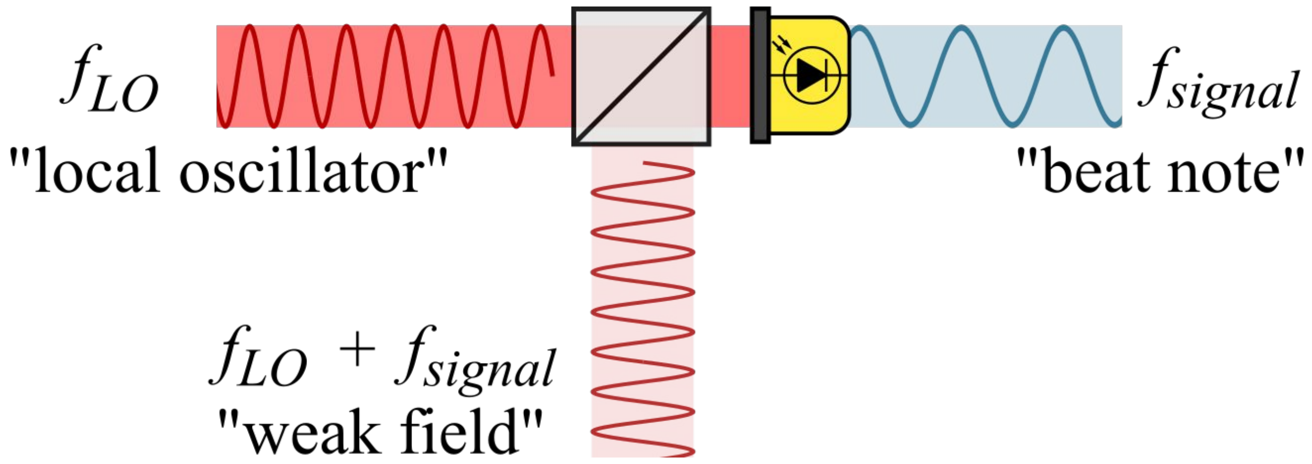

Detector

Heterodyne Interferometry

- if we maintain a fixed frequency and phase offset between the two fields, the detection is coherent and allows us to integrate away noise
  - only stray light, or spuriously-sourced light from the high power laser, is present as a background
  - latest measurements show that phase evolution of the stray light background also allows us to integrate it away over long (million second) measurement periods
- current “open shutter measurement” phase stability (the phase stability of our expected signal) better than **0.1 radians / day**
- current stray light background rate measured with the science photodetector **< 1 ph / 100 s** and improving with each light-tightness upgrade
  - two orders of magnitude above our target, largest outstanding technical challenge

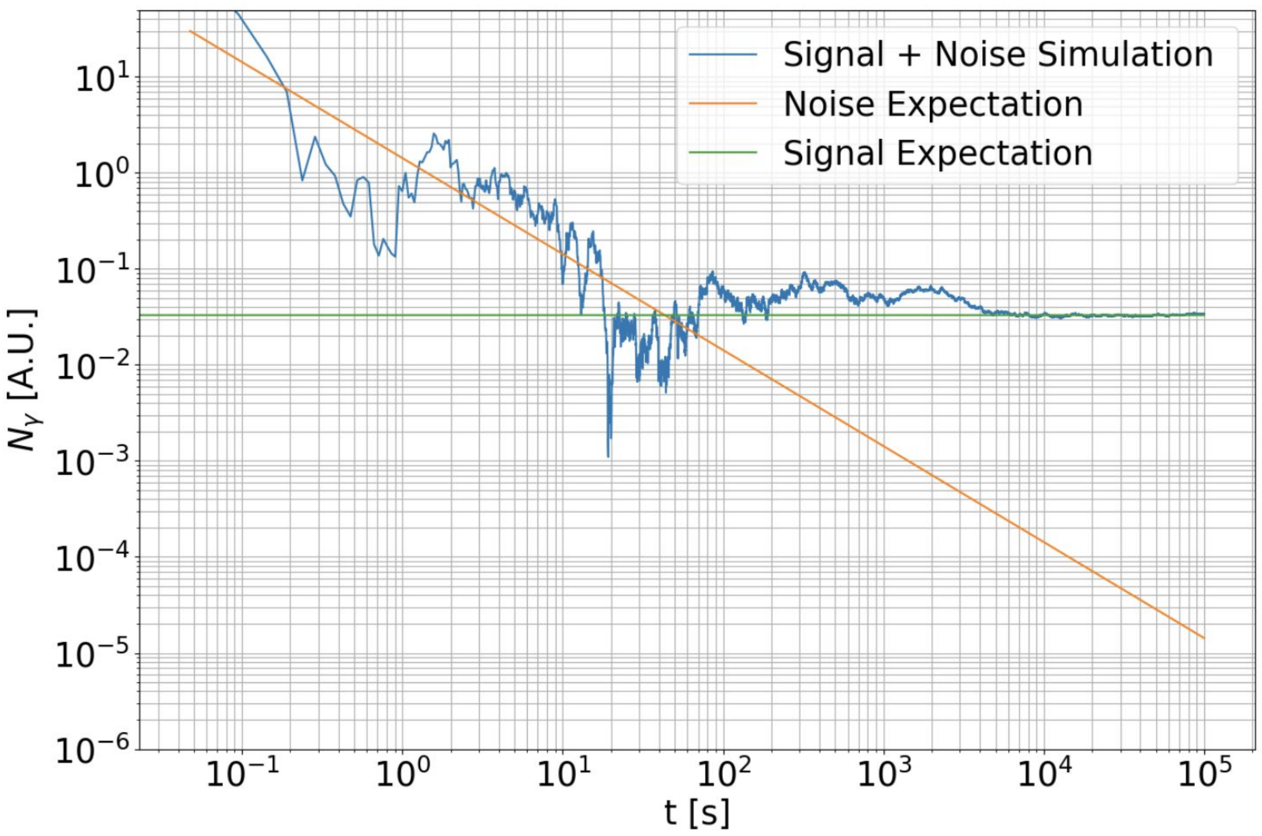

X-Ray Detectors

Post Discovery Technologies

- Beyond baseline: precision technologies
  - ➡ Better energy resolution: few eV - 100 eV
  - ➡ Lower energy threshold: ~ 0.1 keV
- Very active R&D ongoing: designs, materials, readout

Keep in mind!

GridPix
(U. Bonn)

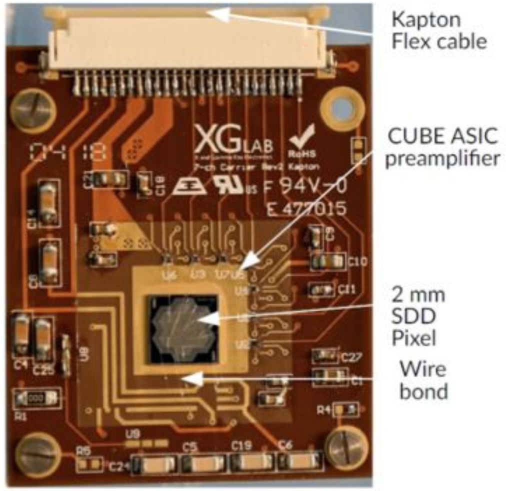

SDD: Silicon Drift
Detectors (TUM)

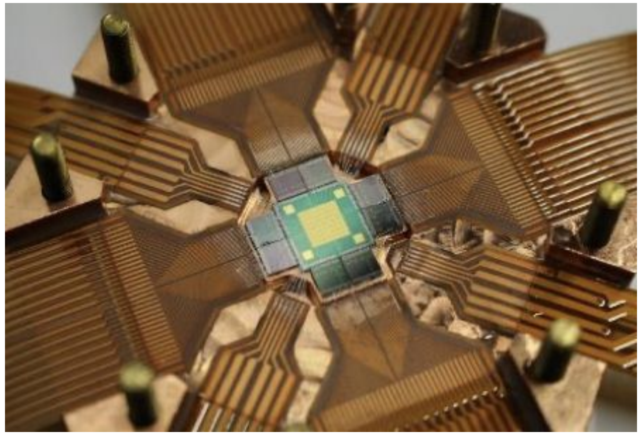

MMC: Metallic Magnetic
Calorimeters (U. Heidelberg)

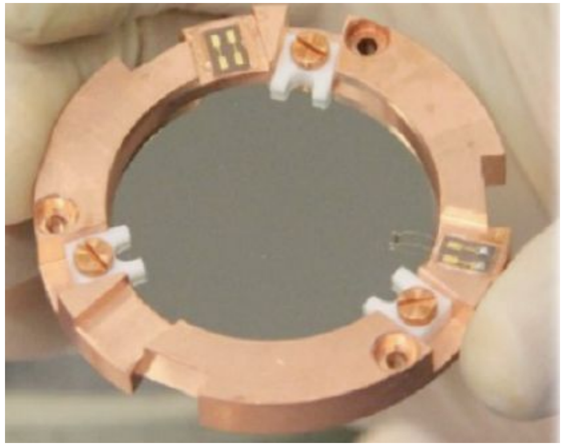

TES: Transition Edge Sensors
(DESY/UHH + INMA-ICMAB CSIC)

Magnet (Design by CERN)

Prospects and Challenges

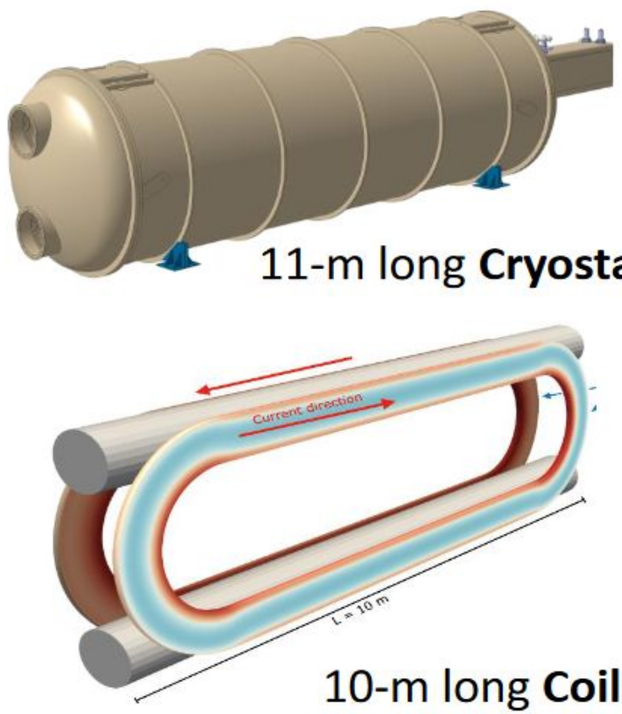

11-m long **Cryostat**

10-m long **Coils**

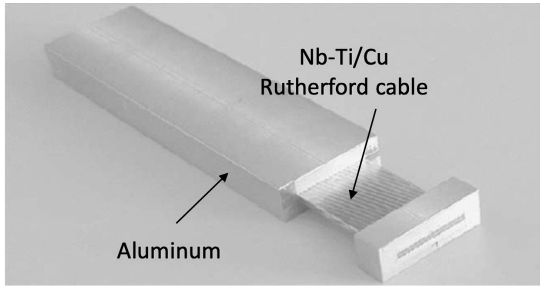

20-km long **Conductor**

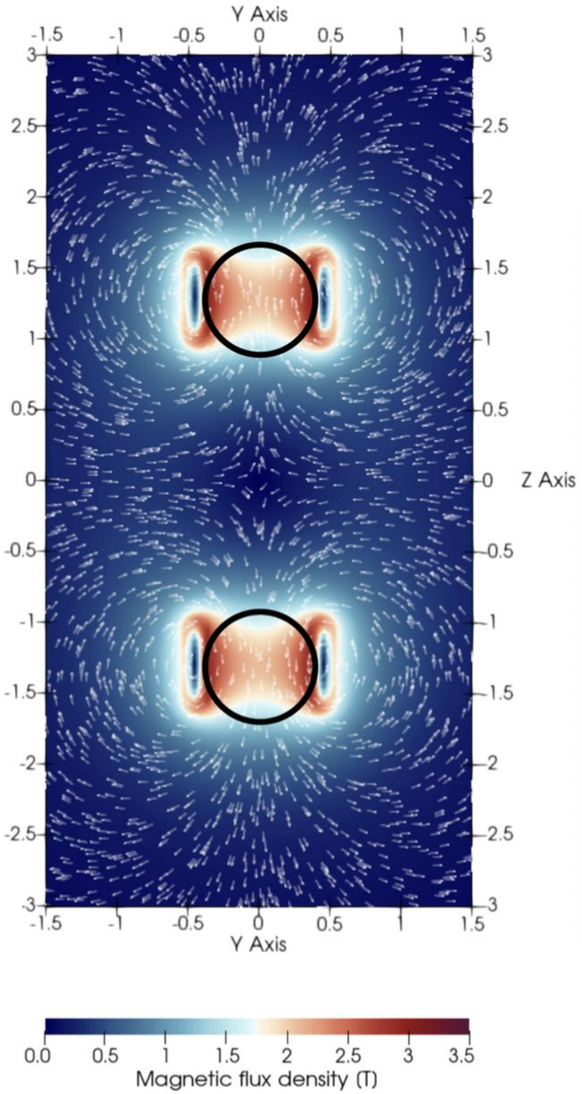

- Two 10 m long bores with common coil racetrack design, cryocooler concept
- Ongoing discussion mainly due to difficulties in building Al-stabilised superconducting cables, **critical item**
  - ➡ Potential Russian companies not available
  - ➡ Causing additional costs and delays
- Collaboration of magnet experts (DESY+CERN)
  - ➡ Build up competence to build cable at CERN or let it built by a suitable industrial partner
  - ➡ Constantly improving cryogenic system
  - ➡ Conceptual design under preparation, new magnet review upcoming

H

DESY.

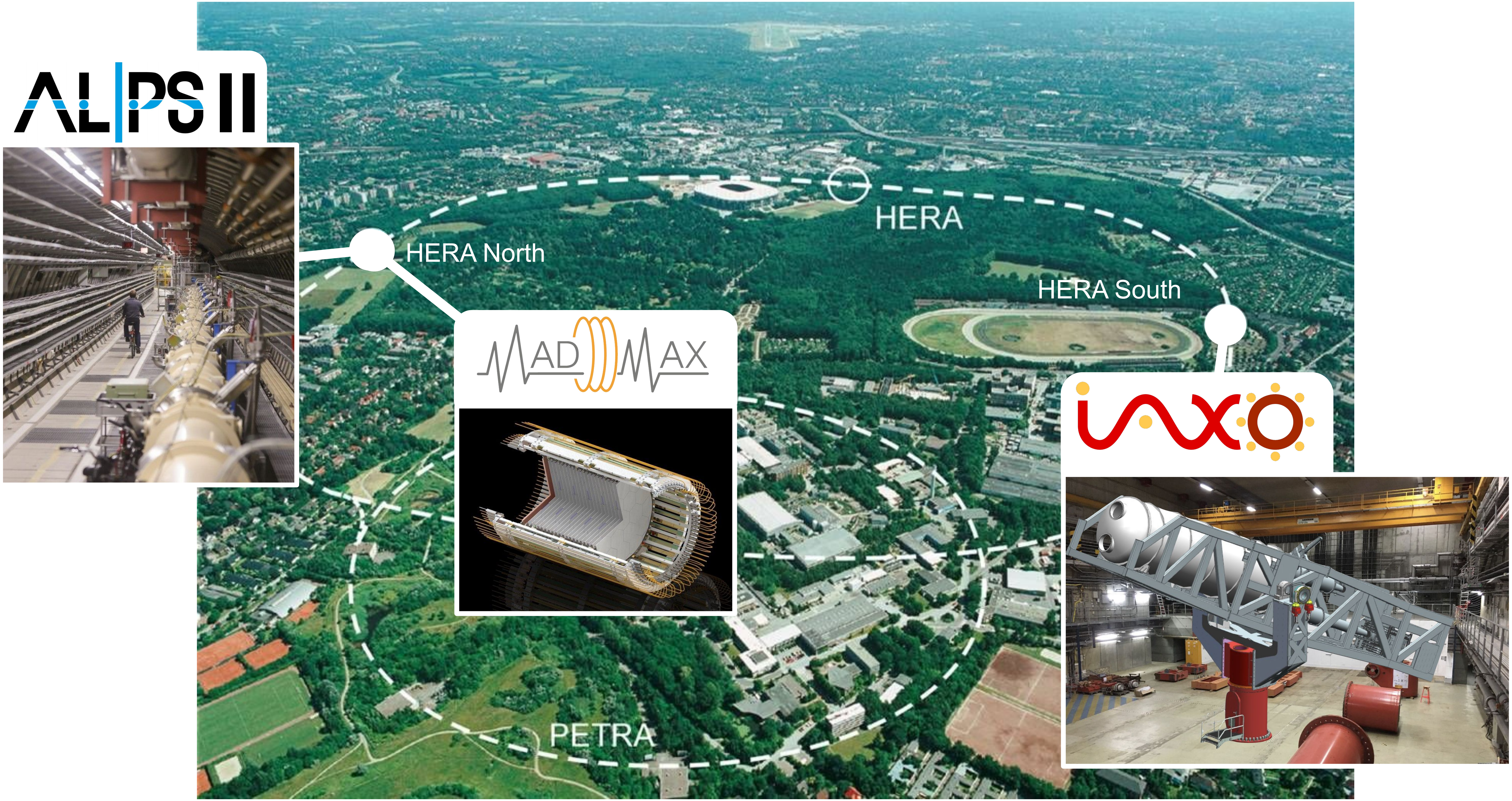

ALPS II
HERA North
HERA
HERA South
MADMAX
IAXO
PETRA